3. Eigene Forschungsergebnisse zur Pathophysiologie des unreifen Hirns

3.1. Hirnschäden durch Trauma

Bittigau P, Sifringer M, Pohl D, Stadthaus D, Ishimaru M, Shimizu H, Ikeda M, Lang D, Speer A, Olney JW, Ikonomidou C. (1999) Apoptotic neurodegeneration following trauma is markedly enhanced in the immature brain. Ann Neurol. 45:724-35.

JCR 2005 **7,17**

Bittigau P, Sifringer M, Felderhoff-Mueser U, Hansen HH, Ikonomidou C. (2003) Neuropathological and biochemical features of traumatic injury in the developing brain. Neurotox Res. 5:475-90.

Felderhoff-Mueser, Sifringer M, Pesditschek S, Kuckuck H, **Bittigau P**, Ikonomidou C. (2002) Pathways leading to apoptotic neurodegeneration following trauma to the developing brain. Neurobiol Dis. 11:231-45.

JCR 2005 **4,782**

3.2. Hirnschäden durch Blockade von NMDA-Rezeptoren

Pohl D, **Bittigau P**, Ishimaru MJ, Stadthaus D, Hubner C, Olney JW, Turski L, Ikonomidou C. (1999) N-Methyl-D-aspartate antagonists and apoptotic cell death triggered by head trauma in developing rat brain. Proc Natl Acad Sci U S A. 96:2508-13.

JCR 2005 **10.272**

3.3. Hirnschäden durch Äthanol

Ikonomidou C, **Bittigau P**, Ishimaru MJ, Wozniak DF, Koch C, Genz K, Price MT, Stefovska V, Horster F, Tenkova T, Dikranian K, Olney JW. (2000) Ethanol-induced apoptotic neurodegeneration and fetal alcohol syndrome. Science. 287:1056-60.

JCR 2005 **29.781**

3.4. Hirnschäden durch Antiepileptika

Bittigau P, Sifringer M, Genz K, Reith E, Pospischil D, Govindarajalu S, Dzietko M, Pesditschek S, Mai I, Dikranian K, Olney JW, Ikonomidou C. (2002) Antiepileptic drugs and apoptotic neurodegeneration in the developing brain. Proc Natl Acad Sci U S A. 99:15089-94.

JCR 2005 **10.272**

Apoptotic Neurodegeneration following Trauma Is Markedly Enhanced in the Immature Brain

Petra Bittigau, MD,* Marco Sifringer, BA,* Daniela Pohl, MD,* Daniel Stadthaus,* Masahiko Ishimaru, MD,† Hiroki Shimizu, PhD,‡ Masuhiro Ikeda, PhD,‡ Dieter Lang,* Astrid Speer, MD,§ John W. Olney, MD,† and Chrysanthy Ikonomidou, MD*

Age dependency of apoptotic neurodegeneration was studied in the developing rat brain after percussion head trauma. In 7-day-old rats, mechanical trauma, applied by means of a weight drop device, was shown to trigger widespread cell death in the hemisphere ipsilateral to the trauma site, which first appeared at 6 hours, peaked at 24 hours, and subsided by 5 days after trauma. Ultrastructurally, degenerating neurons displayed features consistent with apoptosis. A decrease of bcl-2 in conjunction with an increase of c-jun mRNA levels, which were evident at 1 hour after trauma and were accompanied by elevation of CPP 32-like proteolytic activity and oligonucleosomes in vulnerable brain regions, confirmed the apoptotic nature of this process. Severity of trauma-triggered apoptosis in the brains of 3- to 30-day-old rats was age dependent, was highest in 3- and 7-day-old animals, and demonstrated a subsequent rapid decline. Adjusting the mechanical force in accordance with age-specific brain weights revealed a similar vulnerability profile. Thus, apoptotic neurodegeneration contributes in an age-dependent fashion to neuropathological outcome after head trauma, with the immature brain being exceedingly vulnerable. These results help explain unfavorable outcomes of very young pediatric head trauma patients and imply that, in this group, an antiapoptotic regimen may constitute a successful neuroprotective approach.

Bittigau P, Sifringer M, Pohl D, Stadthaus D, Ishimaru M, Shimizu H, Ikeda M, Lang D, Speer A, Olney JW, Ikonomidou C. Apoptotic neurodegeneration following trauma is markedly enhanced in the immature brain. Ann Neurol 1999;45:724–735

Although children younger than 6 years of age sustain traumatic brain injury more frequently than any other age group,[1] there has been a dearth of research focusing on traumatic brain injury to the developing brain. Progress toward understanding the mechanisms and developing neuroprotective measures for traumatic brain injuries in children has therefore been very limited.

Clinical observations suggest that age decidedly influences both morbidity and mortality after head injury in children, with those less than 4 years of age showing worst outcomes.[2–6] In a study by Koskiniemi and colleagues[5] it was demonstrated that of the children suffering severe head injury before the age of 4 years none was able to work independently outside a structured environment years later. Children older than 4 years at the time of injury had a significantly better outcome.

Brain damage resulting from mechanical trauma can be classified into primary damage, which occurs immediately or shortly after impact, and secondary or delayed damage, which may appear several hours or even days later.[7–10] Two pathogenetic mechanisms for secondary traumatic damage stand out among those proposed, excitotoxicity and apoptosis.[8–35] Blocking each of these processes elicits protective effects in experimental models for brain and spinal cord trauma.[13–17,19–30,34]

Excitotoxic and apoptotic cell death can be distinguished histologically.[35] Excitotoxic degeneration is characterized by rapid swelling of dendrites, cell bodies, and intracytoplasmic organelles, nuclear flocculation, and cell lysis.[36] Apoptotic cell death is characterized by cytoplasmic and nuclear condensation, preservation of the plasma membrane and cytoplasmic organelles, internucleosomal cleavage, and cell shrinkage and fragmentation into apoptotic bodies that are engulfed and

From the *Department of Pediatric Neurology, Charité, Virchow Campus, Children's Hospital, Humboldt University, and §Technische Fachhochschule Berlin, Berlin, Germany; †Department of Psychiatry, Washington University School of Medicine, St Louis, MO; and ‡Tsukuba Research Laboratories for Drug Discovery, Eisai Co, Ltd, Ibaraki, Japan.

Received Oct 27, 1998, and in revised form Jan 7, 1999. Accepted for publication Jan 21, 1999.

Address correspondence to Dr Ikonomidou, Department of Pediatric Neurology, Charité, Virchow Campus, Children's Hospital, Humboldt University, Augustenburger Platz 1, 13353 Berlin, Germany.

degraded by neighboring cells in the absence of an inflammatory reaction.[37–40]

Within the pathways that lead to apoptotic deletion, the transcription factor c-jun has proapoptotic properties,[41,42] whereas bcl-2 inhibits apoptosis and ameliorates neuronal degeneration after hypoxic and traumatic central nervous system insults.[43–49] Expression of immediate early genes including c-jun, and of the survival gene bcl-2, has been demonstrated in the context of experimental brain and spinal cord injury in vivo and in vitro.[50–53]

Activation of caspases constitutes a subsequent critical step within the apoptotic cascade. Caspases contribute to cell cleavage via inactivation of nuclease inhibitors and survival proteins, direct disassembly of cell structures, destruction of proteins involved in cytoskeleton regulation, and inactivation of proteins involved in DNA repair and replication.[54]

Pioneering attempts to model pediatric head trauma were made by Prins and associates,[55] Prins and Hovda,[56] and Adelson and colleagues,[57,58] who adopted the lateral fluid percussion and closed head injury model, initially described by Marmarou and collaborators,[59] to 17-day-old rats. Our goal was to study the response of the rat brain to head trauma in even earlier developmental stages, and examine mechanisms that contribute to unfavorable outcomes of very young pediatric patients to head trauma. For that purpose, we developed a model with the weight drop device described by Allen[60] for the spinal cord and by Feeney and colleagues[61] for the brain. By using this approach initially in 7-day-old rats, we found that mechanical trauma to the immature brain causes an acute excitotoxic lesion within the area of impact that rapidly expands within 4 hours after trauma.[62] This local excitotoxic response is followed by disseminated cell death affecting many brain regions ipsilateral and contralateral to the trauma site, which is detected long after the excitotoxic degeneration has run its course. Here, we investigated whether this disseminated degenerative response displays features consistent with apoptosis and examined the vulnerability profile of the developing brain to apoptotic neurodegeneration after mechanical trauma.

Materials and Methods

Traumatic Brain Injury and the Contusive Device

Wistar rat pups (BGVV, Berlin, Germany), age 3, 7, 10, 14, and 30 days, were anesthetized with halothane and placed in a stereotaxic apparatus. A skin incision was made to expose the skull surface. In initial experiments with 3- and 7-day-old rats, craniotomy caused substantial subarachnoid bleeding and was therefore abandoned. To ensure that severity of brain injury was not influenced by bone thickness and consistency in older rats, the parietal bone was carefully thinned in 10-, 14-, and 30-day-old rats by using a drill to reach bone consistency similar to that in 7-day-old animals. This was achieved when the bone could be easily depressed by the experimenter's finger applying light pressure onto a curved forceps.

The contusing device consisted of a hollow stainless steel tube 40 cm in length, perforated at 1-cm intervals. The device was kept perpendicular to the surface of the skull and guided a falling weight onto a circular footplate (2.0 mm in diameter) resting on the surface of the parietal bone. To traumatize corresponding cortical areas (sensorimotor cortex) in all studied ages, stereotaxic coordinates were modified age dependently, based on the atlas of Sherwood and Timiras.[63] The center of the footplate was positioned onto the parietal bone at 2 mm anterior and 2 mm lateral to lambda in 3-day-old rats, 3 mm anterior and 2 mm lateral to lambda in 7-day-old rats, 3.5 mm anterior and 2.5 mm lateral to lambda in 10- and 14-day-old rats, and 4 mm anterior and 3 mm lateral to lambda in 30-day-old rats. The contusion force was delivered unilaterally to the right side of the skull. Group size for each experimental condition was 5 to 9 animals, and for corresponding sham-operated age-matched controls 6 animals.

Two experimental protocols were used. In the first series of experiments, the same traumatic force (160 g-cm) was used in all age groups. In the second, the force was adjusted, taking into account the mean brain weight at each of the ages studied, using the formula: Height (age x) = height (age 7 days) $\times$ brain weight (age x)^2/brain weight (age 7 days)^2, so that pressure/brain weight ratios in all age groups were comparable with that in the 7-day-old group (160 g-cm; mean brain weight 0.71 $\pm$ 0.008 g). This formula was derived from the following pressure equation: Pressure = {mass $\times$ $\sqrt{\text{height} \times g}$}/(duration of impact $\times$ surface). The calculated heights are depicted in Table 1. Animals were kept on a heating pad maintained at 37.5°C until returned to their mothers at 4 hours after the trauma or sham surgery. Rats survived 6, 16, 24, or 48 hours or 5 days after the trauma.

Table 1. Heights and Weights Used to Traumatize Rats of Different Ages

		Trauma Device	
Age	Brain Weight (g) Mean $\pm$ SEM	Weight (g)	Height (cm)
3 days	0.50 $\pm$ 0.01	10	8
7 days	0.71 $\pm$ 0.01	10	16
14 days	0.97 $\pm$ 0.03	10	29
30 days	1.56 $\pm$ 0.03	20	19

Mechanical forces were modified to achieve the same pressure/brain weight ratios in all age groups. Mean brain weights (perfused brains, n = 6) were calculated for each age (row 2). The height from which the weight fell at age x days was calculated according to the formula: Height (age x) = height (age 7 days) $\times$ brain weight (age x)^2/brain weight (age 7 days)^2. At the age of 30 days a modified trauma device was used, which accommodated a 20-g weight. Because the radius of the footplate in the trauma device used for 30-day-old rats was twice the radius size in the footplate used for younger rats, the formula was modified as follows: Height (age 30 days) = height (age 7 days) $\times$ brain weight (age 30 days)^2/4 $\times$ brain weight (age 7 days)^2.

To exclude that anesthesia and surgery might cause apoptotic neurodegeneration in the developing brain, 6 animals per age group were subjected to anesthesia and sham surgery only.

Physiological Monitoring

Because of small animal size, invasive monitoring was not performed. Skin temperature was measured by using a skin probe at the axilla. Heart rate and oxygen saturations (monitored by means of transcutaneous pulse oximetry) were recorded 5 minutes before and immediately after induction of anesthesia, immediately after trauma, as well as at 10, 20, and 30 minutes, and 1, 2, 3, and 4 hours after trauma. The experiments were performed in accordance to the guidelines of the Humboldt University in Berlin and the Washington University in St Louis.

Morphometry

Rats were anesthetized with an overdose of chloral hydrate and perfused through the heart and ascending aorta for 15 minutes with a solution containing paraformaldehyde (1%) and glutaraldehyde (1.5%) in pyrophosphate buffer (for combined light and electron microscopy) or paraformaldehyde (4%) in phosphate buffer (for TUNEL [terminal dUTP nick end-labeling] or DeOlmos cupric silver staining).

DEOLMOS CUPRIC SILVER STAINING. To visualize degenerating cells, coronal sections of the whole brain were stained with silver nitrate and cupric nitrate according to the method of DeOlmos and Ingram.[64] This technique stains degenerating cells dying via an apoptotic[65] or a nonapoptotic mechanism.[66] Degenerating cells assumed a distinct dark appearance caused by silver impregnation.

TUNEL STAINING. To visualize nuclei with DNA cleavage serial coronal sections (70 μm) of the entire brain were cut on a Vibratome (OTS-3000-03, Science Services, Munich, Germany) and residues of peroxidase-labeled digoxigenin nucleotides were catalytically added to DNA fragments by terminal deoxynucleotidyl transferase (ApopTag, Oncor, Heidelberg, Germany).

LIGHT MICROSCOPY ON PLASTIC SECTIONS AND ELECTRON MICROSCOPY. Brains were sliced into 1-mm-thick slabs, fixed in osmium tetroxide, dehydrated in alcohols, and embedded in Araldite (EPON-812, Science Services). For light microscopy, 1-μm transverse serial sections were cut and stained with methylene blue/azure II. Ultrathin sections were cut and stained with uranyl acetate/lead citrate and examined by electron microscopy.

QUANTITATION OF DAMAGE IN THE BRAIN. Distant damage was quantified in TUNEL- or silver-stained sections in the frontal, parietal, cingulate, retrosplenial cortex, caudate nucleus (mediodorsal part), thalamus (laterodorsal, mediodorsal, and ventral nuclei), dentate gyrus, and subiculum by using a stereological optical disector, estimating mean numerical densities (N_v) of degenerating cells.[67] An unbiased counting frame (0.05 × 0.05 mm; disector height, 0.07 mm) and a high aperture objective were used for the sampling. The N_v for each brain region was determined with eight to 10 disectors.

To assess overall severity of damage and enable comparisons among age groups, a scoring system was created. In each hemisphere, 14 regions were analyzed by using the stereological optical disector to determine the densities of degenerating cells. Each region was subsequently given a number of points (score: 1,000 degenerating cells/mm^3 reflects a score of 1) and the scores from all evaluated regions (total of 28) were added to give a cumulative severity score for the brain.

Reverse Transcription–Polymerase Chain Reaction

Total cellular RNA was isolated by acidic phenol/chloroform extraction[68] and DNase treated (AGS GmbH, Boehringer Mannheim, Germany); 5 μg of RNA was reverse transcribed with Moloney murine leukemia virus reverse transcriptase (Promega, Madison, WI) in 25 μl of reaction mixture. The resulting cDNA (5 μl, 1:100 solution) was amplified by polymerase chain reaction. Primers to amplify the rat c-jun were 5′-GGAAACGACCTTCTACGAC-3′ (sense primer, positioned at nucleotide 15; GenBank sequence X17163) and 5′-GTGGTGATGTGCCCATTG-3′ (antisense primer, positioned at nucleotide 269; GenBank sequence X17163). The primers to amplify bcl-2 were 5′-TTATAAGCTGTCGCAGAGG-3′ (sense primer, positioned at nucleotide 60; GenBank sequence U34964) and 5′-TGAAGAGTTCCTCCACCAC-3′ (antisense primer, positioned at nucleotide 406; GenBank sequence U34964). cDNA was amplified in 35 cycles, consisting of denaturing over 30 seconds at 94°C, annealing over 45 seconds at 55°C, and primer extension over 45 seconds at 72°C. Amplified cDNA was analyzed by polyacrylamide gel electrophoresis and subsequent silver staining.[69]

For internal standard we used glyceraldehyde-3-phosphate dehydrogenase (GAPDH). Primers to amplify GAPDH were 5′-TATCCGTTGTGGATCTGAC-3′ (sense primer, positioned at nucleotide 743;, GenBank sequence M17701) and 5′-TGGTCCAGGGGTTTCTTAC-3′ (antisense primer, positioned at nucleotide 1047; GenBank sequence M17701).

Assays for DNA Fragmentation and Caspase 3-Like Activity

Frozen tissue samples from selected brain regions were homogenized and diluted in homogenization buffer (1 g of tissue/20 ml volume). Aliquots of cytosolic extracts were preincubated at 37°C for 30 minutes. Homogenates were centrifuged at 14,000 rpm for 5 minutes, the supernatant was further diluted 20-fold in incubation buffer, and 100 μl was then used directly as the antigen source in the cell death detection enzyme-linked immunosorbent assay (Boehringer Mannheim, Germany). This method is based on the quantitative sandwich enzyme immunoassay principle with mouse monoclonal antibodies directed against DNA and histones, respectively, and detects mononucleosomes and oligonucleosomes. The primary antihistone antibody is coated to the microplates and the secondary anti-DNA antibody is coupled to peroxidase. Quantitation is performed colorimetrically by measuring light absorption at 405 nm wavelength. DNA fragmentation was evaluated in cingulate and parietal cortices, thalamus, striatum, and hippocampus ipsilateral and

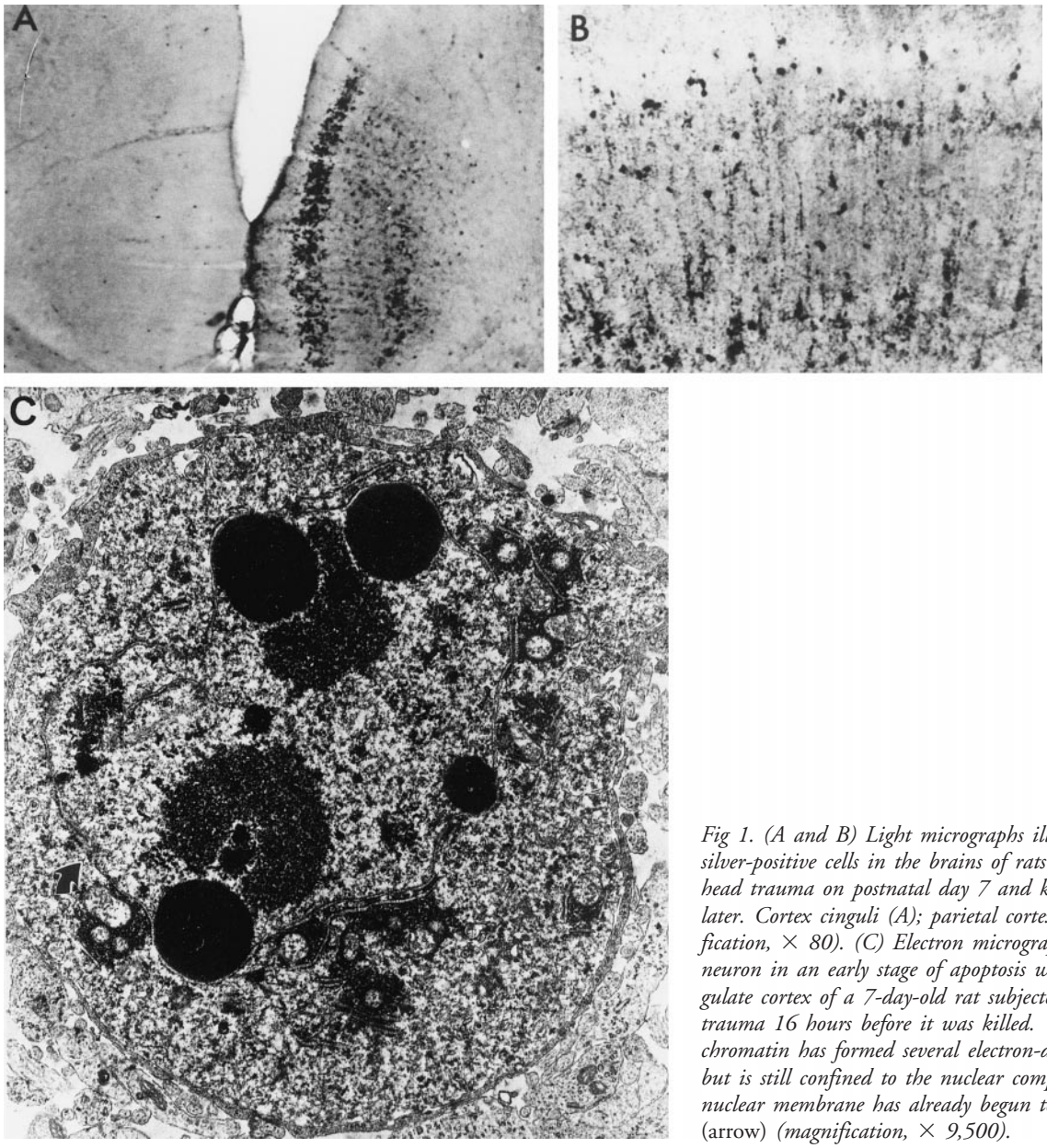

Fig 1. (A and B) Light micrographs illustrating silver-positive cells in the brains of rats subjected to head trauma on postnatal day 7 and killed 24 hours later. Cortex cinguli (A); parietal cortex (B) (magnification, × 80). (C) Electron micrograph depicting a neuron in an early stage of apoptosis within the cingulate cortex of a 7-day-old rat subjected to head trauma 16 hours before it was killed. The nuclear chromatin has formed several electron-dense masses but is still confined to the nuclear compartment. The nuclear membrane has already begun to break down (arrow) *(magnification, × 9,500).*

contralateral to the traumatized hemisphere at 24 hours after trauma in 7-day-old rats.

To determine caspase 3 (CPP 32)-like activity, 30 μl of the same supernatant was diluted with 170 μl of assay buffer [50 mM HEPES, pH 7.5, 1% sucrose, 0.1% 3-(3-cholamidopropyldimethylammonio)-1-propanesulfonate (CHAPS), and 10 mM dithiothreitol] and incubated at 37°C for 2 hours with the fluorogenic tetrapeptide substrate Ac-DEVD-AMC (50 μM, Peptide Institute Inc, Osaka, Japan). Free aminomethylcoumarin (AMC) accumulation, resulting from cleavage of the aspartate–AMC bond, was measured using a Cytofluor II fluorometer (Perspective Biosystems), at 380 nm excitation and 460 nm emission wavelengths. Specific activity was defined as the difference of total activity in the presence and absence of the specific caspase inhibitor Ac-DEVD-CHO (10 nM, Peptide Institute Inc). Serial dilutions of AMC were used as standards.

Changes in CPP 32-like enzymatic activity were evaluated in cingulate and parietal cortices, thalamus, striatum, and hippocampus in 8-day-old rats that had been subjected 24 hours earlier (on postnatal day 7) to trauma (n = 6) or sham surgery (n = 6). In rats subjected to head trauma, separate measurements were made in the hemisphere ipsilateral and contralateral to the trauma.

Statistics

Statistical analysis of numerical densities of degenerating cells and cumulative scores was performed by means of Student's *t* test. For the caspase activity assay and DNA fragmentation (oli-

gonucleosomal) assay, data were analyzed by one-way analysis of variance. Post hoc individual comparisons were performed by using the Bonferroni/Dunn test.

Results

Physiological Parameters

Rats subjected to sham surgery or trauma recovered within 10 to 15 minutes after anesthesia. There was no mortality. Axillar temperature was maintained between 36.5°C and 37.8°C throughout the 4 hours the pups were away from their mothers. Oxygen saturations remained above 91%.

Histology in the Seven-Day-Old Rat Brain

At 24 hours after trauma, widespread degeneration was detected in the brains by means of DeOlmos cupric silver staining (Fig 1). Frontal, parietal, cingulate, and retrosplenial cortices, laterodorsal, mediodorsal, and ventral thalamic nuclei, hippocampal dentate gyrus, subiculum, and striatum were affected. Degeneration did occur bilaterally, with the ipsilateral hemisphere being more severely involved at all time points studied.

Examination of histological sections by TUNEL staining revealed that TUNEL-positive cells displayed a similar distribution pattern as silver-accumulating cells. By morphometric analysis, densities of silver-positive and TUNEL-positive cells obtained from parallel sections within affected brain areas did not significantly differ from each other. Thus, cells that degenerated in a delayed fashion after head trauma in the 7-day-old rat brain displayed nuclear DNA fragmentation.

To confirm the apoptotic nature of the delayed degenerative reaction to trauma in the 7-day-old rat brain, and taking into account that degenerating neurons dying by a nonapoptotic process can also show TUNEL positivity,[70] we examined large numbers of degenerating cells by electron microscopy within the affected brain regions (frontoparietal and cingulate/retrosplenial cortices, thalamus, and caudate nucleus). Within all regions examined, the presence of cells undergoing apoptotic degeneration was a very consistent finding at 16 to 24 hours after trauma. The first detectable ultrastructural changes consisted of clumping of nuclear chromatin and mild to moderate condensation of the entire cell. Nuclear chromatin became transformed into flocculent densities that formed one or more large electron-dense spherical balls (see Fig 1C). The nuclear envelope separated into fragments, and finally the cell became unpartitioned with nucleoplasmic contents freely intermingling with cytoplasmic contents. Large chromatin masses migrated often toward the periphery of the cell and in some cases the cell divided into separate independent bodies consisting of a contingent of cytoplasm and one or more nuclear chromatin balls. This type and sequence of changes are identical to those seen in neurons undergoing apoptosis in physiologically developing brain[70] and meet all the criteria set for diagnosing apoptosis.[40] At 24 hours after trauma, cells in both early and late stages of apoptosis were detected, indicating that the process of cell suicide was still progressing. We did not identify cells undergoing nonapoptotic degeneration by electron microscopy in the brain regions and at the time points analyzed in the context of this study (16–24 hours after trauma), which indicates that, at those times, apoptosis is the predominant form of degeneration in the developing rat brain. In contrast, at 0.5 to 6 hours after trauma, excitotoxic degeneration is the predominant form of neuronal death in the infant rat brain.[62]

Trauma-Induced Changes in c-jun and bcl-2 mRNA Levels in the Seven-Day-Old Rat Brain

A profound increase in c-jun mRNA levels was detectable in the cingulate, parietal, and retrosplenial cortices and the striatum ipsilateral and the cingulate cortex

Fig 2. Bcl-2 (A) and c-jun (B) mRNA expression in right cingulate cortex (ipsilateral to trauma site) in sham-operated control rats and rats subjected to head trauma at 1, 2, 4, 6, 12, and 24 hours after trauma. mRNA was reverse transcribed to cDNA, amplified by polymerase chain reaction, using specific primers for c-jun, bcl-2, and GAPDH (internal standard) and subjected to polyacrylamide gel electrophoresis and silver staining. There is an obvious increase in mRNA levels for c-jun at 1 hour after trauma, whereas levels for bcl-2 are decreased within that same time frame. The GAPDH band shows equal signal intensity in all columns, verifying cDNA integrity. GAPDH = glyceraldehyde-3-phosphate dehydrogenase.

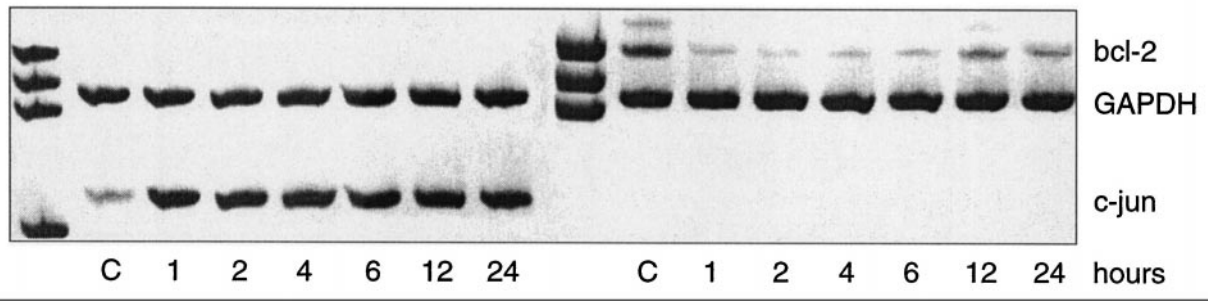

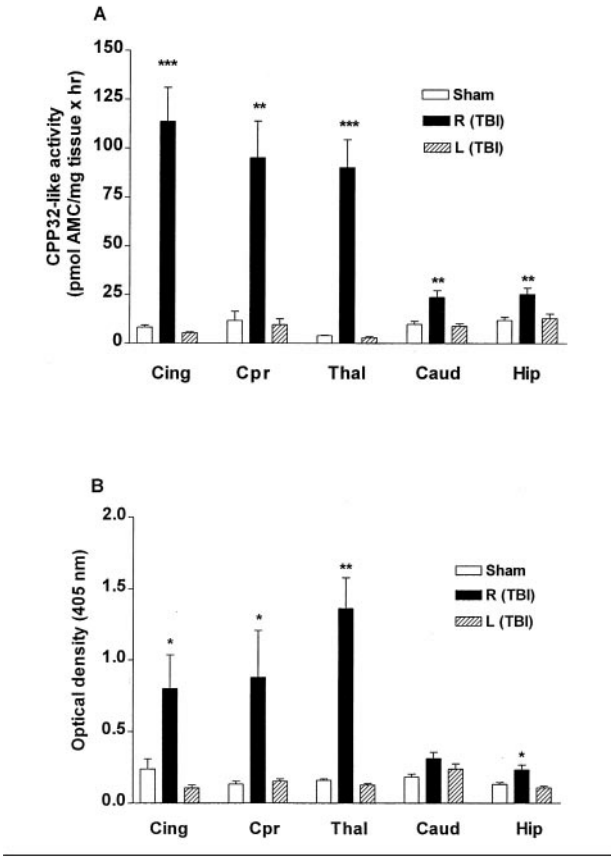

*Fig 3. (A) Caspase 3 (CPP32)-like activity in cytosolic protein extracts from cingulate (Cing) and parietal (Cpr) cortices, thalamus (Thal), caudate nucleus (Caud), and hippocampus (Hip) of sham rats (n = 6) and rats subjected to head trauma (n = 6) on postnatal day 7. Pups were killed 24 hours after trauma or sham surgery. In rats subjected to head trauma, separate measurements were performed ipsilateral and contralateral to the traumatized hemisphere. Caspase 3-like activity was measured fluorometrically by using the specific fluorogenic tetrapeptide substrate Ac-DEVD-AMC by determining the accumulation of free aminomethylcoumarin (AMC). Specific protease activity was defined as the difference between the values obtained in the presence and absence of the specific inhibitor Ac-DEVD-CHO and is expressed as picomoles of AMC per milligram of tissue per hour. Head trauma induced significant elevations of CPP 32-like activity in extracts from ipsilateral cingulate and parietal cortex, thalamus, striatum and hippocampus. No significant increase of CPP 32-like activity was detected in the contralateral hemisphere in 7-day-old rats. (**p < 0.01; ***p < 0.001, compared with sham; Bonferroni/Dunn post hoc test). (B) Enrichment of oligonucleosomes in the cytoplasmic fraction of tissue obtained from the cingulate (Cing) and parietal (Cpr) cortices, thalamus (Thal), caudate nucleus (Caud), and hippocampus (Hip) of 7-day-old rats 24 hours after head trauma (n = 6) or sham surgery (n = 6). Tissue homogenates were centrifuged, the supernatant was further diluted and used directly as an antigen source in the cell death detection enzyme-linked immunosorbent assay to detect histone-associated DNA fragments (oligonucleosomes). Head trauma induced significant elevations of oligonucleosomes (reflected in an increased optical density at 405 nm wavelength) in extracts from ipsilateral cingulate and parietal cortices, thalamus, and hippocampus. No significant increase of oligonucleosomes was detected in the contralateral hemisphere in 7-day-old rats. (*p < 0.05; **p < 0.01, compared with shams; Bonferroni/Dunn post hoc test). TBI = traumatic brain injury.*

contralateral to the trauma site within 1 hour and lasted up to 24 hours after trauma. This increase in c-jun mRNA expression was accompanied by a decrease in mRNA levels for bcl-2 that was already apparent at 1 hour and persisted for up to 24 hours after trauma (Fig 2).

Trauma-Induced Changes in CPP 32-Like Enzymatic Activity in the Seven-Day-Old Rat Brain

Head trauma induced significant elevations of CPP 32-like activity in extracts from ipsilateral cingulate (624% increase compared with sham rats) and parietal cortex (889% increase), thalamus (2,835% increase), striatum (168% increase), and hippocampus (95% increase). Activity was measured at 24 hours after trauma. No significant increases of CPP 32-like activity were detected in the contralateral hemisphere in 7-day-old rats (Fig 3A).

Trauma-Induced DNA Breakdown in the Seven-Day-Old Rat Brain

Compared with sham rats, a profound increase of DNA fragmentation (oligonucleosomes) was detected in the ipsilateral cingulate (300% increase compared with sham rats) and parietal cortices (780% increase), thalamus (580% increase), and hippocampus (130% increase; see Fig 3B). No significant changes were detected with this method in the contralateral hemisphere in 7-day-old rats.

Age-Dependent Distribution Patterns and Severity of Apoptotic Cell Death after Trauma

SAME MECHANICAL FORCE. Apoptotic cell death was detected 24 hours after head trauma in 3-, 7-, 10-, and 14-day-old rats (Fig 4). No distant lesions were seen at this time point in the brains of 30-day-old rats. Silver and TUNEL stains gave similar distribution patterns in all age groups.

In 3-day-old rats, apoptotic cells were found in the frontal, parietal, cingulate, and retrosplenial cortices, thalamic nuclei, dentate gyrus, caudate nucleus, and the subiculum (Table 2; see Fig 4). TUNEL- and silver-positive cells were in addition detected in the contralateral hemisphere, with the laterodorsal and anterior thalamus, cingulate, and retrosplenial cortices and the subiculum being most vulnerable (see Fig 4).

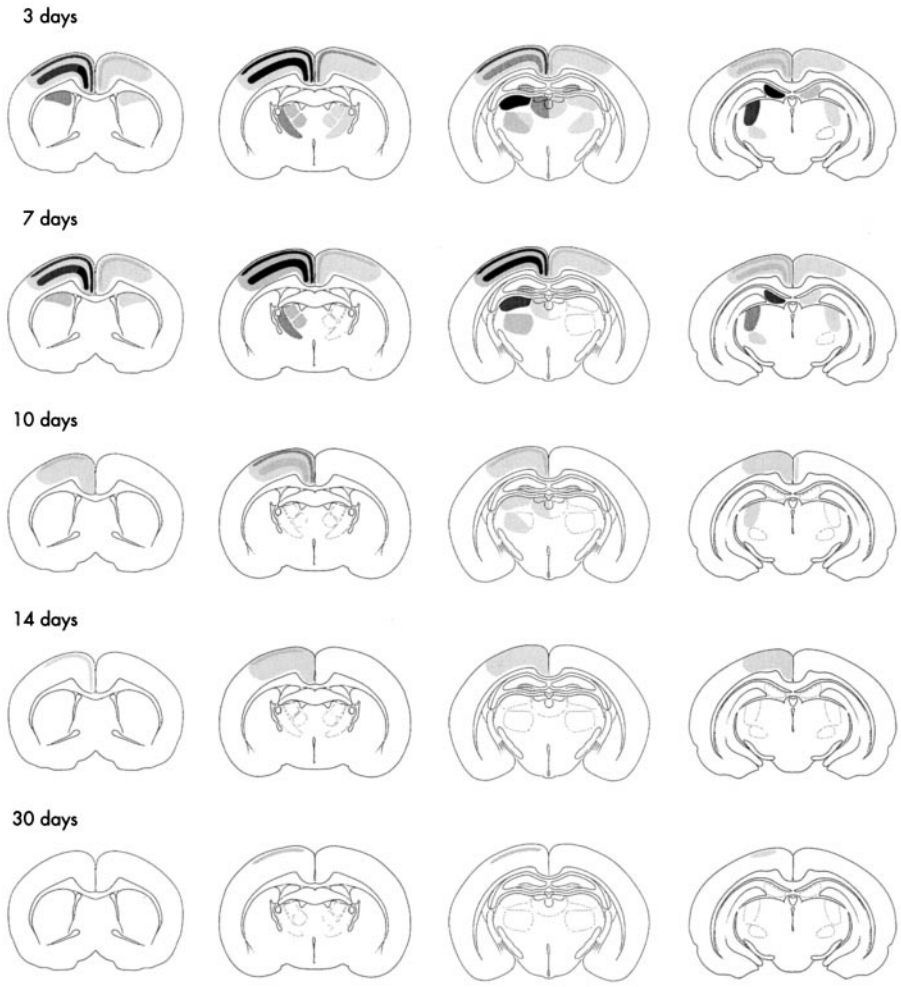

Fig 4. Schematic illustration depicting the distribution patterns of TUNEL-positive cells (shaded areas) in different age groups at 24 hours after trauma. Darker tones indicate higher densities of degenerating cells. Rats were traumatized on postnatal days 3, 7, 10, 14, and 30. TUNEL = terminal deoxynucleotide transferase-mediated dUTP nick end-labeling.

In 7-day-old rats the same brain regions were affected, but the contralateral hemisphere was minimally involved (see Table 2 and Fig 4). Within the contralateral hemisphere, the cingulate/retrosplenial cortices were most vulnerable.

In 10-day-old rats, degenerating cells were found only in the ipsilateral hemisphere in the frontal, parietal, cingulate, and retrosplenial cortices and the thalamus (see Fig 4).

In 14-day-old rats, TUNEL- and silver-positive cells were found ipsilaterally in the frontal, parietal, cingulate, and retrosplenial cortices (see Fig 4).

In 30-day-old rats, no distant lesions were detected at the time points studied when the force of 160 g-cm was used.

In sham rats, pattern and magnitude of apoptotic neurodegeneration was similar to that in nontreated age-matched rats, indicating that anesthesia and surgery by themselves did not trigger apoptotic neuronal death.

MODIFIED MECHANICAL FORCE. Distribution patterns of degenerating cells were similar when the mechanical force was modified; however, severity of apoptotic cell death was less pronounced at the age of 3 days. In 30-day-old rats, isolated degenerating cells were detected within the CA3 hippocampal region by silver staining at 24 hours after trauma.

AGE-DEPENDENT SEVERITY OF APOPTOTIC DAMAGE. When the same force of 160 g-cm was used to traumatize pups of all age groups, severity of apoptotic cell death was highest in 3-day-old rats and decreased significantly with increasing age (Fig 5A). Even when the force was adjusted (see Table 1) to achieve the same pressure/brain weight ratios in all age groups, distant apoptotic damage in older animals remained minimal compared with 3- and 7-day-old rats. Under this experimental setting, 7-day-old rats were most vulnerable to distant apoptotic damage triggered by mechanical trauma (see Fig 5A).

The wave of apoptotic cell death reached a peak at 24 hours after trauma in the brains of pups in all ages studied and had subsided at 5 days after the insult (see Fig 5B).

Table 2. Numerical Densities of TUNEL-Labeled Cells

Brain Region	4 Days		8 Days	
	Sham	Trauma	Sham	Trauma
Cfr II	0.0028 ± 0.0007	0.014 ± 0.006[c]	0.0032 ± 0.0003	0.050 ± 0.008[b]
Cfr IV	0.0012 ± 0.0002	0.035 ± 0.012[b]	0.0002 ± 0.00003	0.010 ± 0.002[a]
Cpr II	0.0033 ± 0.0008	0.060 ± 0.008[c]	0.0022 ± 0.0006	0.107 ± 0.012[c]
Cpr IV	0.0006 ± 0.0001	0.040 ± 0.008[c]	0.0003 ± 0.00008	0.046 ± 0.009[c]
Cing II	0.0102 ± 0.0013	0.035 ± 0.003[c]	0.0030 ± 0.0004	0.084 ± 0.011[c]
Cing IV	0.0034 ± 0.0003	0.066 ± 0.013[b]	0.0002 ± 0.00003	0.047 ± 0.008[c]
RSC II	0.0056 ± 0.0003	0.047 ± 0.010[b]	0.0016 ± 0.0003	0.066 ± 0.006[c]
RSC IV	0.0023 ± 0.0002	0.082 ± 0.008[c]	0.0004 ± 0.00007	0.089 ± 0.006[c]
Caud	0.0044 ± 0.0007	0.014 ± 0.004[a]	0.0006 ± 0.0001	0.023 ± 0.007[b]
Dentate gyrus	0.0086 ± 0.0009	0.010 ± 0.001	0.0014 ± 0.0002	0.006 ± 0.002[a]
Mdth	0.0037 ± 0.0005	0.021 ± 0.006[a]	0.0002 ± 0.00004	0.002 ± 0.0004[c]
Ldth	0.0027 ± 0.0008	0.064 ± 0.015[c]	0.0004 ± 0.00006	0.011 ± 0.001[c]
Vth	0.0004 ± 0.0001	0.012 ± 0.003[b]	0.0001 ± 0.00003	0.004 ± 0.001[c]
Sub	0.0041 ± 0.0009	0.084 ± 0.023[c]	0.0004 ± 0.00006	0.041 ± 0.013[b]

Cells were from the frontal (Cfr), parietal (Cpr), cingulate (Cing), retrosplenial (RSC) cortex, caudate nucleus (Caud), dentate gyrus, mediodorsal (Mdth), laterodorsal (Ldth), ventral (Vth) thalamus, and subiculum (Sub) in sham-operated and traumatized rats at the ages of 4 or 8 days, ipsilateral to the trauma site. Pups were traumatized on day 3 or 7 and killed 24 hours later. Assessment of cell densities was performed in TUNEL-stained sections of the whole brain. Densities (N_v values) of apoptotic cells were determined by using an unbiased stereological optical disector technique and are shown as mean ± SEM values × $10^6/mm^3$ in 6 to 8 rats. II and IV stand for cortical layers II and IV. Densities of degenerating cells in sham-operated rats represent spontaneous apoptosis and are significantly lower than the densities of apoptotic cells in these same brain regions in rats subjected to head trauma.

[a]$p < 0.05$; [b]$p < 0.01$; [c]$p < 0.001$, Student's t test.

TUNEL = terminal deoxynucleotidyl transferase-mediated dUTP nick end-labeling.

Discussion

These results demonstrate that apoptosis plays a crucial role in the pathogenesis of traumatic brain damage in developing rats and that the threshold for triggering apoptotic cell death is much lower in younger compared with older age groups.

Our conclusion that disseminated lesions caused by head trauma in the immature rat brain are apoptotic in nature is based on the combined use of histological, molecular, and biochemical techniques. TUNEL staining enables visualization of cells with nuclear DNA fragmentation. At the time points studied after trauma, degenerating cells in the infant rat brain displayed DNA fragmentation. Histological data are consistent with oligonucleosomal assays, which revealed profound DNA cleavage in the same brain regions.

Because, however, some forms of excitotoxic cell death may also lead to DNA fragmentation,[70] TUNEL may only be used to map apoptotic cell death after apoptotic morphology has been confirmed ultrastructurally. For that reason we analyzed cells degenerating in a delayed fashion in the infant rat brain after trauma by electron microscopy and found that these cells display morphological features consistent with apoptosis. Further support is provided by profound increases of CPP 32-like activity and up-regulation of c-jun in conjunction with down-regulation of bcl-2 mRNA levels in affected brain regions.

Why the same traumatic insult that triggers no detectable apoptotic cell death in the 30-day-old rat brain gives rise to a massive, disseminated apoptotic response in infant rats is unclear. Certainly age-specific differences in the degree of myelination and brain water content will allow traumatic forces to transmit the easier to deeper brain structures the more immature the brain is at the time of injury. Our data suggest that increased transcription of c-jun and decreased transcription of bcl-2 occur very rapidly (within 1 hour) after trauma and may therefore contribute to this process. Up-regulation of c-jun contributes to tissue repair after axonal injury, provided appropriate levels of anti-apoptotic genes are maintained.[42] The combination of c-jun overexpression and bcl-2 down-regulation, however, is potentially lethal.[42] In the adult central nervous system, up-regulation of bcl-2 expression has been reported to occur in the context of traumatic brain[11] and spinal cord injury[53] and appears to represent one mechanism by which damaged cells manage to survive after trauma.[11] In transgenic bcl-2–overexpressing mice subjected to optic nerve transection, most retinal ganglion cells survived, whereas most axotomized retinal ganglion cells degenerated in an apoptotic fashion in wild-type mice.[49] Failure to maintain appropriate levels of bcl-2 in the traumatized immature rat brain may represent one potential mechanism to explain its remarkable susceptibility to apoptotic neurodegeneration. A similar reduction of bcl-2 mRNA expression was observed in association with apoptotic neurodegeneration

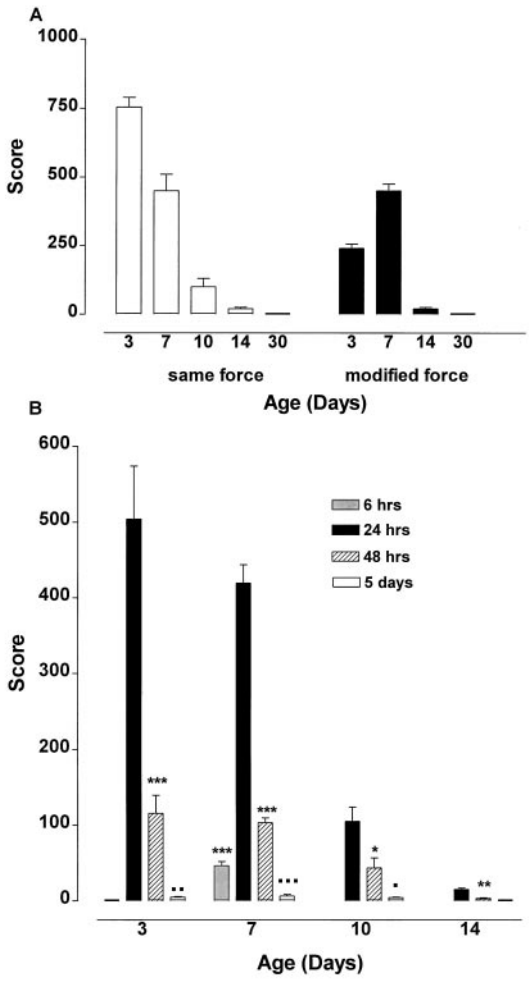

Fig 5. (A) Severity of posttraumatic apoptotic cell death in relation to age. Quantitation of damage was performed by means of the stereological optical disector in sections stained by the TUNEL method. Each region was given a score 1 for every 1,000 degenerating cells/mm^3 (1,000 cells/mm^3 = 1), and the scores from 14 regions ipsilateral and 14 regions contralateral to the trauma were added to give a cumulative severity score for the brain. Depicted are mean scores ± SEM values from 5 to 9 rats. Open columns *represent mean scores from rats traumatized with the same mechanical force.* Black columns *represent mean scores from rats that were traumatized by using the same pressure/brain weight ratio in all age groups (see Table 1). In both groups, severity of apoptotic damage at 24 hours after trauma was significantly* ($p < 0.001$; *Student's* t *test) higher in 3- and 7-day-old rats compared with 10-, 14-, or 30-day-old animals. (B) Time course of apoptotic cell death after head trauma in different age groups. Morphological analysis was performed by means of the stereological optical dissector in sections stained by the DeOlmos cupric silver method. Rats were given a cumulative severity score for apoptotic damage, as described in A. Depicted are mean scores ± SEM values from 5 to 7 rats. Brains were analyzed at 24 or 48 hours or 5 days after trauma, and in 7-day-old rats also at 6 hours after trauma. Apoptotic cell death in all ages studied showed a maximum at 24 hours after trauma.* (*$p < 0.05$; ***$p < 0.001$, *compared with 24 hours;* ·$p < 0.05$; ··$p < 0.01$; ···$p < 0.001$, *compared with 48 hours; Student's* t *test*).

in the fetal rat brain after γ-radiation.[71] It remains a goal for future studies to clarify which factors lead to these changes in the infant rat brain (eg, intracellular and extracellular ionic shifts, release of death factors, oxidative stress, and axonal dysfunction and resulting lack of trophic support). These mechanisms can trigger c-jun phosphorylation and increased c-jun transcription. Important in this respect is the observation that up-regulation of c-jun mRNA occurred rapidly (within 1 hour) after trauma, making its induction via growth factor deprivation unlikely. In sympathetic neurons, growth factor deprivation leads to detectable increase of Jun kinase (JNK) activity, the earliest at 6 to 8 hours after deprivation.[72] Oxidative stress or release of death factors (Fas-L and tumor necrosis factor) may contribute to rapid JNK activation and c-jun transcription. In support of this hypothesis, the radical scavenger 2-sulfo-α-phenyl-*N*-tert-butylnitrone, the antioxidant *N*-acetylcysteine, and the tumor necrosis factor inhibitor pentoxifylline elicit a protective effect in the infant rat trauma model.[73]

It is noteworthy that the infant rat brain is most sensitive to apoptotic neurodegeneration after trauma during the *N*-methyl-D-aspartate (NMDA) receptor hypersensitivity period,[74,75] with peak vulnerability on postnatal day 7. This exactly coincides with the age at which the infant rat brain is most sensitive to NMDA excitotoxicity. In view of reports that NMDA receptor stimulation may trigger both excitotoxic and apoptotic neurodegeneration depending on intensity of stimulation,[76] the question arises as to whether endogenous glutamate, acting on NMDA receptors, may be mediating apoptosis after trauma in infant rats. However, while attempting to block this apoptotic response with NMDA antagonists, we observed an unexpected potentiating effect[77] indicating that, if NMDA receptors are mechanistically involved in this process, they are rather playing a protective role.

Our results are in accordance with reports showing that apoptosis occurs in the context of traumatic brain and spinal cord injury in rodents and primates.[32–34,78–80] Colicos and Dash[78] reported that dentate granule cells of adult rats exhibit apoptotic morphology after experimental cortical injury. Numbers of apoptotic cells were highest at 24 hours after trauma, the time point at which we also found the apoptotic response to have reached its maximum in infant and juvenile rats. Apoptosis has also been documented in traumatized spinal cord tissue of rodents and primates[9,79,80] with a peak at 24 hours after trauma.[80] Activation of CPP 32-like caspases appears to play a critical role in apoptotic cell deletion after trauma to the immature brain. In contrast to the adult brain, however, CPP 32-like proteolytic activity rises not just up to 130%, as described in a study by Yakovlev and associates,[34] but up to 2,830% of control

values. Together with our histological data, this highlights a novel aspect of our findings, which is the disproportionately large magnitude of the apoptosis contribution to posttraumatic brain damage in the immature brain. By using combined optical dissector stereology and volumetry, we calculated that in the brains of 7-day-old rats subjected to head trauma 2.7 ± 0.5 million cells (n = 9) were dying an apoptotic death in the brain at 24 hours after trauma as opposed to 16,400 ± 2,435 cells (n = 12) dying an excitotoxic death at 4 hours after trauma. Because apoptotic cells can be detected histologically for a few hours (clearance time, 2 hours and 20 minutes)[81] and apoptosis is occurring in the infant rat brain for several days after trauma, the numbers of cells eventually deleted by this mechanism are much higher.

It is noteworthy that, at a given age, the highest densities of apoptotic cells after trauma were detected in areas that also displayed the highest densities of cells undergoing physiological (programmed) death (see Table 2). This possibly indicates that neurons and glia may be most vulnerable to die via apoptosis when exposed to an exogenous insult during a certain period of their maturation and differentiation process. It has been proposed that the ratio of proapoptotic versus antiapoptotic factors within a cell primarily determines its vulnerability and likelihood to undergo programmed cell death.[44,82] Thus, the ontogenetically regulated expression of potential proapoptotic factors early in development, such as c-jun, c-fos, and p53,[83] which, under physiological conditions, promote differentiation of immature neurons and glia may, under pathological circumstances, predispose these same cells to undergo suicide. P53, for example, promotes cell differentiation but initiates apoptotic deletion after irradiation.[71,84,85] Progressive axonal injury and secondary axotomy after trauma may be an additional mechanism that promotes neuronal apoptosis, caused by deafferentiation and loss of trophic support.[86]

Considering the magnitude to which apoptosis contributes to posttraumatic brain damage in the young, development of an antiapoptotic regimen to treat pediatric head trauma appears to be a very reasonable goal for future research.

Supported by BMBF grant 01KO95151TPA3.

References

1. Diamond PT. Brain injury in the Commonwealth of Virginia: an analysis of Central Registry data 1988-1993. Brain Injury 1996;10:413–419
2. Adelson PD, Kochanek PM. Head injury in children. J Child Neurol 1998;13:2–15
3. Brink JD, Garrett AL, Hale WR, et al. Recovery of motor and intellectual function in children sustaining severe head injuries. Dev Med Child Neurol 1970;12:565–571
4. Levin HS, Eisenberg HM, Wigg NE, Kobayashi K. Memory and intellectual ability after head injury in children and adolescents. Neurosurgery 1982;11:668–673
5. Koskiniemi M, Kyykka T, Nybo T, Jarho L. Long-term outcome after severe brain injury in preschoolers is worse than expected. Arch Pediatr Adolesc Med 1995;149:249–254
6. Mahoney WJ, D'Souza BJ, Haller A, et al. Long-term outcome of children with severe head trauma and prolonged coma. Pediatrics 1983;71:756–762
7. Adams JH. Head injury. In: Adams JH, Duchen LW, eds. Greenfield's neuropathology. London: Arnold, 1992:106–152
8. Colicos MA, Dixon CE, Dash PK. Delayed, selective neuronal death following experimental cortical impact injury in rats: possible role in memory deficits. Brain Res 1996;739:111–119
9. Crowe MJ, Bresnahan JC, Shuman SL, et al. Apoptosis and delayed degeneration after spinal cord injury in rats and monkeys. Nat Med 1997;3:73–76
10. Stein SC, Spettell CM. Delayed and progressive brain injury in children and adolescents with head trauma. Pediatr Neurosurg 1995;23:299–304
11. Clark RS, Chen J, Watkins SC, et al. Apoptosis-suppressor gene bcl-2 expression after traumatic brain injury in rats. J Neurosci 1997;17:9172–9182
12. Conti AC, Raghupathi R, Trojanowski JQ, et al. Experimental brain injury induces regionally distinct apoptosis during the acute and delayed post-traumatic period. J Neurosci 1998;18:5663–5672
13. Faden AI, Demediuk P, Panter SS, Vink R. The role of excitatory amino acids and NMDA receptors in traumatic brain injury. Science 1989;44:798–800
14. Faden AI, Simon RP. A potential role for excitotoxins in the pathophysiology of spinal cord injury. Ann Neurol 1988;23:623–626
15. Belluardo N, Mudo G, Dell'Albani P, et al. NMDA receptor-dependent and -independent immediate early gene expression induced by focal mechanical brain injury. Neurochemistry 1996;26:443–453
16. Golding EM, Vink R. Efficacy of competitive vs noncompetitive blockade of the NMDA channel following traumatic brain injury. Mol Chem Neuropathol 1995;24:137–150
17. Hayes RL, Jenkins LW, Lyeth BG, et al. Pretreatment with phencyclidine, an *N*-methyl-D-aspartate antagonist, attenuates long-term behavioral deficits in the rat produced by traumatic brain injury. J Neurotrauma 1988;5:259–274
18. Katoh H, Sima K, Nawashiro H, et al. The effect of MK-801 on extracellular neuroactive amino acids in hippocampus after closed head injury followed by hypoxia in rat. Brain Res 1997;758:153–162
19. Kroppenstedt S-N, Schneider G-H, Thomale U-W, Unterberg AW. Protective effects of aptiganel HCl (Cerestat) following controlled cortical impact injury in the rat. J Neurotrauma 1998;15:191–197
20. McIntosh TK, Smith DH, Voddi M, et al. Riluzole, a novel neuroprotective agent, attenuates both neurologic motor and cognitive dysfunction following experimental brain injury in the rat. J Neurotrauma 1996;13:767–780
21. McIntosh TK, Vink R, Soares HD, et al. Effects of noncompetitive blockade of *N*-methyl-D-aspartate receptors on the neurochemical sequelae of experimental brain injury. J Neurochem 1990;55:1170–1179
22. McIntosh TK, Vink R, Yamakami I, Faden AI. Magnesium deficiency exacerbates and pretreatment improves outcome following traumatic brain injury in rats: ^{31}P magnetic resonance spectroscopy and behavioral studies. J Neurotrauma 1988;5:17–31
23. Okiyama K, Smith DH, White WF, McIntosh TK. Effects of the NMDA antagonist CP-98,113 on regional cerebral edema

and cardiovascular, cognitive, and neurobehavioral function following experimental brain injury in the rat. Brain Res 1998; 792:291–298
24. Okiyama K, Smith DH, White WF, et al. Effects of the novel NMDA antagonists CP-98,113, CP-101,581, and CP-101,606 on cognitive function and regional cerebral edema following experimental brain injury in the rat. J Neurotrauma 1997;14: 211–222
25. Panter SS, Faden AI. Pretreatment with the NMDA antagonists limits release of excitatory amino acids following traumatic brain injury. Neurosci Lett 1992;136:165–168
26. Phillips LL, Lyeth BG, Hamm RJ, et al. Effect of prior receptor antagonism on behavioral morbidity produced by combined fluid percussion injury and entorhinal cortical lesion. J Neurosci Res 1997;49:197–206
27. Shapira Y, Yadid G, Cotev S, et al. Protective effect of MK-801 in experimental brain injury. J Neurotrauma 1990;7:131–139
28. Toulmond S, Serrano A, Benavides J, Scatton B. Prevention by eliprodil (SL 82.0715) of traumatic brain damage in the rat. Existence of a large (18 h) therapeutic window. Brain Res 1993; 620:32–41
29. Wrathall JR, Choiniere D, Teng YD. Dose-dependent reduction of tissue loss and functional impairment after spinal cord trauma with the AMPA/kainate antagonist NBQX. J Neurosci 1994;14:6598–6607
30. McIntosh TK, Juhler M, Wieloch T. Novel pharmacologic strategies in the treatment of experimental traumatic brain injury: 1998. J Neurotrauma 1998;15:731–769
31. Linnik MD. Role of apoptosis in acute neurodegenerative disorders. Restor Neurol Neurosci 1996;9:219–225
32. Rink A, Trojanowski JQ, Lee VM, et al. Evidence of apoptotic cell death after experimental traumatic brain injury in the rat. Am J Pathol 1995;147:1575–1583
33. Shah PT, Yoon KW, Xu XM, Broder LD. Apoptosis mediates cell death following traumatic injury in rat hippocampal neurons. Neuroscience 1997;79:999–1004
34. Yakovlev AG, Knoblach SM, Fan L, et al. Activation of CPP32-like caspases contributes to neuronal apoptosis and neurological dysfunction after traumatic brain injury. J Neurosci 1997;17:7415–7424
35. Kerr JFR, Wyllie AH, Currie AR. Apoptosis: a basic biological phenomenon with wide-ranging implications in tissue kinetics. Br J Cancer 1972;26:239–257
36. Olney JW, Adamo NJ, Ratner A. Monosodium glutamate effects. Science 1971;172:294–295
37. Bursch W, Kleine L, Tenniswood M. The biochemistry of cell death by apoptosis. Biochem Cell Biol 1990;68:1071–1074
38. Cohen JJ. Apoptosis. Immunol Today 1993;14:126–130
39. Compton MM. A biochemical hallmark of apoptosis: internucleosomal degradation of the genome. Cancer Metastasis Rev 1992;11:105–119
40. Wyllie AH, Kerr JFR, Currie AR. Cell death: the significance of apoptosis. Int Rev Cytol 1980;68:251–306
41. Bossy-Wetzel E, Bakiri L, Yaniv M. Induction of apoptosis by the transcription factor c-jun. EMBO J 1997;16:1695–1709
42. Herdegen T, Skene P, Baehr M. The c-jun transcription factor—bipotential mediator of neuronal death, survival and regeneration. Trends Neurol Sci 1997;20:227–231
43. Jacobson MD, Raff MC. Programmed cell death and Bcl-2 protection in very low oxygen. Nature 1995;374:814–816
44. Kroemer G. The proto-oncogene Bcl-2 and its role in regulating apoptosis. Nat Med 1997;3:614–620
45. Mattson MP, Furukawa K. Programmed cell life: anti-apoptotic signaling and therapeutic strategies for neurodegenerative disorders. Restor Neurol Neurosci 1996;9:191–205
46. Reed J. Double identity of proteins of the Bcl-2 family. Nature 1997;387:773–776
47. Shimizu S, Eguchi Y, Kosaka H, et al. Prevention of hypoxia-induced cell death by Bcl-2 and Bcl-xL. Nature 1995;374:811–813
48. Zhong LT, Sarafian T, Kane DJ, et al. *bcl-2* inhibits death of central neural cells induced by multiple agents. Proc Natl Acad Sci USA 1993;90:4533–4537
49. Porciatti V, Pizzorusso T, Cenni MC, Maffei L. The visual response of retinal ganglion cells is not altered by optic nerve transection in transgenic mice overexpressing Bcl-2. Proc Natl Acad Sci USA 1996;93:14955–14959
50. Raghupathi R, Welsh FA, Lowenstein DH, et al. Regional induction of c-fos and heat shock protein-72 mRNA following fluid-percussion brain injury in the rat. J Cereb Blood Flow Metab 1995;15:467–473
51. Raghupathi R, Grants I, Rosenberg LJ, et al. Increased jun immunoreactivity in an in vitro model of mammalian spinal neuron physical injury. J Neurotrauma 1998;15:555–561
52. Pravdenkova SV, Basnakian AG, James SJ, Andersen BJ. DNA fragmentation and nuclear endonuclease activity in rat brain after severe closed head injury. Brain Res 1996;729:151–155
53. Li GL, Brodin G, Farooque M, et al. Apoptosis and expression of Bcl-2 after compression trauma to rat spinal cord. J Neuropathol Exp Neurol 1996;55:280–289
54. Thornberry NA, Lazebnik Y. Caspases: enemies within. Science 1998;281:1312–1316
55. Prins ML, Lee SM, Cheng CL, et al. Fluid percussion brain injury in the developing and adult rat: a comparative study of mortality, morphology, intracranial pressure and mean arterial blood pressure. Dev Brain Res 1996;95:272–282
56. Prins ML, Hovda D. Traumatic brain Injury in the developing rat: effects of maturation on Morris Water Maze Acquisition. J Neurotrauma 1998;15:799–811
57. Adelson PD, Robichaud P, Hamilton RL, Kochanek PM. A model of diffuse traumatic brain injury in the immature rat. J Neurosurg 1996;85:877–884
58. Adelson PD, Dixon CE, Robichaud P, Kochanek PM. Motor and cognitive deficits following diffuse traumatic brain injury in the immature rat. J Neurotrauma 1997;14:99–108
59. Marmarou A, Abd-Elfattah Foda MA, van den Brink W, et al. A new model of diffuse brain injury in rats. Part I: Pathophysiology and biomechanics. J Neurosurg 1994;80:291–300
60. Allen AR. Surgery of experimental lesion of spinal cord equivalent to crush injury of fracture dislocation of spinal column. JAMA 1911;57:878–880
61. Feeney DM, Boyeson MG, Linn RT, et al. Responses to cortical injury: I. Methodology and local effects of contusions in the rat. Brain Res 1981;211:67–77
62. Ikonomidou C, Quin Y, Labruyere J, et al. Prevention of trauma-induced neurodegeneration in infant rat brain. Pediatr Res 1996;39:1020–1027
63. Sherwood NM, Timiras PS. A stereotaxic atlas of the developing rat brain. Berkeley: University of California Press, 1970
64. DeOlmos JS, Ingram WR. An improved cupric-silver method for impregnation of axonal and terminal degeneration. Brain Res 1971;33:523–529
65. Ikonomidou C, Bosch F, Miksa M, et al. Blockade of NMDA receptors and apoptotic neurodegeneration in the developing brain. Science 1999;283:70–74
66. Corso TD, Sesma MA, Tenkova TI, et al. Multifocal brain damage induced by phencyclidine is augmented by pilocarpine. Brain Res 1997;752:1–14
67. West MJ, Gundersen HJG. Unbiased stereological estimation of the number of neurons in the human hippocampus. J Comp Neurol 1990;296:1–22
68. Chomczynski P, Sacchi N. Single-step method of RNA isolation by acid guanidinium thiocyanate-phenol-chloroform extraction. Anal Biochem 1987;162:156–159

69. Lohmann J, Schickle H, Bosch TC. REN display, a rapid and efficient method for nonradioactive differential display and mRNA isolation. Biotechniques 1995;18:200–202
70. Ishimaru MJ, Ikonomidou C, Dikranian K, Olney JW. CNS apoptosis: how shall it be defined and recognized? Soc Neurosci Abstr 1997;23:895 (Abstract)
71. Borovitskaya AE, Evtushenko VI, Sabol SL. Gamma-radiation-induced cell death in the fetal rat brain possesses molecular characteristics of apoptosis and is associated with specific messenger RNA elevations. Mol Brain Res 1996;35:19–30
72. Eilers A, Whitfield J, Babij C, et al. Role of Jun kinase pathway in the regulation of c-Jun expression and apoptosis in sympathetic neurons. J Neurosci 1998;18:1713–1724
73. Bittigau P, Pohl D, Fuhr S, et al. Pharmacotherapy of secondary traumatic lesions in the immature rat brain. Soc Neurosci Abstr 1998;24:1728 (Abstract)
74. McDonald JW, Silverstein FS, Johnston MV. Neurotoxicity of *N*-methyl-D-aspartate is markedly enhanced in developing rat central nervous system. Brain Res 1988;459:200–203
75. Ikonomidou C, Mosinger JL, Salles KS, et al. Sensitivity of the developing rat brain to hypobaric/ischemic damage parallels sensitivity to *N*-methyl-aspartate neurotoxicity. J Neurosci 1989;9:2809–2818
76. Bonfoco E, Krainc D, Ankarcrona M, et al. Apoptosis and necrosis: two distinct events induced, respectively, by mild and intense insults with *N*-methyl-D-aspartate or nitric oxide/superoxide in cortical cell cultures. Proc Natl Acad Sci USA 1995;92:7162–7166
77. Pohl D, Bittigau P, Lang D, et al. Delayed posttraumatic degeneration is potentiated by NMDA receptor antagonists in the infant rat brain. Soc Neurosci Abstr 1997;23:1123 (Abstract)
78. Colicos MA, Dash PK. Apoptotic morphology of dentate gyrus granule cells following experimental cortical impact injury in rats: possible role in spatial memory deficits. Brain Res 1996;739:120–131
79. Katoh K, Ikatah T, Katoh S, et al. Induction and its spread of apoptosis in rat spinal cord after mechanical trauma. Neurosci Lett 1996;216:9–12
80. Liu XZ, Xu XM, Hu R, et al. Neuronal and glial apoptosis after traumatic spinal cord injury. J Neurosci 1997;17:5395–5406
81. Thomaidou D, Mione MC, Cavanagh JFR, Parnavelas JG. Apoptosis and its relation to the cell cycle in the developing cerebral cortex. J Neurosci 1997;17:1075–1085
82. Barinaga M. Forging a path to cell death. Science 1996;273:735–737
83. Ferrer I, Olivé M, Ribera J, Planas AM. Naturally occurring (programmed) and radiation-induced apoptosis are associated with selective c-jun expression in the developing rat brain. Eur J Neurosci 1996;8:1286–1298
84. Almog N, Rotter V. Involvement of p53 in cell differentiation and development. Biochim Biophys Acta 1997;1333:F1–F27
85. Norimura T, Nomoto S, Katsuki M, et al. *p53*-dependent apoptosis suppresses radiation-induced teratogenesis. Nat Med 1996;2:577–580
86. Maxwell WL, Povlishock JT, Graham DL. A mechanistic analysis of nondisruptive axonal injury: a review. J Neurotrauma 1997;14:419–440

F.P. Graham Publishing Co.

Neuropathological and Biochemical Features of Traumatic Injury in the Developing Brain

PETRA BITTIGAU[a], MARCO SIFRINGER[a], URSULA FELDERHOFF-MUESER[b], HENRIK H. HANSEN[a,c] and CHRYSANTHY IKONOMIDOU[a,*]

[a]*Departments of Pediatric Neurology and* [b]*Neonatology, Charité Children's Hospital, Humboldt University, Augustenburger Platz 1, 13353 Berlin, Germany;* [c]*Department of Pharmacology, The Danish University of Pharmaceutical Sciences, DK-2100, Copenhagen, Denmark. hrissanthi.ikonomidou@charite.de*

(Received 19 August 2003; Revised 26 September 2003; In final form 26 September 2003)

Trauma to the developing brain constitutes a poorly explored field. Some recent studies attempting to model and study pediatric head trauma, the leading cause of death and disability in the pediatric population, revealed interesting aspects and potential targets for future research.

Trauma triggers both excitotoxic and apoptotic neurodegeneration in the developing rat brain. Excitotoxic neurodegeneration develops and subsides rapidly (within hours) whereas apoptotic cell death occurs in a delayed fashion over several days following the initial traumatic insult. Apoptotic neurodegeneration contributes in an age-dependent fashion to neuronal injury following head trauma, with the immature brain being exceedingly sensitive. In the most vulnerable ages the apoptosis contribution to the extent of traumatic brain damage far outweighs that of the excitotoxic component.

Molecular and biochemical studies indicate that both extrinsic and intrinsic mechanisms are involved in pathogenesis of apoptotic cell death following trauma. Interestingly, in infant rats a pancaspase inhibitor ameliorated apoptotic neurodegeneration with a therapeutic time window of up to 8 h after trauma.

These results help explain unfavorable outcomes of very young pediatric head trauma patients and imply that regimen which target slow active forms of cell death may comprise a successful neuroprotective approach.

Key words: Apoptosis; Excitotoxicity; Neuroprotection

INTRODUCTION

Traumatic brain injury (TBI) constitutes a major cause of morbidity and mortality in the industrialized world (Goldstein, 1990; Sosin *et al.*, 1995; Thurman *et al.*, 1999). According to the National Center for Injury Prevention and Control, an estimated 1.5 million Americans sustain TBI each year. As a result, 50,000 people die, 230,000 are hospitalized and survive and an estimated 80,000-90,000 people experience the onset of long-term disability every year (Thurman *et al.*, 1999). A large proportion of TBI patients are never hospitalized but may suffer varying degrees of cognitive impairment, behavioral and personality changes, irritability, post-traumatic vertigo, sleep disturbances, attentional deficits and headaches.

Although children under six years of age sustain TBI more frequently than any other age group (Adelson and Kochanek, 1998; Diamond, 1996), there has been limited research focusing on traumatic injury to the developing brain. The assumption that pathophysiology of TBI is identical in the adult and developing central nervous system is incorrect. Clinical studies suggest that age decidedly influences both morbidity and mortality after head injury in children, with those under 4 years of age showing the worst outcomes (Mahoney *et al.*, 1983; Koskiniemi *et al.*, 1995; Adelson and Kochanek, 1998). A study by Koskiniemi and colleagues (1995) demonstrated that in a cohort of children suffering severe head injury prior to the age of 4 years none was able to work independently outside a structured environment years later. Children older than 4 years at the time of injury had a significantly better outcome. Differences in the mechanisms by which TBI

*Corresponding author. Tel: +49-30-450566103; Fax: +49-30-450566920; E-Mail: hrissanthi.ikonomidou@charite.de
ISSN 1029 8428 print/ ISSN 1476-3524 online.

was sustained and the higher incidence of non-accidental closed head traumata in the very young (Kraus *et al.*, 1987; James, 1999) may partly account for these findings. Nevertheless, it is important to consider whether the developing brain may be more vulnerable to suffering irreversible neuronal loss and/or axonal injury and, if so, what mechanisms may be involved.

In this review we will first summarize recent clinical, neuropathological and biochemical data pertaining to TBI in infants, toddlers and young children. Then we will present own experimental work on TBI in the developing rat brain with focus on cellular injury and the involved pathomechanisms.

CLINICAL AND NEUROPATHOLOGICAL FEATURES OF TBI IN INFANTS AND CHILDREN

People under the age of 18 years constitute the majority of victims of TBI. In children there are two peak periods of incidence: early childhood (less than 5 years of age) and mid-to-late adolescence (Luerssen *et al.*, 1988). Ten to 15% of children with head trauma suffer severe head injury with the majority of survivors having permanent deficits.

TBI can be grouped into different types, depending on the mechanism of injury: focal versus diffuse, closed head versus penetrating injuries and primary versus secondary injuries. Diffuse injuries are more common in children than focal injuries and closed head injuries account for the majority of cases in children.

Child abuse tends to occur more often in the very young (less than 4 years) and may even be the major cause of severe brain injury in this group, representing almost two-thirds of severe brain injury cases in the 0- to 4-year old range in some series. Shaken baby syndrome, which can be associated with head impact, is most common between 3 and 6 months of age (Barlow and Minns, 1993) and results in a high mortality rate (10-40%), acute neurological signs and poor neurological outcome, mental retardation, cerebral palsy, blindness, epilepsy and major behavioral problems (Oliver, 1975; Jaspan *et al.*, 1992; Bonnier *et al.*, 1995; 2002; Duhaime *et al.*, 1996; Shaver *et al.*, 1996).

Another major cause of head trauma among infants, toddlers and young children are falls. In older children, falls and assaults result in less than 20% of TBI.

Primary traumatic injury elicits a secondary response from the brain as a reaction to that injury, which is believed to contribute to the diffuse cerebral swelling and tissue damage seen following pediatric TBI. This secondary response includes loss of cerebral autoregulation, breakdown of the blood-brain barrier, intracellular and extracellular edema, and ischemic brain injury. Intracranial hypertension, ischemia and vasospasm are thought to contribute to progression of the injury. A strong association between diffuse brain swelling and hypoxemia or early hypotension has been reported (Aldrich *et al.*, 1992). The very young developing brain can be particularly susceptible to extensive damage and have a higher likelihood for worse outcome. In addition, in inflicted brain injury, the most common form of brain injury in infants and young children, the injuries tend to be multiple and diffuse.

There are few reports in the literature on neuropathology of infant head injury. In shaken baby syndrome, edema, bleeding, infarcts, white matter contusional tears, and axonal injury have been reported (Zimmerman *et al.*, 1979; Vowles *et al.*, 1987; Jaspan *et al.*, 1992; Duhaime *et al.*, 1998). In other studies, contusional tears but no axonal injury in infants were described (Lindenberg and Freytag, 1969). Neuronal eosinophilia, interpreted as hypoxic-ischemic changes, is a very common finding in one study by Shannon *et al.* (1998), in which some axonal injury was also found in infants and toddlers less than 18 months of age.

In a recent study by Geddes *et al.* (1999) the findings in the brains of a series of 37 infants aged 9 months or less, all of whom died from inflicted head injuries, and 14 control infants who died of other causes were summarized. Surprisingly, the most common histological finding was severe and widespread neuronal damage. In this particular study, widespread traumatic axonal injury was only found in association with multiple skull fractures. This is in contrast to earlier reports stating that diffuse axonal injury is one of the inevitable and devastating sequelae of shaken baby syndrome (Brown and Minns, 1993; Munger *et al.*, 1993; David, 1999). The only location where focal axonal damage was consistently found in the series by Geddes *et al.* was the craniocervical junction, the neuropathology being that of stretch injury from cervical hyperextension/flexion. The authors concluded that damage to this area could account for the observed apnea, which could in turn lead to hypoxic damage and brain swelling (Geddes *et al.*, 2001a).

Thus, head injury in infants in the series by Geddes *et al.* was shown to result primarily in neuronal damage, and to a much lesser extent in diffuse axonal injury. According to the authors, this finding could be explained in one of two ways: either the unmyelinated axon of the immature cerebral hemispheres is relatively resistant to traumatic damage, or, in shaking-type injuries, the brain is not exposed to the forces necessary to produce diffuse axonal injury (Geddes *et al.,* 2001b).

Similarly, in a series on inflicted head injury including older victims (aged 20 days to 8 years), severe hypoxic brain damage was present in 77% of the cases. Children over 1 year of age tended to have larger subdural hemorrhages than infants and, in the few cases where traumatic axonal injury was present, patterns of hemispheric white matter damage more akin to those reported in adults were found. Overall and contrary to what one might expect, diffuse axonal injury was an uncommon sequel in both infants and children with inflicted brain injury, whereas widespread neuronal damage (eosinophilia and shrinkage, interpreted as neuronal hypoxia-ischemia) was a very frequent finding (Geddes *et al.*, 2001b).

These two studies raised the assumption that there are significant differences between the pathology of non-accidental head injury in children and adults but also between children of different ages. They also support the notion that pathophysiology of TBI may show age-dependent variations and underline the need for animal models that will allow studying developmental aspects of TBI.

BIOCHEMICAL FEATURES OF TBI IN INFANTS AND CHILDREN

In a study by Bayir *et al.* (2002) antioxidant reserves and oxidative stress in cerebrospinal fluid after severe TBI were assessed in infants and children. Among the eleven studied patients in that group there were five aged 2 months to 4 years. The authors found evidence for marked and progressive compromise of antioxidant defenses and free radical mediated lipid peroxidation, suggesting that these markers could be used to assess the effect of therapies on oxidative stress in patients after TBI. They also suggested that defining the role of oxidative stress in the pathophysiology of TBI in infants and children could help with the development of novel, clinically applicable therapies.

Other biochemical markers that have been studied in children with TBI include serum and cerebrospinal fluid concentrations of S100B and neuron specific enolase (Berger *et al.*, 2002), adenosine levels in the cerebrospinal fluid (Robertson *et al.*, 2001) and concentrations of interleukins 6 and 10 (Bell *et al.*, 1997). All these parameters were found elevated following TBI. Interestingly, neuron specific enolase and S100B concentrations in the CSF of children with TBI showed a unique time course in inflicted brain injury. In this group both an early peak and a late peak of NSE and S100B concentrations were observed, the first occurring at a median of 11 hours after injury and the second one occurring at a median of 63 hours after injury. Interestingly, the group of children assigned to that group were 0.2- 1.8 years old. Such biochemical findings raise the assumption that in inflicted brain injury in infants and toddlers there appears to be a wave of early cell death occurring within hours after injury and a second wave of delayed cell death occurring days after injury, which may represent an important therapeutic target.

In a study by Clark *et al.* (2000a) increases of oligonucleosomes and the antiapoptotic protein bcl-2 in cerebrospinal fluid of infants and children after severe TBI were described. Most profound increases of oligonucleosomes were detected on the second day after trauma. Interestingly, bcl-2 levels showed a significantly higher increase in patients who survived versus those who died. The authors concluded that bcl-2 may participate in the regulation of cell death after TBI in infants and children and that the increase in bcl-2 seen in patients who survived is consistent with a protective role for this anti-apoptotic protein after TBI (Clark *et al.*, 2000a).

HOW TO MODEL PEDIATRIC HEAD TRAUMA

The developing mammalian brain undergoes a period of rapid growth, during which synaptogenesis and physiological cell death, the prototypic example of apoptosis, takes place. This brain growth spurt period begins in the human in the 6th month of pregnancy and extends up to the third year of life. In rodents, this period runs during the first three postnatal weeks, in piglets it also begins prenatally and includes the first 100 days of life. To model phenomena that take place in the developing brain of human infants, toddlers and young children, one needs to study animals during the comparable developmental period. Such experiments have been performed in rats and piglets.

Among the several models that have been developed for studying brain trauma, three have been widely used: the fluid percussion model (McIntosh *et al.*, 1989), the controlled cortical impact model (Dixon *et al.*, 1991) and the weight drop model (Feeney *et al.*, 1981).

In the fluid percussion model, rapid injection of small volumes of saline into the closed cranial cavity against the dura induces brain injury. The pressure pulse is delivered through a craniotomy lateral or central to the midline and induces a short-lasting intracranial pressure increase and tissue deformation. This model has been used in rats, rabbits, cats, pigs and mice. The neuropathology described in this model consists of cortical contusion, selective hippocampal neuronal loss, axonal

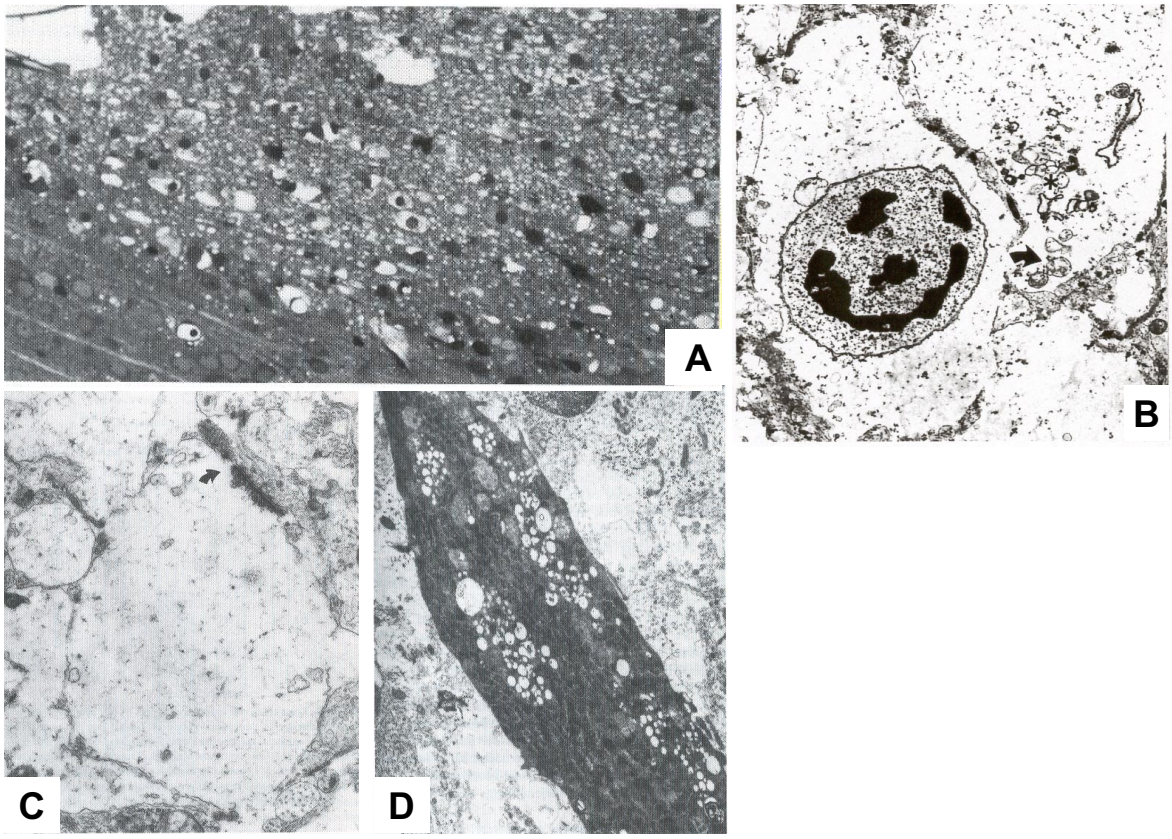

FIGURE 1 Light- and electronmicrographs depicting features of acute excitotoxic neurodegeneration following trauma to the 7 day old rat brain. (**A**) Light micrograph depicting traumatic lesion in the parietal cortex 4 h after the mechanical impact. The areas of necrosis consist of degenerating neurons with swollen cytoplasm and pyknotic nuclei (methylene blue azur II stain, X530). (**B**) Electron micrograph from the traumatized cortex of a rat pup 4 h after trauma showing an acutely degenerating neuron. The cytoplasm is massively swollen as are intracellular organelles, the endoplasmic reticulum (star) and mitochondria (arrow). The nucleus demonstrates clumps of nuclear chromatin. Magnification x6,500. (**C**) Electron micrograph taken at 2 h after trauma depicting a swollen dendrite with several areas of membrane breakdown. A presynaptic axon terminal appears intact, it contains synaptic vesicles, is of normal size and is forming an axodendritic synapse with the degenerating dendrite (arrow). Degeneration of dendritic elements with preservation of presynaptic axons is a typical feature of excitotoxic lesions. Magnification x9,000. (**D**) Pyramidal neuron undergoing dark cell degeneration 2 h after mechanical trauma. The cytoplasm is condensed and contains several vacuoles. Magnification x14,000.

injury and regional cerebral edema.

In the controlled cortical impact model, a pneumatically driven piston directly impacts the animal´s brain through a craniotomy positioned lateral or central to the midline. This model has been described in adult rats and mice. Tissue deformations can be well controlled by adjusting the depth and velocity of impact, which produces a cortical contusion, hippocampal cell loss and cognitive dysfunction.

In the weight drop model, injury is produced by a metal rod which falls through a guide tube onto the animal´s skull or the exposed brain. Weight and height of the rod determine injury severity. In this model, as in the other two, a cortical contusion, hippocampal cell loss and cognitive dysfunction are produced.

Attempts to model pediatric head trauma were initially made by Prins and Hovda (Prins *et al.*, 1996; Prins and Hovda, 1998) and Adelson and colleagues (Adelson *et al.*, 1996; 1997) who adopted the lateral fluid percussion and the closed head injury model, initially described by Marmarou and colleagues (Marmarou *et al.*, 1994), to 17-day-old rats.

Our group studied the response of the rat brain to head trauma in even earlier developmental stages in an attempt to examine mechanisms that contribute to unfavorable outcomes of very young pediatric patients to head trauma. For that purpose, a model using the weight drop device described by Allen for the spinal cord (Allen, 1911) and by Feeney for the brain (Feeney *et al.*, 1981) was developed. In the following we will

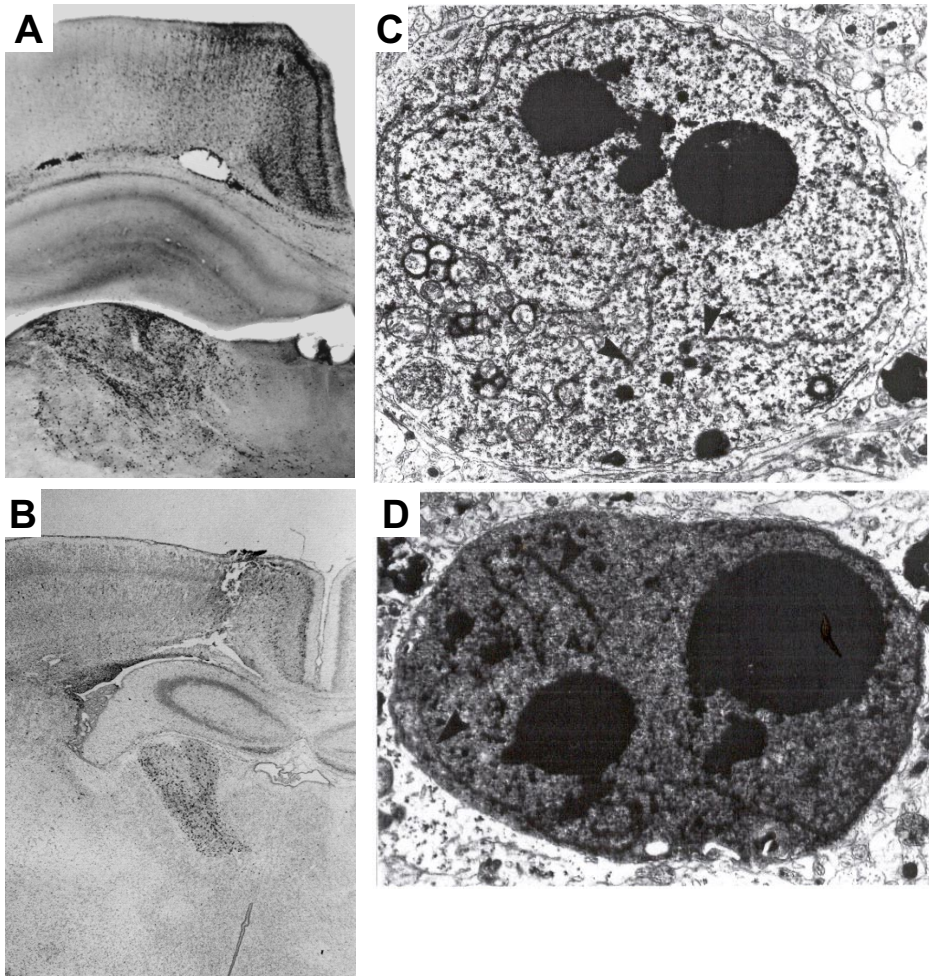

FIGURE 2 Light- and electronmicrographs depicting features of delayed apoptotic neurodegeneration following trauma to the 7 day old rat brain. Silver-positive (**A**, DeOlmos cupric silver staining) and TUNEL-positive (**B**) cells in the brains of 8 day old rats subjected to head trauma on day 7. (**C, D**) Electron microscopic evaluation of the cingulate cortex 16 h after parietal trauma reveals that the type and sequence of morphological changes meet the classical criteria for apoptosis and are identical to the changes in neurons undergoing physiological cell death in the developing brain. The neuron in **C** is showing very early signs of apoptotic cell death which consist of the formation of electron dense spherical chromatin masses in the nucleus and a discontinuity in the nuclear membrane (arrow heads). In this early stage cytoplasmic organelles appear essentially normal. As the apoptotic process evolves (**D**), the nuclear membrane decomposes into fragments (arrow heads), the contents of the nucleoplasm and cytoplasm freely intermix and the entire cell becomes uniformly condensed. In later stages, apoptotic bodies are formed and these are extruded into the neuropil (not shown). Finally, both the main cell mass and the apoptotic bodies are transformed into shrunken amorphous masses of debris and are phagocytized. Magnifications: **C**, x10,500; **D**, x9,750.

review neuropathological and biochemical data we obtained using this head trauma model in developing rats.

NEUROPATHOLOGICAL FINDINGS IN TBI IN THE DEVELOPING BRAIN

Using the weight drop device initially in 7 day old rats, we found that mechanical trauma to the immature brain causes an acute excitotoxic lesion within the area of impact which rapidly expands within 4 h after trauma (Ikonomidou et. al., 1996) (FIG. 1). This local excitotoxic response is followed by disseminated cell death affecting many brain regions ipsi- and contralateral to the trauma site, which is detected by means of DeOlmos silver staining (DeOlmos and Ingram, 1971) and TUNEL staining for a period of hours after the excitotoxic degeneration has run its course (FIG. 2). Delayed cell death is detected in frontal, parietal, cingulate and retrosplenial cortices, laterodorsal, mediodorsal and ventral thalamic nuclei, hippocampal dentate gyrus, subiculum and striatum (Bittigau *et al.*, 1999; Pohl *et al.*, 1999).

Examination of histological sections by TUNEL staining revealed that TUNEL positive cells displayed a similar distribution pattern. By morphometric analysis, densities of silver positive- and TUNEL-positive cells obtained from parallel sections within affected brain areas did not significantly differ from each other. Thus, cells which degenerated in a delayed fashion after head

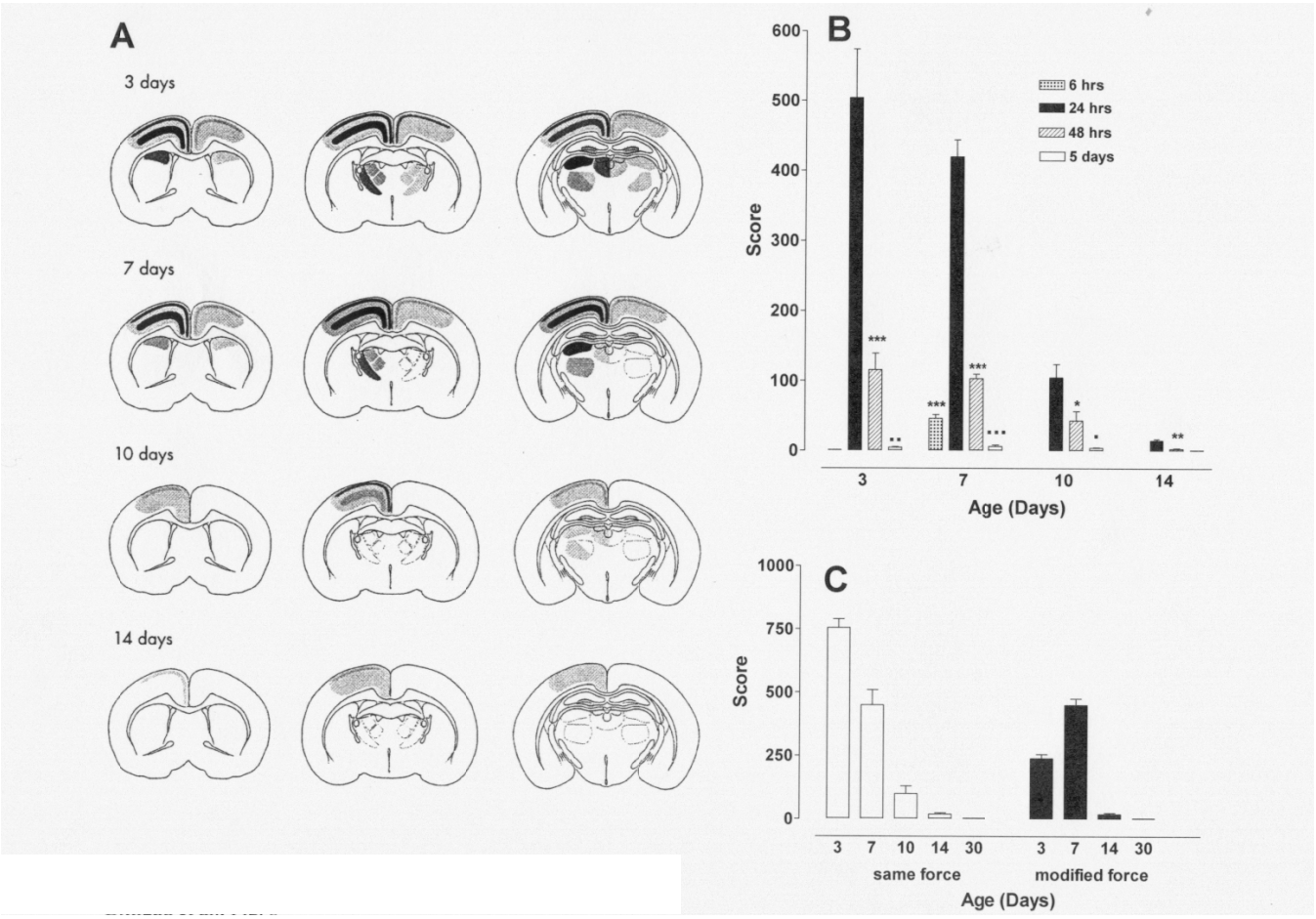

FIGURE 3 (**A**) Schematic illustration depicting the distribution patterns of TUNEL positive cells (shaded areas) in different age groups at 24 h after trauma. Darker tones indicate higher densities of degenerating cells. Rats were traumatized on postnatal days 3, 7, 10, 14 and 30. (**B**) Time course of apoptotic cell death following head trauma in different age groups. Morphological analysis was performed by means of the stereological optical dissector in sections stained with the DeOlmos cupric silver method. Rats were given a cumulative severity score for apoptotic damage. Depicted are mean scores ± SEM from 5-7 rats. Brains were analysed at 24, 48 h or 5 days after trauma, in 7 day old rats also at 6 h after trauma. Apoptotic cell death in all ages studied showed a maximum at 24 h after trauma. (**P* <0.05, ****P* <0.001 compared to 24 h; •*P* <0.05, ••*P* <0.01, •••*P* <0.001 compared to 48 h; Student´s *t* test). (**B**) Severity of posttraumatic apoptotic cell death in relation to age. Quantitation of damage was performed by means of the stereological optical dissector in sections stained with the TUNEL method. Each region was given a score 1 for every 1000 degenerating cells/mm^3 (1000 cells mm^3=1) and the scores from 14 regions ipsilateral and 14 regions contralateral to the trauma were added to give a cumulative severity score for the brain. Depicted are mean scores ± SEM from 5-9 rats. Open bars represent mean scores from rats traumatized with the same mechanical force. Black bars represent mean scores from rats which were traumatized using the same pressure/brain weight ratio in all age groups. In both groups, severity of apoptotic damage at 24 h after trauma was significantly (*P* <0.001; Student´s *t* test) higher in 3 and 7 day old rats as compared to 10, 14 or 30 day old animals.

trauma in the 7 day old rat brain displayed nuclear DNA-fragmentation (Bittigau *et al.*, 1999).

To confirm the apoptotic nature of this delayed degenerative reaction to trauma in the 7 day old rat brain, and taking into account that degenerating neurons dying by a non-apoptotic process can also show TUNEL positivity (Ishimaru *et al.*, 1999), large numbers of degenerating cells were examined by electron microscopy. In all regions examined (frontoparietal and cingulate/retrosplenial cortices, thalamus, caudate nucleus), the cells undergoing delayed degeneration displayed ultrastructural changes characteristic of apoptosis. The first detectable ultrastructural changes consisted of clumping of nuclear chromatin and mild to moderate condensation of the entire cell. Nuclear chromatin became transformed into flocculent densities which formed one or more large electron dense spherical balls (FIG. 2C, 2D). The nuclear envelope separated into fragments, and finally the cell became unpartitioned with nucleoplasmic contents freely intermingling with cytoplasmic contents. Large chromatin masses migrated often towards the periphery of the cell

and in some cases the cell divided into separate independent bodies consisting of a contingent of cytoplasm and one or more nuclear chromatin balls. This type and sequence of changes are identical to changes seen in neurons undergoing physiological cell death, a natural apoptotic process by which redundant or unsuccessful neurons are deleted from the developing brain (Ishimaru *et al.*, 1999) and meet established criteria for diagnosing apoptosis (Wyllie *et al.*, 1980). At 24 h after trauma, cells in both early and late stages of apoptosis were detected, indicating that the process of cell suicide was still progressing. We did not identify cells undergoing non-apoptotic degeneration by electron microscopy in affected brain regions at 16-24 h after trauma, which indicates that, at those times, apoptosis is the predominant form of degeneration, whereas up to 6 h after trauma excitotoxic degeneration primarily takes place in the infant rat brain (Ikonomidou *et al.*, 1996; Bittigau *et al.*, 1999).

These results demonstrate that both acute excitotoxic and slower active or apoptotic cell death occur in the context of traumatic brain damage in developing rats.

AGE-DEPENDENT DISTRIBUTION PATTERNS AND SEVERITY OF APOPTOTIC CELL DEATH FOLLOWING TRAUMA

We studied age dependent severity of apoptotic neurodegeneration following TBI by performing two series of experiments, one in which the brains of rats at all ages (3-30 days old) were subjected to the same mechanical force and one in which the mechanical force was modified in order to achieve the same pressure/brain weight ratio (Bittigau *et al.*, 1999). In both series we detected apoptotic cell death at 24 h after head trauma in 3-14 day old rats. Silver and TUNEL stains gave similar distribution patterns in all age groups. The age-dependent distribution patterns are shown in figure 3.

When the same force of 160gcm was used to traumatize pups of all age groups, severity of apoptotic cell death was highest in 3 day old rats and decreased significantly with increasing age (FIG. 3C). Even when the force was adjusted to provide the same pressure/brain weight ratio in all age groups, distant apoptotic damage in older animals remained minimal as compared to 3 and 7 day old rats. Under this experimental condition (fixed pressure/brain weight ratio), 7 day old rats were most vulnerable to distant apoptotic damage triggered by mechanical trauma (FIG. 3C).

Apoptotic cell death reached a peak at 24 h following trauma in the brains of pups at all ages studied and was non-detectable at 5 days after the insult (FIG. 3B).

In our studies in infant animals, we found that, at a given developmental age, highest densities of apoptotic cells following trauma were detected in areas that also displayed highest densities of cells undergoing physiologic cell death (Bittigau *et al.*, 1999). This possibly indicates that neurons and glia may be most vulnerable to die via apoptosis when exposed to an exogenous insult during a certain period of their maturation and differentiation process. It has been proposed that the ratio of pro- versus antiapoptotic factors within a cell primarily determines its vulnerability and likelihood to undergo active cell death (Kroemer, 1997; Hengartner, 2000). Thus, the ontogenetically regulated expression of potential proapoptotic factors early in development, such as c-jun, c-fos, p53 (Ferrer *et al.*, 1996), which, under physiological conditions, promote differentiation of immature neurons and glia may, under pathological circumstances, predispose these same cells to undergo suicide. P53, for example, promotes cell differentiation but initiates apoptotic deletion following irradiation (Borovitskaya *et al.*, 1996; Norimura *et al.*, 1996; Almog and Rotter, 1997). Progressive axonal injury and secondary axotomy after trauma may be an additional mechanism that promotes neuronal apoptosis, due to deafferentiation and loss of trophic support (Maxwell *et al.*, 1997).

Why the same traumatic insult that triggers no detectable apoptotic cell death in the 30-day-old rat brain gives rise to a massive, disseminated apoptotic response in infant rats is unclear. Certainly age-specific differences in the degree of myelination and brain water content will allow traumatic forces to transmit more easily to deeper brain structures the more immature the brain is at the time of injury. Interestingly, the infant rat brain is most sensitive to apoptotic neurodegeneration following trauma during the *N*-methyl-D-aspartate (NMDA) -receptor-hypersensitivity period (McDonald *et al.*, 1988; Ikonomidou *et al.*, 1989), with peak vulnerability on postnatal day 7. This exactly coincides with the age at which the infant rat brain is most sensitive to NMDA-excitotoxicity. In view of reports that NMDA receptor stimulation may trigger both excitotoxic and apoptotic neurodegeneration depending on intensity of stimulation (Bonfoco *et al.*, 1995), the question arises whether stimulation of NMDA receptors by endogenous glutamate, may promote apoptosis following trauma in infant rats. However, while attempting to block this apoptotic response with NMDA antagonists, we observed an unexpected potentiating effect (Pohl *et al.*, 1999), indicating that NMDA receptor blockade promotes apopto-

sis and NMDA receptor stimulation may be neuroprotective against apoptosis. Radical scavengers and antioxidants elicited a protective effect against delayed apoptotic cell death in the infant rat TBI model (Pohl *et al.*, 1999), suggesting contribution of free radicals in pathogenesis of this form of neurodegeneration.

Other factors likely to complicate tissue injury and potentially further entertain apoptotic deletion are progressive axonal injury and secondary axotomy after trauma with resulting deafferentation, decrease in the levels of neurotrophic factors and loss of trophic support, activation of glial cells and inflammatory pathways involving death receptors. Our attempts to explore some of these mechanisms will be illustrated in the following.

PATHWAYS LEADING TO APOPTOTIC NEURODEGENERATION

Apoptosis can be initiated by diverse signals and executed via different biochemical pathways (Hengartner, 2000). Triggers include growth factor deprivation, DNA damage, cytokine production and activation of death receptors, as well as release of cytochrome c from the mitochondria into the cytoplasm. Although biochemical pathways differ considerably, they all converge upon activation of effector caspases (Krammer, 2000; Meier *et al.*, 2000; Nicholson, 2000; Rich *et al.*, 2000; Savill and Fadok, 2000; Yuan and Yankner, 2000).

An intrinsic and extrinsic apoptotic pathway have been defined, the first initiated by release of cytochrome c into the cytoplasm and the second by activation of death receptors. Cytochrome c release leads to activation of effector caspases via recruitment of caspase-9 (Hengartner, 2000). Aggregation of the death receptor Fas (CD95/Apo-1), a member of the TNF-α superfamily, follows Fas ligand binding and leads to formation of a death-inducing signaling complex (DISC): Fas itself, an adapter protein named Fas associated death domain (FADD) and the inactive form of caspase-8 (Martin-Villalba *et al.*, 1999). After formation of the DISC, procaspase-8 is proteolytically cleaved, activated and released from the DISC (Chinnaiyan *et al.*, 1995; Muzio *et al.*, 1996; Medema *et al.*, 1997; Krammer, 2000). Caspase-8 then activates downstream caspases, such as caspase-3, which execute the cell.

Activation of caspases comprises a subsequent critical step within the apoptotic cascade. Caspases contribute to cell cleavage via inactivation of nuclease inhibitors and survival proteins, direct disassembly of cell structures, destruction of proteins involved in cytoskeleton regulation and inactivation of proteins involved in DNA repair and replication (Thornberry and Lazebnik, 1998).

To investigate involvement of the intrinsic apoptotic pathway in the pathogenesis of apoptotic neurodegeneration following trauma to the developing brain, we analyzed changes in the expression of antiapoptotic proteins of the bcl-2 group that decrease mitochondrial membrane permeability, changes in cytochrome c immunoreactivity in the cytosolic fraction and changes in caspase-9 activity in the infant rat brain trauma model. To investigate involvement of the extrinsic pathway, Fas-expression and caspase-8 activity in brain tissue were measured. To investigate the role of neurotrophins, endogenous mRNA levels for neurotrophin-3 (NT-3) and brain derived neurotrophic factor (BDNF) were analyzed. Finally, to test the potential benefit of caspase inhibition in TBI to the developing brain, the pancaspase inhibitor z-VAD.FMK was administered to infant rats and neurodegeneration was quantitated. Our findings indicate that trauma leads to activation of the intrinsic and the extrinsic apoptotic pathways in the developing rat brain and that inhibition of effector caspases confers neuroprotection over a time window of at least 8 h after trauma.

TRAUMA-INDUCED CHANGES IN CASPASE-3-LIKE ENZYMATIC ACTIVITY AND DNA-BREAKDOWN IN THE INFANT RAT BRAIN

Head trauma induced significant elevations of caspase 3/CPP32-like activity and DNA fragmentation (oligonucleosomes) in extracts from ipsilateral cingulate and parietal cortex, thalamus, striatum and hippocampus as measured at 24 h after trauma (Bittigau *et al.*, 1999).

These findings indicate that activation of CPP32-like caspases play a critical role in active cell deletion following trauma to the immature brain. In contrast to the adult brain, CPP32-like proteolytic activity rose not just up to 130%, as described in a study by Yakovlev *et al.* (1997), but up to 2,830% of control values. Together with our histological data, this highlights the disproportionately large magnitude of the apoptosis contribution to posttraumatic brain damage in the immature brain. Using combined optical dissector stereology and volumetry we calculated that in the brains of 7 day old rats subjected to head trauma, millions of cells were dying an apoptotic death in the brain at 24 h after trauma as opposed to a few thousand cells dying an excitotoxic death at 4 h after trauma (Bittigau

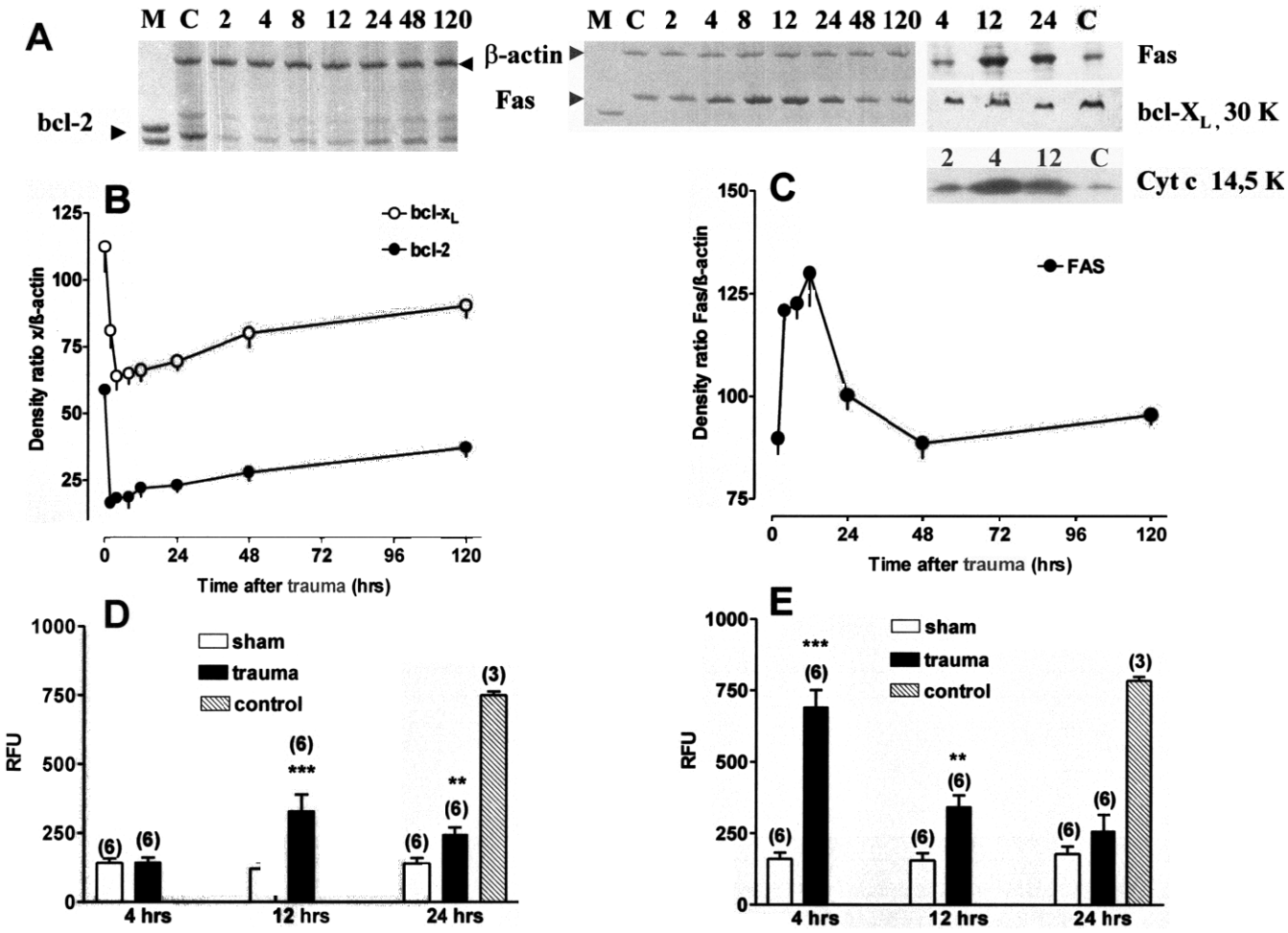

FIGURE 4 (**A**) Bcl-2 (left) and Fas (right) mRNA expression in right thalamus (ipsilateral to trauma site) in a sham operated rat at 0 hrs after trauma and in rats subjected to head trauma at 2-120 h after trauma. mRNA was reverse transcribed to cDNA, amplified by polymerase chain reaction using specific primers for bcl-2 and ß-actin and subjected to polyacrylamide gel electrophoresis and silver staining. There is obvious decrease in mRNA levels for bcl-2. There is an increase in mRNA levels for Fas at 4 h, peaking at 12 h after the insult and lasting up to 24 h. These are representative gels from a series performed to analyze bcl-2 and Fas mRNA expression. On the right, Western blot analysis for Fas and bcl-x_L in brain extracts prepared from the thalamus of sham operated rats (C) and rats traumatized on day 7, at 4-24 h after trauma. Representative blots of a series performed (thalamus, striatum, cortex), demonstrating an increase in Fas and decrease in bcl-x_L protein expression 4 h after trauma in the ipsilateral thalamus. Western blot analysis of cytochrome c immunoreactivity in the cytoplasmic fractions of brain extracts taken from the thalamus of a sham operated rat (C) and rats traumatized on day 7, at 2, 4 and 12 h after trauma is also shown. There is an increase in cytochrome c immunoreactivity in the cytosolic fraction by 2 h after trauma. (**B**) The results of densitometric analysis of bcl-2 and bcl-x_L specific mRNA-bands on the gels from traumatized rats are presented in reference to ß-actin. Data represent the ratio (%) of the density of the bcl-2 or bcl-x_L band to the ß-actin band ± SEM. Two way ANOVA revealed that trauma had a highly significant effect on the mRNA-levels for bcl-2 [$F(7,44)=40.9$, $P<0.001$] and bcl-x_L [$F(7,44)=31.71$, $P<0.001$] in the thalamus. There was a highly significant effect of time (posttraumatic interval) on the mRNA-levels for bcl-2 [$F(1,44)=155.1$, $P<0.001$] and bcl-x_L [$F(1,44)=648.8$] in the thalamus as well, compared to sham operated rats. (**C**) The results of densitometric analysis of the Fas specific mRNA bands from the thalamus of traumatized rats are presented in reference to ß-actin. Data represent the ratio (%) of the density of the Fas band to the ß-actin band ± SEM. Comparison between sham rats and rats subjected to brain trauma by ANOVA revealed that trauma had a highly significant effect on Fas mRNA levels in the thalamus [$F(1,44) = 804.5$, $P<0.001$]. (**D**) Caspase-9 activity in cytosolic protein extracts from thalamus of sham rats and rats subjected to head trauma. Specimen were analyzed at 4, 12 and 24 h after trauma or sham surgery. Caspase-9-like activity was measured fluorometrically, using the specific substrate LEHD and by determining accumulation of free aminotrifluoromethyl coumarin (AFC). Data are expressed in relative fluorescent units (RFU) as means ± SEM after subtraction of the appropriate buffer controls. The numbers in parentheses represent the number of specimen in each group. Two way ANOVA revealed that trauma had a highly significant effect on caspase-9 activity in the thalamus [$F(1,30) = 17.56$, $P<0.001$]. The grey column depicts recombinant caspase-9 activity which served as control. (**E**) Caspase-8 activity in cytosolic protein extracts from right thalamus in rats subjected to head trauma compared to sham rats. Specimens were analyzed at 4, 12 and 24 h after trauma or sham surgery. Caspase-8 like activity was measured fluorometrically using the specific substrate IETD and by determining accumulation of free AFC. Data are expressed in relative fluorescent units (RFU) as the mean ratios ± SEM of signal obtained in specimen from traumatized and sham operated brains after subtraction of the appropriate buffer controls. The numbers in parentheses represent the number of specimen in each group. Two way ANOVA revealed that trauma had a highly significant effect on caspase-8 activity in the thalamus [$F(1,30) = 63.27$, $P<0.001$]. The grey column depicts recombinant caspase-8 activity which served as control.

et al., 1999). Since apoptotic cells can be detected histologically for a few hours (clearance time, 2 h and 20 min) (Thomaidou *et al.*, 1997) and apoptosis is occurring in the infant rat brain for several days after trauma, the numbers of cells eventually deleted by this mechanism are much higher.

ACTIVATION OF THE INTRINSIC APOPTOTIC PATHWAY BY TRAUMA

Downregulation in the Expression of Antiapoptotic Genes

The expression of bcl-2 and bcl-x_L, two proteins with antiapoptotic properties which have been shown to decrease mitochondrial membrane permeability was first investigated at the transcriptional level. Trauma triggered marked and rapid downregulation in the expression of bcl-2- and bcl-x_L-specific mRNA in thalamus and cingulate cortex, which was evident within 2 h following the insult, persisted up to 48 h and demonstrated a slow, incomplete recovery by 120 h after trauma (FIG. 4A, 4B).

Downregulation of bcl-2 family members was confirmed at the protein level in that immunoreactivity of bcl-x_L was analyzed by Western blotting in brain extracts from thalamus, striatum and cortex. Decreased levels of bcl-x_L protein were found in these areas at various time points after trauma (FIG. 4A).

Cytochrome c Release and Caspase-9 Activation

Cytochrome c immunoreactivity was analyzed by Western blotting in the cytosolic fraction of brain extracts from thalamus, striatum and cortex of 7 day old rats subjected to head trauma. Cytochrome c immunoreactivity increased at 2 h after trauma in the cytosolic fraction (FIG. 4A), at a time point when no signs of delayed neurodegeneration were detectable by histological techniques.

The activity of the initiator caspase-9 was measured in thalamic tissue using the specific substrate (LEHD) in sham rats and rats subjected to head trauma. Compared to sham operated rats, there was a significant increase of caspase-9 activity in the thalamus in rats subjected to head trauma at 12 and 24 h after trauma (FIG. 4D).

Activation of the intrinsic apoptotic pathway has previously been reported in *in vivo* trauma models (Morita-Fujimura *et al.*, 1999; Raghupathi *et al.* 2000; Keane *et al.* 2001). How cytochrome c manages to cross the mitochondrial membrane is not understood. In all proposed models (Hengartner, 2000), members of the bcl-2 family play a key role in that they decrease mitochondrial membrane permeability and prevent release of cytochrome c into the cytoplasm (Nicholson, 2000). In the infant rat brain we demonstrate downregulation of the expression of bcl-2 and bcl-x_L following trauma, which is expected to result in increased permeability of the mitochondrial membranes. Changes at the mRNA levels correlated with decreased protein levels (Felderhoff-Mueser *et al.*, 2002). Reasons for decreased expression of antiapoptotic bcl-2 family proteins remain unclear. Transcription of antiapoptotic bcl-2 family members is influenced by CREB, whose activity level is regulated by growth factors (Xing *et al.*, 1996). It has been shown that release of trophic factors and their trophic effects on developing neurons depend upon the level of neuronal activity (Mc Callister *et al.*, 1996; Liou and Fu, 1997). Spreading depression triggered by trauma disrupts physiological synaptic activity. Even in the presence of increased neurotrophin levels, it is possible that disruption of physiological synaptic activity may lead to impairment of intracellular neurotrophin-initiated signaling pathways and result in decrease in the transcription of survival genes.

APOPTOSIS BY DEATH RECEPTOR ACTIVATION (EXTRINSIC PATHWAY) FOLLOWING TRAUMA TO THE DEVELOPING BRAIN

Changes in expression of the death receptor Fas following trauma to the 7 day old rat brain were determined at defined time points post-injury. Trauma triggered increase of Fas-mRNA levels at 4 h after trauma which lasted up to 24 hours and subsequently decreased to pre-trauma levels (FIG. 4A). Increased protein levels for Fas were found in the ipsilateral thalamus, striatum and cortex starting at 4 hours after trauma, with this increase being most pronounced at 12 and 24 h after trauma (FIG. 4A).

In the intact developing brain there is moderate physiological expression of Fas. Fas immunoreactivity increased particularly in the cortex and in the thalamus ipsilateral to the injury after trauma (FIG. 4A, 4C). At 48 h, reduction of Fas immunoreactivity occurred in affected brain regions, possibly reflecting evacuation of cells that overexpressed the receptor (Felderhoff *et al.*, 2002).

To further confirm activation of the extrinsic apoptotic pathway following trauma, caspase-8 activity was measured fluorometrically in the thalamus using the specific caspase-8 substrate IETD. Trauma had a highly significant effect on caspase-8 activity in the thala-

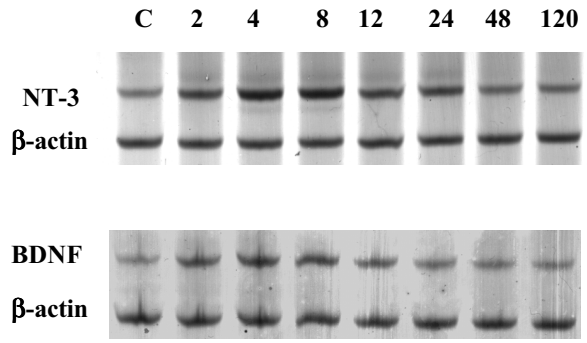

FIGURE 5 NT-3 and BDNF mRNA expression in right thalamus (ipsilateral to trauma site) in a sham operated rat (C) at 0 h after surgery, and rats subjected to head trauma at 2, 4, 8, 12, 24, 48 and 120 h after trauma. There is an increase in mRNA levels for both neurotrophins at 4 h, with peaks between 4-8 h after the insult and decline to control values by 48 h after trauma. The ß-actin band shows equal signal intensity in all columns, verifying cDNA integrity.

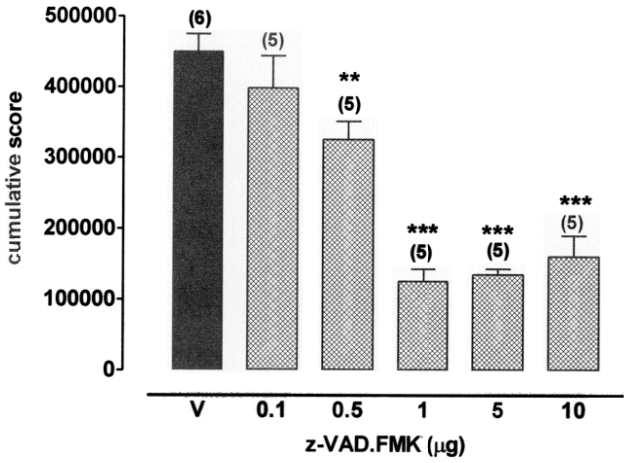

FIGURE 6 Neuroprotective effect of z-VAD.FMK in infant TBI. Seven day old rats received 0.1-10 μg z-VAD.FMK (grey columns) or DMSO vehicle (V, dark column) i.c.v. at 2 h after trauma and were perfused at 24 h after trauma (n=6 per group). In sections stained by the DeOlmos technique, the frontal, parietal, cingulate, retrosplenial cortices, caudate nucleus, thalamus, dentate gyrus and subiculum were subjected to morphometric analysis by stereological dissector method, estimating numerical densities of silver positive cells. Each region was given a score of 1000 for every 1000 degenerating cells/mm^3, and the scores of 14 regions ipsilateral to the trauma side were added to a cumulative score. Columns represent cumulative scores ± SEM (numbers in parentheses represent the number of animals per group). ANOVA revealed that the effect of treatment with z-VAD.FMK was significant [$F(5,30) = 30.06$, $P<0.0001$]. Pairwise comparisons revealed that the dose of 0.5 mg/kg z-VAD.FMK significantly protected from apoptotic neurodegeneration following trauma to the developing brain. $^{**}P<0.01$; $^{***}P<0.001$ compared to DMSO-treated rats, Student´s *t*-test.

mus after trauma (FIG. 4E). Previous studies have demonstrated Fas expression in the context of trauma to the adult brain and in infant hypoxia-ischemia (Nakashima *et al.*, 1999; Beer *et al.*, 2000; Felderhoff-Mueser *et al.*, 2000). Our findings imply Fas receptor involvement in activation of caspase-8 after neonatal brain trauma but do not exclude the possibility that other death receptors and their ligands (TNF, TRAIL) may also contribute to activation of this extrinsic apoptotic pathway.

A cross talk between the extrinsic pathway and the mitochondria has been postulated (Hengartner, 2000). Activation of caspase-8 leads to proteolysis of the proapoptotic protein bid. Truncated bid enters the mitochondria and promotes cytochrome c release. Time course studies suggest that activation of caspase-8 occurs early (within 4 h) after trauma. Therefore, it is possible that caspase-8 mediated bid cleavage may constitute one additional mechanism to facilitate release of cytochrome c into the cytoplasm.

Trauma Triggers Transcription of Neurotrophins

To determine whether downregulation of neurotrophins may contribute to apoptotic neurodegeneration after trauma, mRNA levels for BDNF and NT-3 were analyzed by RT-PCR in brain samples from rats subjected to head trauma at the age of 7 days. Trauma triggered increase of NT-3 and BDNF specific mRNA. This effect was evident at 2 h after trauma, demonstrated a peak at 8 h and returned to basal levels by 48 h after trauma (FIG. 5).

In accordance, BDNF immunoreactivity was quite prominent in the cortex and thalamus ipsilateral to the injury at 24 h after trauma (Felderhoff-Mueser *et al.*, 2002).

Thus, our studies did not demonstrate downregulation in the expression of the neurotrophins BDNF and NT-3. In contrast, neurotrophin mRNA levels and immunoreactivity increased within hours after trauma, suggesting that neurotrophin-upregulation may represent an endogenous compensatory mechanism to counteract neuronal destruction in the developing central nervous system and provide modes for regeneration and repair.

PHARMACOLOGICAL INTERVENTIONS IN DEVELOPMENTAL BRAIN TRAUMA

NMDA Antagonists Block Excitotoxic but Enhance Trauma-induced Apoptotic Neurodegeneration

To assess whether antagonists at the NMDA receptor may have neuroprotective effects in the neonatal head trauma model, we administered NMDA antagonists to

7 day old rats and evaluated the extent of excitotoxic and apoptotic neurodegeneration following such treatment.

Quantitative evaluation 4 h after trauma of the brains of 7-day-old rats treated with the NMDA antagonist dizocilpine 1 h prior to trauma revealed reduction of the extent of excitotoxic damage in the parietal cortex (Ikonomidou *et al.*, 1996; Pohl *et al.*, 1999).

Quantitative evaluation of the brains 24 h after head trauma however revealed that the apoptotic degeneration was more severe in rats treated with dizocilpine than in those subjected to vehicle (Pohl *et al.*, 1999). NMDA antagonists also gave rise to apoptotic degeneration in the brains of 7-day-old sham-operated rats, indicating that they promote physiological apoptosis at this age. In 7-day-old rats subjected to head trauma and subsequent treatment with NMDA antagonists the severity of apoptotic cell death was higher (by 27% after treatment with dizocilpine and 37% after treatment with CPP) than would be expected if the combined effect were due to a simple additive mechanism (Pohl *et al.*, 1999).

These results indicate that NMDA antagonists have opposite effects on the two components of TBI in the developing brain; they reduce the relatively small excitotoxic component, while markedly increasing the substantially larger apoptotic component, the net effect being increased neurodegeneration. Thus, NMDA antagonists are singularly unsuitable for neuroprotection in TBI to the developing brain.

Treatment with the Pancaspase Inhibitor z-VAD.FMK Blocks Trauma-induced Apoptotic Cell Death

To assess the neuroprotective potential of caspase-inhibition in TBI in infant rats, the pancaspase inhibitor z-VAD.FMK was administered intracerebroventricularly (i.c.v.) to 7 day old rats in doses of 0.1-10 µg at 2 h after trauma. Treatment with z-VAD.FMK had a significant effect on severity of apoptotic brain damage following trauma. Rats receiving a single dose of z-VAD.FMK displayed a reduction in cumulative scores for degenerating cells (FIG. 6) compared to rats subjected to head trauma and i.c.v. injection of DMSO.

The therapeutic time window for z-VAD.FMK was at least 8 h, since delayed administration of z-VAD.FMK up to 8 h following trauma resulted in lower scores for apoptotic brain damage compared to vehicle treated rats (Felderhoff-Mueser *et al.*, 2002).

In order to exclude the possibility that caspase inhibition might delay but not inhibit apoptosis, we injected z-VAD.FMK (1 µg) 2 h after trauma to 7 day old rats and analyzed their brains at 24, 48 h and 5 days after trauma. A protective effect of z-VAD.FMK was still evident at 48 h after trauma in comparison to vehicle. At 5 days after trauma densities of degenerating cells in both vehicle and z-VAD.FMK treated rats were equally low and did not significantly differ between groups (Felderhoff *et al.*, 2002)

Finally, to provide additional evidence that treatment with z-VAD.FMK offered lasting protection against TBI, we injected 7 day old rats subjected to brain trauma i.c.v. with the protective dose of 1 µg z-VAD.FMK or vehicle at 2 h after trauma. All animals were sacrificed 7 days after trauma or sham surgery without transcardial perfusion, the forebrains were hemisected and their weights monitored. Trauma resulted in significant weight reduction of the right (traumatized) hemisphere in vehicle treated rats compared to the non traumatized left side (Felderhoff-Mueser *et al.*, 2002). Treatment with z-VAD.FMK resulted also in a significant but less pronounced reduction of right hemispheric weights compared to vehicle treated traumatized rats and sham operated rats. These time studies suggest amelioration of the neurodegenerative response to trauma (Felderhoff *et al.*, 2002).

In adult animal models, caspase inhibition may confer neuroprotection in cerebral ischemia (Hara *et al.*, 1997; Endres *et al.*, 1998; Fink *et al.*, 1998; Himi *et al.*, 1998). Furthermore, early treatment of experimental pneumococcal meningitis with z-VAD.FMK was shown to have a beneficial effect, whereas delayed application of this compound did not result in substantial reduction of neuronal loss (Braun *et al.*, 1999). In traumatic injury to the adult brain, z-VAD.FMK and the selective caspase-3 inhibitor z-DEVD.FMK can block neuronal death (Yakovlev *et al.*, 1997; Clark *et al.*, 2000b). In hippocampal and cortical neuronal cultures, the cell permeable pancaspase inhibitor boc-aspartyl(OMe)-fluoromethylketone (BAF) and the more selective caspase-8 inhibitor IETD-FMK (IETD) reduced Fas-induced apoptosis (Felderhoff-Mueser *et al.*, 2000). The only existing *in vivo* study on caspase inhibition in the immature brain demonstrated neuroprotection with the pancaspase inhibitor BAF in an infant model of hypoxic-ischemic injury (Cheng *et al.*, 1998). Our data indicate a beneficial effect of caspase inhibition in brain trauma for neuronal death occurring distant to the impact site. More importantly, the protective effect could be achieved even when the compound was administered in a delayed fashion, indicating relevance in the clinical setting.

TRAUMA ACTIVATES THE ENDOGENOUS CANNABINOID LIGAND-RECEPTOR SYSTEM

Transcriptional mRNA expression and ligand binding capacity of cerebral cannabinoid receptors were assessed at defined time points post-trauma and compared to levels of the endogenous cannabinoid receptor ligands, anandamide and 2-arachidonoyl glycerol (2-AG). While loss of a neuron-specific mRNA marker was observed after induction of head trauma, levels of cannabinoid CB_1 receptor mRNA transcription and ligand binding capacity were upregulated in the ipsilateral cerebral cortex. These alterations were most prominent in the proximity of the impact site of the contusive force (Hansen *et al.*, 2001a). Accumulation of anandamide and its precursor, but not 2-AG, was apparent in the ipsilateral cortex after induction of head trauma, in particular 24 hours post-injury (Hansen *et al.*, 2001a,b), which suggest an enhanced activity of the endogenous cannabinoid receptor-ligand system in the developing brain as a response to contusive head trauma.

Since central presynaptically located cannabinoid receptors suppress the activity of a range of neurotransmitter systems, including glutamatergic and GABAergic neurotransmission (Schlicker and Kathmann, 2001; Wilson and Nicoll, 2002), and endogenous cannabinoids are found in much higher concentrations when neurons are in an injured state (Hansen *et al.*, 2000), it is believed that these substances and their receptors may constitute a putative endogenous response aiming at dampening the destructive impact of brain insults (Hansen *et al.*, 2000; Piomelli *et al.*, 2000). Paradoxically, exogenously induced overactivation of neuronal cannabinoid receptors can also induce apoptotic-like neurodegeneration, presumably depending on the cell type, cell developmental state and degree of activation (Downer *et al.*, 2001; Guzmán *et al.*, 2001). Also, blockade of cannabinoid receptors induces neuroprotection in a developmental model of NMDA-induced excitotoxic brain damage (Hansen *et al.*, 2002). It therefore remains to be established under what circumstances and in which direction intrinsically upregulated cannabinoid ligand-receptor function affects pro-survival signaling pathways in the immature brain and whether the endogenous cannabinoid system may represent a target for pharmacotherapy in pediatric TBI.

CONCLUSIONS

Traumatic injury to the developing central nervous system has two major components, an acute excitotoxic component at the site of the insult and a delayed apoptotic component affecting the impact site as well as deeper brain structures. The number of brain cells affected by the apoptotic component is disproportionally larger than the number of cells degenerating by an excitotoxic mechanism (Bittigau *et al.*, 1999). Given our findings, targeting the downstream effectors of neuronal apoptosis in the acute phase of the insult has therapeutic potential in the treatment of traumatic injury to the immature brain. Antiapoptotic therapies may give cells enough time to establish intrinsic protection systems and restore cellular homeostasis and function (Han and Holtzman, 2000). However, since apoptosis is also a physiological process in the developing brain, studies addressing the long-term functional effects following caspase inhibition appear to be potential targets for future research (Gillardon *et al.*, 1999).

Acknowledgements

This work was supported by BMBF grant 01KO95151TPA3 and a Rahel-Hirsch award from the Humboldt University.

References

Adelson PD, P Robichaud, RL Hamilton and PM Kochanek (1996) A model of diffuse traumatic brain injury in the immature rat. *J. Neurosurg.* **85**, 877-884.

Adelson PD, CE Dixon, P Robichaud and PM Kochanek (1997) Motor and cognitive deficits following diffuse traumatic brain injury in the immature rat. *J. Neurotrauma* **14**, 99-108.

Adelson PD and PM Kochanek (1998) Head injury in children. *J. Child Neurol.* **13**, 2-15.

Aldrich EF, HM Eisenberg, C Saydjari, TG Luerssen, MA Foulkes, JA Jane, LF Marshall, A Marmarou and HF Young (1992) Diffuse brain swelling in severely head-injured children. A report from the NIH Traumatic Coma Data Bank. *J. Neurosurg.* **76**, 450-454.

Allen AR (1911) Surgery of experimental lesion of spinal cord equivalent to crush injury of fracture dislocation of spinal column. *J. Am. Med. Assoc.* **57**, 878-880.

Almog N and V Rotter (1997) Involvement of p53 in cell diffentiation and development. *Biochim. Biophys. Acta* **1333**, F1-F27.

BarlowKM and RA Minns (2000) Annual incidence of shaken impact syndrome in young children. *Lancet* **356**, 1571-1572.

Bayir H, VA Kagan, YY Tyurina, V Tyurin, RA Ruppel, PD Adelson, SH Graham, K Janesko, RSB Clark and PM Kochanek (2002) Assessment of antioxidant reserves and oxidative stress in cerebrospinal fluid after severe traumatic brain injury in infants and children. *Pediatric Res.* **51**, 571-578.

Beer R, G Franz, M Schopf, M Reindl, B Zelger, E Schmutzhard, W Poewe and A Kampfl. (2000) Expression of Fas and Fas ligand after experimental traumatic brain injury in the rat. *J. Cereb. Blood Flow Metab.* **20**, 669-677.

Bell MJ, PM Kochanek, LA Doughty, JA Carcillo, PD Adelson, RSB Clark, SR Wisniewski, MJ Whalen and ST DeKosky

(1997) Interleukin-6 and interleukin-10 in cerebrospinal fluid after severe traumatic brain injury in children. *J. Neurotrauma* **14**, 451-457.

Berger RP, MC Pierce, SR Wisniewski, PD Adelson and PM Kochanek (2002) Serum S100B concentrations are increased after closed head injury in children: a preliminary study. *J. Neurotrauma* **19**, 1405-1409.

Bittigau P, M Sifringer, D Pohl, D Stadthaus, M Ishimaru, H Shimizu, M Ikeda, D Lang, A Speer, JW Olney and C Ikonomidou (1999) Apoptotic neurodegeneration following trauma is markedly enhanced in the immature brain. *Ann. Neurol.* **45**, 724-735.

Bonfoco E, D Krainc, M Ankarcron, P Nicotera and SA Lipton (1995) Apoptosis and necrosis: two distinct events induced, respectively, by mild and intense insults with *N*-methyl-D-aspartate or nitric oxide/superoxide in cortical cell cultures. *Proc. Natl. Acad. Sci. USA* **92**, 7162-7166.

Bonnier C, MC Nassogne and P Evrard (1995) Outcome and prognosis of whiplash shaken infant syndrome: late consequences after a symptom free interval. *Dev. Med. Child Neurol.* **37**, 943-956.

Bonnier C, B Mespiès, S Carpentier, D Henin, and P Gressens (2002) Delayed white matter injury in a murine model of shaken baby syndrome. *Brain Pathol.* **12**, 320-328.

Borovitskaya AE, VI Evtushenko and SL Sabol (1996) Gamma-radiation-induced cell death in the fetal rat brain possesses molecular characteristics of apoptosis and is associated with specific messenger RNA elevations. *Brain Res. Mol. Brain Res.* **35**, 19-30.

Braun JS, R Novak, KH Herzog, SM Bodner, JL Cleveland and EI Tuomanen (1999) Neuroprotection by a caspase inhibitor in acute bacterial meningitis. *Nat. Med.* **5**, 298-302.

Brown JK and RA Minns (1993) Non-accidental head injury, with particular reference to whiplash shaking injury and medico-legal aspects. *Dev. Med. Child Neurol.* **35**, 849-869.

Cheng Y, M Deshmukh, A D'Costa, JA Demaro, JM Gidday, A Shah, Y Sun, MF Jacquin, EM Johnson and DM Holtzman (1998) Caspase inhibitor affords neuroprotection with delayed administration in a rat model of neonatal hypoxic-ischemic brain injury. *J. Clin. Invest.* **101**, 1992-1999.

Chinnaiyan AM, K O´Rourke, M Tewari and VM Dixit (1995) FADD, a novel death domain-containing protein interacts with the death domain of Fas and initiates apoptosis. *Cell* **81**, 505-512.

Clark RSB, PM Kochanek, PD Adelson, MJ Bell, JA Carcillo, M Chen, SR, Wisniewski, K Janesko, MJ Whalen and SH Graham (2000a) Increases in bcl-2 protein in cerebrospinal fluid and evidence for programmed cell death in infants and children after severe traumatic brain injury. *J. Pediatr.* **137**, 197-204.

Clark RSB, PM Kochanek, SC Watkins, M Chen, CE Dixon, NA Seidberg, J Melick, JE Loeffert, PD Nathaniel, KL Jin and SH Graham (2000b) Caspase-3 mediated neuronal death after traumatic brain injury in rats. *J. Neurochem.* **74**, 740-753.

David TJ (1999) Shaken baby (shaken impact) syndrome: non-accidental head injury in infancy. *J. R. Soc. Med.* **92**, 556-561.

DeOlmos JS and WR Ingram (1971) An improved cupric-silver method for impregnation of axonal and terminal degeneration. *Brain Res.* **33**, 523-529.

Diamond PT (1996) Brain injury in the Commonwealth of Virginia: an analysis of Central registry data 1988-1993. *Brain Injury* **10**, 414-419.

Dixon CE, GL Clifton, JW Lighthall, A Yaghmai and RL Hayes (1991) A controlled cortical impact model of traumatic brain injury in the rat. *J. Neurosci. Meth.* **39**, 253-262.

Downer E, B Boland, M Fogarty and V Campbell (2001) Delta9-tetrahydrocannabinol induces the apoptotic pathway in cultured cortical neurones via activation of the CB1 receptor. *Neuroreport* **12**, 3973-3978.

Duhaime AC, CW Christian, E Moss and T Seidl (1996) Long-term outcome in infants with the shaking impact syndrome. *Pediatr. Neurosurg.* **24**, 292-298.

Duhaime AC, CW Christian, LB Rorkea and RA Zimmerman (1998) Nonaccidental head injury in infants - The shaken-baby syndrome. *N. Engl. J. Med.* **338**, 1822-1829.

Endres M, S Namura, M Shimizu-Sasamata, C Weber, L Zhang, T Gomez-Isla, BT Hyman and MA Moskowitz (1998) Attenuation of delayed neuronal death after mild focal ischemia in mice by inhibition of the caspase family. *J. Cereb. Blood Flow Metab.* **18**, 238-247.

Feeney DM, MG Boyeson, R Linn, HM Murray and WG Dail (1981) Responses to cortical injury: I. Methodology and local effects of contusions in the rat. *Brain Res.* **211**, 67-77.

Felderhoff-Mueser U, DL Taylor, K Greenwood, M Kozma, D Stibenz, UC Joashi, AD Edwards and H Mehmet (2000) Fas/CD95/Apo-1 can function as a death receptor for neuronal cells *in vitro* and *in vivo* and is upregulated following cerebral hypoxic-ischemic injury to the developing rat brain. *Brain Pathol.* **10**, 17-29.

Felderhoff-Mueser U, M Sifringer, S Pesditschek, H Kuckuck, A Moysich, P Bittigau and C Ikonomidou (2002) Pathways leading to apoptotic neurodegeneration following trauma to the developing rat brain. *Neurobiol. Dis.* **11**, 231-245.

Ferrer I, M Olivé, J Ribera and AM Planas (1996) Naturally occuring (programmed) and radiatio-induced apoptosis are associated with selective c-jun expression in the developing rat brain. *Eur. J. Neurosci.* **8**, 1286-1298.

Fink K, J Zhu, S Namura, M Shimizu-Sasamata, M Endres, J Ma, T Dalkara, J Yuan and MA Moskowitz (1998) Prolonged therapeutic window for ischemic brain damage caused by delayed caspase activation. *J. Cereb. Blood Flow Metab.* **18**, 1071-1076.

Geddes JF, GH Vowles, JA Nicoll and T Revesz (1999) Neuronal cytoskeletal changes are an early consequence of repetitive head injury. *Acta Neuropathol. (Berl.)* **98**, 171-178.

Geddes JF, AK Hackshaw, GH Vowles, CD Nickols and HL Whitwell (2001a) Neuropathology of inflicted head injury in children I. Patterns of brain damage. *Brain* **124**, 1290-1298.

Geddes JF, GH Vowles, AK Hackshaw, CD Nickols, IS Scott and HL Whitwell (2001b) Neuropathology of inflicted head injury in children II. Microscopic brain injury in infants. *Brain* **124,** 1299-1306.

Gillardon F, I Kiprianova, J Sandkuhler, HA Hossmann and M Spranger (1999) Inhibition of caspases prevents cell death of hippocampal CA1 neurons, but not impairment of hippocampal long-term potentiation following global ischemia. *Neuroscience* **93**, 1219-1222.

Goldstein M (1990) Traumatic brain injury: a silent epidemic. *Ann. Neurol.* **27**, 327.

Guzmán M, C Sánchez and I Galve-Roperh (2001) Control of the cell survival/death decision by cannabinoids. *J. Mol. Med.* **78**, 613-625.

Han BH and DM Holtzman (2000) BDNF protects the neonatal brain from hypoxic-ischemic injury *in vivo* via the ERK pathway. *J. Neurosci.* **20**, 5775-5781.

Hansen HS, B Moesgaard, HH Hansen and G Petersen (2000) *N*-

acylethanolamines and precursors - relation to cell injury. *Chem. Phys. Lipids* **108**, 135-150.

Hansen HH, C Ikonomidou, P Bittigau, SH Hansen and HS Hansen (2001a) Accumulation of the anandamide precursor and other N-acylethanolamine phospholipids in infant rat models of *in vivo* necrotic and apoptotic neuronal cell death. *J. Neurochem.* **76**, 39-46.

Hansen HH, PC Schmid, P Bittigau, L Lastres-Becker, F Berrendero, J Manzanares, C Ikonomidou, HHO Schmid, JJ Fernández-Ruiz and HS Hansen (2001b) Anandamide, but not 2-arachidonoylglycerol, accumulates during *in vivo* neurodegeneration. *J. Neurochem.* **78**, 1415-1427.

Hansen HH, I Azcoitia, S Pons, J Romero, LM Garcia-Segura, JA Ramos, HS Hansen and JJ Fernández-Ruiz (2002) Blockade of cannabinoid CB1 receptor function protects against *in vivo* disseminating brain damage following NMDA-induced excitotoxicity. *J. Neurochem.* **82**, 1-5.

Hara H, RM Friedlander, V Gagliardini, C Ayata, K Fink, Z Huang, M Shimizu-Sasamata, J Yuan and MA Moskowitz (1997) Inhibition of interleukin 1 beta converting enzyme family proteases reduces ischemic and excitotoxic neuronal damage. *Proc. Natl. Acad. Sci. USA* **94**, 2007-2012.

Hengartner MO (2000) The biochemistry of apoptosis. *Nature* **407**, 770-776.

Himi T, Y Ishizaki and S Murota (1998) A caspase inhibitor blocks ischaemia-induced delayed neuronal death in the gerbil. *Eur. J. Neurosci.* **10**, 777-781.

Ikonomidou C, JL Mosinger, KS Salles, J Labruyere and JW Olney (1989) Sensitivity of the developing rat brain to hypobaric/ischemic damage parallels sensitivity to *N*-methyl-D-aspartate neurotoxicity. *J. Neurosci.* **9**, 2809-2818.

Ikonomidou C, Y Qin, J Labruyere, C Kirby and JW Olney (1996) Prevention of trauma-induced neurodegeneration in infant rat brain. *Pediatr. Res.* **39**, 1020-1027.

Ishimaru MJ, C Ikonomidou, TI Tenkova, TC Der, K Dikranian, MA Sesma and JW Olney (1999) Distinguishing excitotoxic from apoptotic neurodegeneration in the developing rat brain. *J. Comp. Neurol.* **408**, 461-476.

James HE (1999) Pediatric head injury: what is unique and different. *Acta Neurochir.* Suppl. (Wien.) **73**, 85-88.

Jaspan T, G Narorough, JAG Punt and J Lowe (1992) Cerebral contusional tears as marker of child abuse - detection by cranial sonography. *Pediatr. Radiol.* **22**, 237-245.

Keane RW, S Kraydieh, G Lotocki, OF Alonso, P Aldana and WD Dietrich (2001) Apoptotic and antiapoptotic mechanisms after traumatic brain injury. *J. Cereb. Blood Flow Metab.* **21**, 1189-1198.

Koskiniemi M, T Tykka, T Nybo and L Jarho (1995) Long-term outcome after severe brain injury in preschoolers is worse than expected. *Arch. Pediatr. Adolesc. Med.* **149**, 249-254.

Krammer PH (2000) CD95's deadly mission in the immune system. *Nature* **407**, 789-795.

Kraus JF, D Fife and C Conroy (1987) Pediatric brain injuries: the nature, clinical course and early outcomes in a defined United States population. *Pediatrics* **79**, 501-507.

Kroemer G (1997) The proto-oncogene Bcl-2 and its role in regulating apoptosis. *Nat. Med.* **3**, 614-620.

Lindenberg R and E Freytag (1969) Morphology of brain lesions from blunt trauma in early infancy. *Arch. Pathol.* **87**, 298-305.

Liou JC and WM Fu (1997) Regulation of quantal secretion from developing motoneurons by postsynaptic activity-dependent release of NT-3. *J. Neurosci.* **17**, 2459-2468.

Luerssen TG, MR Klauber and LF Marshall (1988) Outcome from head injury related to patient´s age. A longitudinal prospective study of adult and pediatric head injury. *J. Neurosurg.* **68**, 409-416.

Mahoney WJ, BJ D´Souza, A Haller, MC Rogers, MH Epstein and JM Freeman (1983) Long-term outcome of children with severe head trauma and prolonged coma. *Pediatrics* **71**, 756-762.

Marmarou A, MA Abd-Elfattah Foda, W van den Brink, J Campbell, H Kita and K Demetriadou (1994) A new model of diffuse brain injury in rats. Part I: Pathophysiology and biomechanics. *J. Neurosurg.* **80**, 291-300.

Martin-Villalba A, I Herr, I Jeremias, M Hahne, R Brandt, J Vogel, J Schenkel, T Herdegen and KM Debatin (1999) CD95 ligand (Fas-L/APO-1L) and tumor necrosis factor-related apoptosis-inducing ligand mediate ischemia-induced apoptosis in neurons. *J. Neurosci.* **19**, 3809-3817.

Maxwell WL, JT Povlishock and DL Graham (1997) A mechanistic analysis of nondisruptive axonal injury: a review. *J. Neurotrauma* **14**, 419-440.

McDonald JW, FS Silverstein and MV Johnston (1988) Neurotoxicity of *N*-methyl-D-aspartate is markedly enhanced in developing rat central nervous system. *Brain Res.* **459**, 200-203.

McIntosh TK, R Vink, L Noble, I Yamakami, S Fernyak and AI Faden (1989) Traumatic brain injury in the rat: characterization of a lateral fluid-percussion model. *Neuroscience* **28**, 233-244.

McCallister AK, LC Katz and DC Lo (1996) Neurotrophin regulation of cortical dendritic growth requires activity. *Neuron* **17**, 1057-1064.

Medema JP, C Scaffidi, FC Kischkel, A Shevchenko, M Mann, PH Krammer and ME Peter (1997) FLICE is activated by association with the CD95 death-inducing signaling complex (DISC). *EMBO J.* **16**, 2794-2804.

Meier P, A Finch and G Evan (2000). Apoptosis in development. *Nature* **407**, 796-801.

Morita-Fujimura Y, M Fujimura, M Kawase, SF Chen and PH Chan (1999) Release of mitochondrial cytochrome c and DNA fragmentation after cold injury-induced brain trauma in mice: possible role in neuronal apoptosis. *Neurosci. Lett.* **267**, 201-205.

Munger CE, RL Peiffer, TW Bouldin, JA Kylstra and RL Thompson (1993) Ocular and associated neuropathologic observations in suspected whiplash shaken infant syndrome. A retrospective study of 12 cases. *Am. J. Forensic Med. Pathol.* **14**, 193-200.

Muzio M, AM Chinnaiyan, FC Kischkel, K O'Rouke, A Shevchenko, J Ni, C Scaffidi, JD Bretz, M Zhang, R Gentz, M Mann, PH Krammer, ME Peter and VM Dixit (1996) FLICE, a novel FADD-homologous ICE/CED-3-like protease, is recruited to the CD95 (Fas/APO-1) death-inducing signaling complex. *Cell* **85**, 817-827.

Nakashima K, K Yamashita, S Uesugi and H Ito (1999) Temporal and spatial profile of apoptotic cell death in transient intracerebral mass lesion of the rat. *J. Neurotrauma* **16**, 143-151.

Nicholson DW (2000) From bench to clinic with apoptosis-based therapeutic agents. *Nature* **407**, 810-816.

Norimura T, S Nomoto, M Katsuki, Y Gondo and S Kondo (1996) p53-dependent apoptosis suppresses radiation-induced teratogenesis. *Nat. Med.* **2**, 577-580.

Oliver JE (1975) Microcephaly following baby battering and shaking. *Br. J. Med.* **2**, 262-264.

Piomelli D, A Giuffrida, A Calignano and F Rodriguez de Fonseca (2000) The endocannabinoid system as a target for therapeutic

drugs. *Trends Pharmacol. Sci.* **21**, 218-224.

Pohl D, P Bittigau, MJ Ishimaru, D Stadthaus, C Hubner, JW Olney, L Turski and C Ikonomidou (1999) *N*-Methyl-D-aspartate antagonists and apoptotic cell death triggered by head trauma in developing rat brain. *Proc. Natl. Acad. Sci. USA* **96**, 2508-2513.

Prins ML and D Hovda (1998) Traumatic brain Injury in the Developing rat: effects of maturation on Morris Water Maze Acquisition. *J. Neurotrauma* **15**, 799-811.

Prins ML, SM Lee, CL Cheng, DP Becker and DA Hovda (1996) Fluid percussion brain injury in the developing and adult rat: a comparative study of mortality, morphology, intracranial pressure and mean arterial blood pressure. *Brain Res. Dev. Brain Res.* **95**, 272-282.

Raghupathi R, DI Graham and TK McIntosh (2000) Apoptosis after traumatic brain injury. *J. Neurotrauma* **17**, 927-938.

Rich T, RL Allen and AH Wyllie (2000) Defying death after DNA damage. *Nature* **407**, 777-783.

Robertson CL, MJ Bell, PM Kochanek, PD Adelson, RA Ruppel, JA Carcillo, SR Wisniewski, Z Mi, KL Janeski, RS Clark, DW Marion, SH Graham and EK Jackson (2001) Increased adenosine in cerebrospinal fluid after severe traumatic brain injury in infants and children: association with severity of injury and excitotoxicity. *Crit. Care Med.* **29**, 2287-2293.

Savill J and V Fadok (2000) Corpse clearance defines the meaning of cell death. *Nature* **407**, 784-788.

Schlicker E and M Kathmann (2001) Modulation of transmitter release via presynaptic cannabinoid receptors. *Trends Pharmacol. Sci.* **22**, 565-572.

Shannon P, CR Smith, J Deck, LC Ang, M Ho and L Becker (1998) Axonal injury and the neuropathology of shaken baby syndrome. *Acta Neuropathol. (Berl.)* **95**, 625-31.

Shaver EG, AC Duhaime, M Curtis, LM Gennarelli and R Barret (1996) Experimental acute subdural hematoma in infant piglets. *Pediatr. Neurosurg.* **25**, 123-129.

Sosin DM, JE Sniezek and RJ Waxweiler (1995) Trends in death associated with traumatic brain injury, 1979 through 1992. Success and failure. *JAMA* **273**, 1778-1780.

Thomaidou D, MC Mione, JFR Cavanagh and JG Parnavelas (1997) Apoptosis and its relation to the cell cycle in the developing cerebral cortex. *J. Neurosci.* **17**, 1075-1085.

Thornberry NA and Y Lazebnik (1998) Caspases: enemies within. *Science* **281**, 1312-1316.

Thurman DJ, C Alverson, KA Dunn, J Guerrero and JE Sniezek (1999) Traumatic brain injury in the United States: a public health perspective. *J. Head Trauma Rehabil.* **14**, 602-615.

Vowles GH, CL Scholtz and JM Cameron (1987) Diffuse axonal injury in early infancy. *J. Clin. Pathol.* **40**, 185-189.

Wilson RI and RA Nicoll (2002) Endocannabinoid signaling in the brain. *Science* **296**, 678-682.

Wyllie AH, JFR Kerr and AR Currie (1980) Cell death: the significance of apoptosis. *Int. Rev. Cytol.* **68**, 251-306.

Xing J, DD Ginty and ME Greenberg (1996) Coupling of the RAS-MAPK pathway to gene activation by RSK2, a growth factor-regulated CREB kinase. *Science* **273**, 959-963.

Yakovlev AG, SM Knoblach, L Fan, GB Fox, R Goodnight and AI Faden (1997) Activation of CPP32-like caspases contributes to neuronal apoptosis and neurological dysfunction after traumatic brain injury. *J. Neurosci.* **17**, 7415-7424.

Yuan J and BA Yankner (2000) Apoptosis in the nervous system. *Nature* **407**, 802-809.

Zimmerman RA, LT Bilaniuk, D Bruce, I Schut, B Uzzell and HI Goldberg (1979) Computed tomography of craniocerebral injury in the abused child. *Neuroradiology* **130**, 687-690.

Neurobiology of Disease **11,** 231–245 (2002)
doi:10.1006/nbdi.2002.0521

Pathways Leading to Apoptotic Neurodegeneration Following Trauma to the Developing Rat Brain

Ursula Felderhoff-Mueser,* Marco Sifringer,† Stefanie Pesditschek,† Heike Kuckuck,† Axel Moysich,* Petra Bittigau,† and Chrysanthy Ikonomidou†

†*Department of Pediatric Neurology and* **Department of Neonatology, Charité Children's Hospital, Humboldt University, 13353 Berlin, Germany*

Received December 3, 2001; revised May 13, 2002; accepted for publication August 6, 2002

Trauma triggers diffuse apoptotic neurodegeneration in the developing rat brain. To explore the pathogenesis of this phenomenon we investigated the involvement of three possible mechanisms: death receptor activation, activation of the intrinsic apoptotic pathway by cytochrome *c* release into the cytoplasm, and changes in trophic support provided by endogenous neurotrophins. We detected a decrease in the expression of bcl-2 and bcl-x_L, two antiapoptotic proteins that decrease mitochondrial membrane permeability, an increase in cytochrome *c* immunoreactivity in the cytosolic fraction, and an activation of caspase-9 in brain regions which show apoptotic neurodegeneration following percussion brain trauma in 7-day-old rats. Increase in the expression of the death receptor Fas was revealed by RT-PCR analysis, Western blotting, and immunohistochemistry, as was activation of caspase-8 in cortex and thalamus. Apoptotic neurodegeneration was accompanied by an increase in the expression of BDNF and NT-3 in vulnerable brain regions. The pancaspase inhibitor z-VAD.FMK ameliorated apoptotic neurodegeneration with a therapeutic time window of up to 8 h after trauma. These findings suggest involvement of intrinsic and extrinsic apoptotic pathways in neurodegeneration following trauma to the developing rat brain. Upregulation of neurotrophin expression may represent an endogenous mechanism that limits this apoptotic process.

Key Words: **trauma; caspase; cytochrome *c*; death receptor; Fas; neurotrophin; brain development.**

INTRODUCTION

Traumatic brain injury is a major cause of morbidity in the pediatric population, with a high socioeconomic impact (Goldstein, 1990). Children under 6 years of age show the highest prevalence of brain trauma and the worst clinical outcomes (Koskiniemi *et al.,* 1995; Diamond, 1996; Adelson & Kochanek, 1998).

Two types of neurodegeneration can be triggered by trauma in the developing brain, excitotoxic and apoptotic. Whereas excitotoxic death shows a rapid time course, apoptosis occurs in a delayed fashion and affects brain areas distant from the site of primary impact (Pohl *et al.,* 1999). The magnitude of the apoptotic response to trauma is age dependent. In the young, most vulnerable age groups, this form of cell death decidedly determines the neuropathologic outcome (Bittigau *et al.,* 1999).

Apoptosis can be initiated by diverse signals and executed via different biochemical pathways (Hengartner, 2000). Triggers include growth factor deprivation, DNA damage, cytokine production, and activation of death receptors, as well as release of cytochrome *c* from the mitochondria into the cytoplasm. Although biochemical pathways differ considerably, they all converge upon activation of effector caspases (Krammer, 2000; Meier *et al.,* 2000; Nicholson, 2000; Rich *et al.,* 2000; Savill & Fadok, 2000; Yuan & Yankner, 2000).

An intrinsic and an extrinsic apoptotic pathway have been defined, the first initiated by release of cytochrome *c* into the cytoplasm and the second by

0969-9961/02 $35.00

activation of death receptors. Cytochrome *c* release leads to activation of effector caspases via recruitment of caspase-9 (Hengartner, 2000). Aggregation of the death receptor Fas (CD95/Apo-1), a member of the TNF-α superfamily, follows Fas ligand binding and leads to formation of a death-inducing signaling complex (DISC): Fas itself, an adapter protein, Fas-associated death domain, and the inactive form of caspase-8. After formation of the DISC, procaspase-8 is proteolytically cleaved, activated, and released from the DISC (Chinnaiyan *et al.*, 1995; Muzio *et al.*, 1996; Medema *et al.*, 1997; Krammer, 2000). Caspase-8 then activates downstream caspases, such as caspase-3, which execute the cell.

To investigate involvement of the intrinsic apoptotic pathway in the pathogenesis of apoptotic neurodegeneration following trauma to the developing brain, we used a well-described percussion trauma model in infant rats (Ikonomidou *et al.*, 1996; Bittigau *et al.*, 1999; Pohl *et al.*, 1999) and analyzed changes in the expression of antiapoptotic proteins of the bcl-2 group that decrease mitochondrial membrane permeability, changes in cytochrome *c* immunoreactivity in the cytosolic fraction, and changes in caspase-9 activity. To investigate involvement of the extrinsic pathway, Fas expression and caspase-8 activity in brain tissue were measured. To investigate the role of neurotrophins, endogenous mRNA levels for neurotrophin-3 (NT-3) and brain-derived neurotrophic factor (BDNF) were analyzed. Finally, to test the potential benefit of caspase inhibition in traumatic brain injury to the developing brain, the pancaspase inhibitor z-VAD.FMK was administered to infant rats and neurodegeneration was quantitated. Findings indicate that trauma leads to activation of the intrinsic and the extrinsic apoptotic pathways in the developing rat brain and that inhibition of effector caspases confers neuroprotection over a time window of at least 8 h after trauma.

MATERIAL AND METHODS

Traumatic Brain Injury

Seven-day-old Wistar rat pups (Bundesinstitut für Gesundheitlichen Verbraucherschutz und Veterinärmedizin BgVV, Berlin, Germany), weighing 13–16 g, were anesthetized with halothane (induced with 4% and maintained with 1.5% in balanced room air) and subjected to head trauma as previously described (Bittigau *et al.*, 1999; Pohl *et al.*, 1999). Following fixation of the animal's skull in a stereotaxic frame, a skin incision was made to expose the skull. The trauma device, which was integrated in the stereotaxic apparatus, consisted of a hollow stainless steel tube perforated at 1-cm intervals to prevent air compression. It guided a weight of 10 g which was allowed to fall from a height of 16 cm onto a mobile circular foot plate (2.00 mm in diameter) resting on the surface of the right parietal bone. The device was oriented perpendicular to the parietal bone with the center of the foot plate positioned 3 mm anterior and 2 mm lateral to lambda. The foot plate was first allowed to touch the skull and was then further depressed by 1.5 mm. Rats subjected to sham surgery served as controls.

Tissue Sampling

Animals were sacrificed at 2, 4, 6, 8, 12, 24, 48, and 72 h and 5 days after trauma. Animals whose brains were subjected to histological analysis received an overdose of intraperitoneal chloral hydrate and were transcardially perfused with heparinized 0.1 M PBS, pH 7.4, followed by 4% paraformaldehyde in 0.1 M cacodylate buffer, pH 7.4. Animal weights and brain weights were documented for each experiment. Brains were postfixed for 3 days at 4°C and processed for TUNEL (terminal deoxynucleotide transferase-mediated dUTP nick end-labeling), immunohistochemistry, or DeOlmos silver staining. For RT-PCR, Western blotting, and fluorescence activity assays, fresh tissue was prepared from the cingulate and parietal cortex, the striatum, and the thalamus, subsequently snap frozen in liquid nitrogen, and stored at −80°C until analysis.

All animal experiments were in accordance to the guidelines of Humboldt University in Berlin, Germany.

DeOlmos Cupric Silver Staining and TUNEL

Brains were embedded in agar and coronal sections of 70 μm thickness were serially cut on a Vibratome (Leica VT 1000 S; Nussloch, Germany) and processed for staining with silver nitrate and cupric nitrate according to the method of DeOlmos and Ingram (1971). Degenerating cells were identified by a distinct dark appearance due to the silver impregnation.

TUNEL staining was performed using the ApopTag Peroxidase kit (S 7100; Oncor Appligene, Heidelberg, Germany). Briefly, after pretreatment with proteinase K and quenching of endogenous peroxidase, sections were incubated first in equilibration buffer followed by working-strength TdT enzyme (incorporating

TABLE 1
Oligonucleotide Primer Sequences for RT-PCR Analysis

Gene	Sense primer	Nucleotide position	Antisense primer	Nucleotide position	GenBank Accession No.
Fas	5′-CCGACAACAACTGCTCAGA-3′	174	5′-GCACCTGCACTTGGTATTC-3′	430	D26112
Bcl-2	5′-TTATAAGCTGTCACAGAGG-3′	60–78	5′-TGAAGAGTTCCTCCACCAC-3′	388–406	U34964
Bel-x_L	5′-AATGTCTCAGAGCAACCGG-3′	19–37	5′-CTTCCGACTGAAGAGTGAG-3′	700–718	U34963
BDNF	5′-CGACGTCCCTGGCTGGACACTTTT-3′	2296–2318	5′-AGTAAGGGCCCGAACATACGATTGG-3′	2762–2786	D10938
NT-3	5′-GGTCAGAATTCCAGCCGATGATTGC-3′	308–332	5′-CAGCGCCAGCCTACGAGTTTGTTGT-3′	767–791	M34643
β-Actin	5′-CCCTAAGGCCAACCGTGAAAAGATG-3′	1663	5′-GAACCGCTCATTGCCGATAGTGATG-3′	2559	V01217

digoxigenin-labeled dUTP nucleotides to free 3′-OH DNA termini) (1 h, 37°C). Sections were incubated in stop / wash buffer (30 min, 37°C) and then with anti-digoxigenin–peroxidase conjugate (30 min) followed by diaminobenzidene (DAB) substrate (Sigma, Deisenhofen, Germany).

Immunohistochemistry for Fas and BDNF

Brains were embedded in paraffin and coronal sections, 10 μm thick, were cut on a Microtome HM 360 (Microm) and mounted onto 3-aminopropyltrietoxylane-coated (Sigma) glass slides. Paraffin-embedded sections were microwaved in 10 mM citrate buffer, pH 6.5, at 750 W as previously described (Shi *et al.*, 1997). Endogenous peroxidase activity was blocked with 0.6% v / v hydrogen peroxide (15 min), and sections were incubated with normal goat serum (20 min) and left overnight at 4°C with rabbit polyclonal Fas or rabbit polyclonal BDNF antibody (Santa Cruz, CA; Fas M20, 1:2500; BDNF N20, 1:100). Negative controls were performed by including the peptide immunogen as a competitor of antibody binding according to the manufacturer's instructions. Sections were then treated with a goat anti-rabbit IgG. After detection with the ABC kit (Vector Laboratories, Peterborough, UK), positive cells were visualized with DAB (Sigma) and counterstained with hematoxylin–eosin.

RT-PCR for bcl-2, bcl-x_L, Fas, BDNF, and NT-3

Total cellular RNA was isolated from snap-frozen tissue by acidic phenol / chloroform extraction (Chomczynski & Sacchi, 1987) and DNase treated (Hybaid-GmbH; Roche Diagnostics GmbH, Mannheim, Germany); 200 ng of RNA was reverse transcribed with Moloney murine leukemia virus reverse transcriptase (Promega, Madison, WI) in 25 μl of reaction mixture. The resulting cDNA (2 μl) was amplified by polymerase chain reaction. The oligonucleotide primers used for the PCR for rat bcl-2, bcl-x_L, Fas, BDNF, and NT-3 and the internal standard β-actin are summarized in Table 1. cDNA was amplified in 35 cycles, consisting of denaturing for 30 s at 94°C, annealing for 45 s at 55°C, and primer extension for 45 s at 72°C. Amplified cDNA was subjected to polyacrylamide gel electrophoresis, subsequent silver staining (Lohmann *et al.*, 1995), and densitometric analysis.

Western Blotting for Cytochrome c, bcl-x_L, and Fas

Snap-frozen tissue was homogenized in 1% SDS buffer (pH 7.3, containing 250 mM EDTA and 1 tablet protease inhibitor Boehringer Complete; Roche Diagnostics GmbH, Mannheim, Germany), heated to 90°C, and centrifuged at 15,000*g* (10 min). The supernatant was used as the cytosolic fraction. Total cellular proteins (50–100 μg / lane cytosolic fraction) were separated on a 10% polyacrylamide gel and transferred onto nitrocellulose membrane (Hybond ECL; Amersham International, Buckinghamshire, UK). Primary incubations (12 h, 4°C) were with a mouse monoclonal antibody specific for cytochrome *c* (Pharmingen, Heidelberg, Germany; 1:1000), a mouse monoclonal antibody for Fas (Transduction Laboratories, Heidelberg, Germany; 1:1000), or a rabbit polyclonal antibody for bcl-x_L (Santa Cruz, CA; 1:1000). Secondary incubations were with HRP-linked anti-mouse (for cytochrome *c* and Fas) or anti-rabbit IgG (for bcl-x_L) (1:1000). Positive signals were visualized using enhanced chemiluminescence (Amersham International) and serial exposures were made to radiographic film (Hyperfilm ECL; Amersham International).

Measurements of Caspase-8 and Caspase-9 Enzymatic Activity

The fluorometric caspase-8 and caspase-9 activity assays (Oncogene Research Products, Bad Schwalbach, Germany) take advantage of the specificity of

the enzymes for cleavage of aspartate residues in a particular peptide sequence, present in the substrates IETD (caspase-8) and LEHD (caspase-9). For detection the substrate is labeled with the fluorescent molecule 7-aminotrifluoromethyl coumarin (AFC). Reaction can be monitored by a blue to green shift in fluorescence upon cleavage of the AFC fluorophore.

Frozen tissue from the cingulate cortex and the thalamus was homogenized in extraction buffer (Tris 50 mM, EDTA 5 mM, Triton 1%, KCl 0.166 M, leupeptin 0.5 mg/ml, pepstatin 1 mg/ml, PMSF 0.2 mM, adjusted to pH 8.0) (50 μg of tissue/500 μl volume). Protein concentrations were adjusted to 5 mg/ml and homogenates were diluted in 50 μl extraction buffer/1% 1 M dithiothreitol solution, incubated at room temperature (15 min), and centrifuged (500*g*). Fifty microliters of the lysates was transferred to 96-well microliter plates and an equal volume of assay buffer was added. Following a 2-h incubation with the caspase substrate conjugate AFC, samples were analyzed with a Dynatech G 2.0 fluorometer (Dynex, Frankfurt, Germany), at 400-nm excitation and 505-nm emission wavelengths. Recombinant caspase-8 and -9 served as positive controls. According to the manufacturer's instructions, data are expressed in relative fluorescent units (RFU), which reflect the intensity of the fluorescence signal following subtraction of the signal of the appropriate buffer controls.

Intracerebral Administration of Caspase Inhibitor

To determine whether caspase inhibition mitigates damage following trauma, the tripeptide *N*-benzyloxycarbonyl-Val-Ala-Asp-fluoromethylketone (z-VAD.FMK) (Bachem, Heidelberg, Germany), a broad spectrum caspase inhibitor, was administered. Animals were randomized to receive z-VAD.FMK diluted in 2 μl DMSO intracerebroventricularly (icv) at 2, 4, and 8 h after head trauma at doses of 0.1–10 μg. Controls were subjected to injection with an equal volume of DMSO. For icv injections, rats were subjected to halothane anesthesia and fixed in a stereotaxic frame. A skin incision was performed to expose the skull, and the parietal bone was penetrated using a Hamilton syringe (30-gauge needle) at the stereotaxic coordinates of 1 mm anterior and 1 mm lateral to bregma. A total volume of 2 μl was slowly injected over 2 min into the right lateral ventricle. To exclude a potentially toxic effect of the injection procedure, a number of sham-operated rats received intracerebroventricular injections of 2 μl normal saline.

At 24 h, 48 h, 5 days, and 7 days following the insult animals were transcardially perfused and brain tissue was processed for histology. Animals were weighed daily and brain weights were documented at the end of each experiment.

Quantitation of Neurodegeneration in Different Brain Regions

Following administration of z-VAD.FMK, degenerating cells were determined in sections (70 μm) stained by the DeOlmos cupric–silver method in the frontal, parietal, cingulate, retrosplenial cortex; caudate nucleus (mediodorsal part); thalamus (laterodorsal, mediodorsal, ventral nuclei); hippocampal dentate gyrus; and subiculum by means of stereological disector (West & Gundersen, 1990), estimating mean numerical cell densities (N_v) of degenerating cells (cells/mm^3). An unbiased counting frame (0.05 $\times$ 0.05 mm, disector height 0.07 mm) and a high aperture objective were used for the sampling. The N_v for each brain region was determined with 8 to 10 disectors. To assess overall severity of damage and enable comparisons among treatment groups, a scoring system was created as follows: In each hemisphere, 14 regions were analyzed by using the stereological disector to determine the mean numerical densities of degenerated cells in each brain region. Each region was subsequently given a number of points (score: 1000 degenerating cells/mm^3 reflects a score of 1000) and scores from all evaluated regions were added to give a cumulative severity score for degeneration within each brain.

RESULTS

Histological Evaluation of Apoptotic Neurodegeneration after Trauma in the 7-Day-Old Rat Brain

Rats subjected to sham surgery (n = 10) or trauma (n = 15) recovered within 10 min after anesthesia. There was no mortality. At 24 h following percussion head trauma in 7-day-old rats, widespread cell death was detected by silver and TUNEL staining in the frontal, parietal, cingulate, and retrosplenial cortex; the thalamus; the dentate gyrus; the subiculum; and the striatum (Figs. 1A–1C). Degeneration occurred bilaterally, with the side ipsilateral to the trauma being more severely affected. TUNEL staining displayed a similar distribution pattern of degenerating cells as

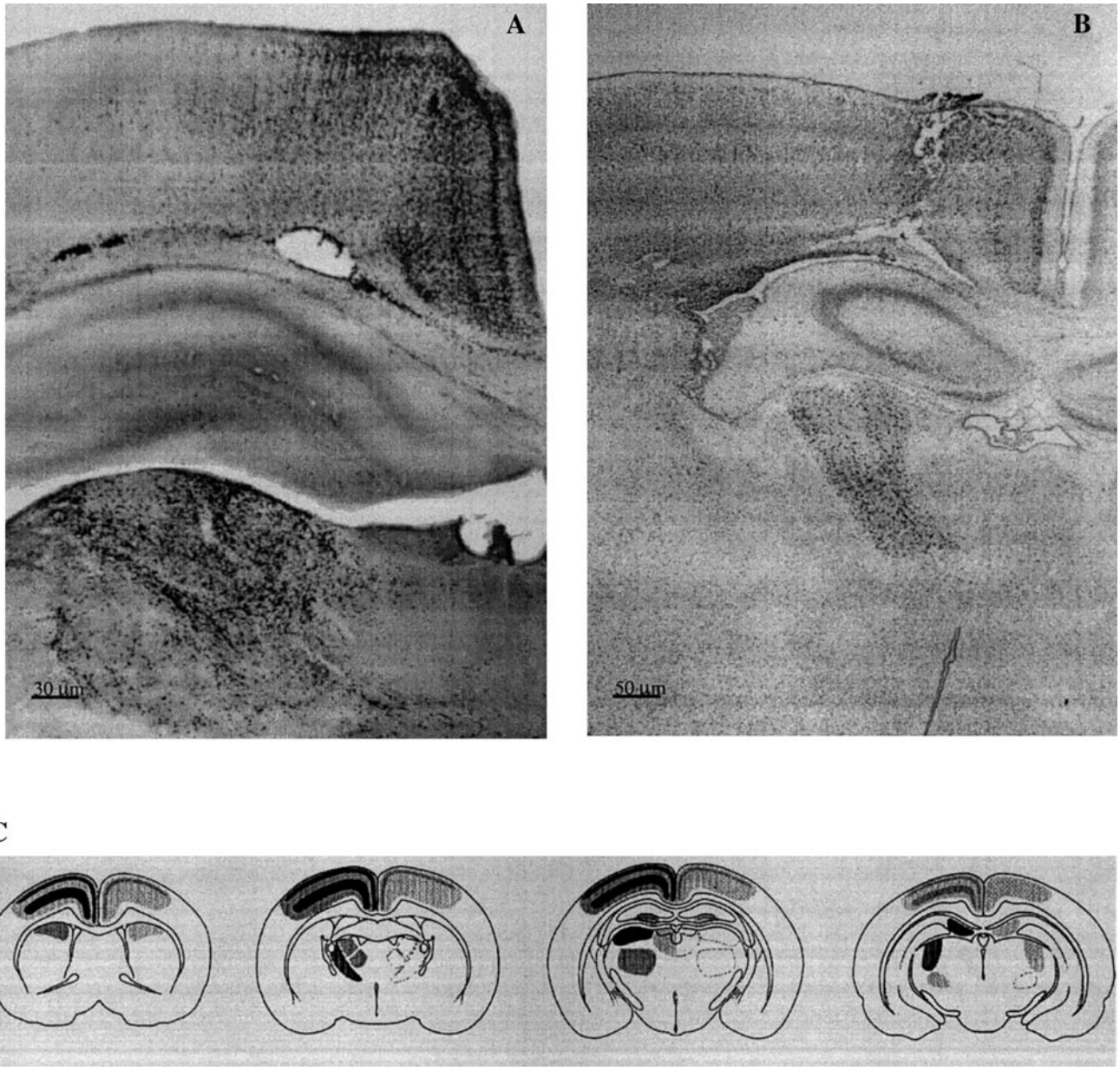

FIG. 1. Light micrographs illustrating silver-positive (A; DeOlmos cupric–silver staining) and TUNEL-positive (B) cells in the brains of 8-day-old rats subjected to head trauma on day 7. (C) Schematic illustration depicting the distribution pattern of silver-positive cells (shaded areas) in the brain at 24 h after trauma. Darker shades indicate higher densities of degenerating cells. Rats were traumatized on postnatal day 7.

silver staining, confirming that nuclear DNA fragmentation occurred (Fig. 1B). Previously, we reported that brain trauma to 7-day-old rats initially triggers an excitotoxic lesion which remains localized at the impact site in the parietal cortex. This excitotoxic lesion has a rapid evolution, reaches a peak at 4 h after trauma, and subsides thereafter (Pohl *et al.*, 1999). Subsequently and starting at 6 h after trauma a delayed neurodegenerative response becomes evident in the parietal cortex at the impact site but also in many other brain regions distant to the site of impact. We have provided a detailed description of the distribution pattern and time course of this delayed neurodegenerative response to brain trauma in 7-day-old rats,

which reaches a peak at 24 h after trauma and subsides thereafter. We have presented evidence obtained from parallel vibratome sections indicating that silver staining and TUNEL staining depict comparable distribution patterns and densities of degenerating cells in affected brain regions (Bittigau *et al.*, 1999). Furthermore, we have performed a detailed analysis of this delayed neurodegenerative response to trauma by electron microscopy, which has confirmed that neurons which degenerate in a disseminated and delayed fashion in the 7-day-old rat brain fulfill ultrastructural criteria for apoptosis (Bittigau *et al.*, 1999). In addition, we have reported that marked activation of caspase 3 occurs in affected brain regions. This morphological and biochemical evidence will not be presented here in more detail but it represents the basis for our assumption that, in the study outlined here, we have been investigating mechanisms pertaining solely to apoptotic neurodegeneration following trauma to the developing rat brain.

Activation of the Intrinsic Apoptotic Pathway by Trauma

Downregulation of the expression of antiapoptotic genes. The expression of bcl-2 and bcl-x_L, two proteins with antiapoptotic properties which have been shown to decrease mitochondrial membrane permeability, was first investigated at the transcriptional level. mRNA levels for bcl-2 and bcl-x_L were analyzed using semiquantitative RT-PCR in the laterodorsal thalamus, cingulate cortex, and striatum of sham-operated controls and rats subjected to head trauma at the age of 7 days at 0 ($n = 4$ per group), 2 ($n = 4$ per group), 4 ($n = 4$ per group), 8 ($n = 4$ per group), 12 ($n = 4$ per group), 24 ($n = 4$ per group), 48 ($n = 3$ per group), and 120 ($n = 3$ per group) h after trauma. Polyacrylamide gels were subjected to densitometric analysis and density ratios (bcl-2 and bcl-x_L in reference to β-actin) were statistically analyzed. Trauma triggered marked and rapid downregulation in the expression of bcl-2 and bcl-x_L, which was evident within 2 h following the insult, persisted up to 48 h, and demonstrated a slow, incomplete recovery by 120 h after trauma. In Figs. 2A and 2B downregulation of bcl-2 and bcl-x_L in the thalamus is shown. Two-way ANOVA revealed that trauma had a highly significant effect on the mRNA levels for bcl-2 [$F(7,44) = 40.9$, $P < 0.001$] and bcl-x_L [$F(7,44) = 31.71$, $P < 0.001$] in the thalamus. There was a significant effect of time (posttraumatic interval) on the mRNA levels for bcl-2 [$F(1,44) = 155.1$, $P < 0.001$] and bcl-x_L [$F(1,44) = 648.8$] in the thalamus as well (Fig. 2B). Similar findings were obtained in the cingulate cortex and the striatum.

To further confirm downregulation of bcl-2 family members at the protein level, immunoreactivity of bcl-x_L was analyzed by Western blotting in brain extracts from thalamus, striatum, and cortex. Seven-day-old rats were examined at 4 ($n = 4$ per group), 12 ($n = 4$ per group), and 24 ($n = 4$ per group) h after trauma. Decreased levels of bcl-x_L protein were found in the ipsilateral thalamus at 4, 12, and 24 h after trauma (Fig. 2C). Analysis of protein samples from striatum and cortex revealed similar results.

Cytochrome c release and caspase-9 activation. To determine whether head trauma induces release of cytochrome *c* into the cytoplasm, cytochrome *c* immunoreactivity was analyzed by Western blotting in the cytosolic fraction of brain extracts from thalamus, striatum, and cortex of 7-day-old rats subjected to head trauma. Analysis was performed in sham-operated rats ($n = 3$) and rats subjected to head trauma at 2 ($n = 3$), 4 ($n = 3$), and 12 ($n = 3$) h after trauma. Cytochrome *c* immunoreactivity increased at 2 h and was most pronounced at 4 h after trauma in the cytosolic fraction (Fig. 2D). It should be noted here that at 4 h after trauma no signs of delayed neurodegeneration are detectable in the thalamus, cingulate cortex, or striatum by histological techniques.

The activity of the initiator caspase-9 was measured using the specific substrate (LEHD) in sham-operated rats and rats subjected to head trauma, at 4 ($n = 6$ per group), 12 ($n = 6$ per group), and 24 ($n = 6$ per group) h after trauma in the thalamus. Two-way ANOVA revealed that trauma had a highly significant effect on caspase-9 activity in the thalamus [$F(1,30) = 17.56$, $P < 0.001$]. Activity of caspase-9 was also dependent on posttraumatic interval [$F(2,30) = 3.57$, $P < 0.05$]. Compared to sham-operated rats, there was a significant increase in caspase-9 activity in the thalamus in 7-day-old rats subjected to head trauma, at 12 ($P < 0.001$) and 24 h ($P < 0.01$; Bonferroni/Dunn test) after trauma (Fig. 2E).

Apoptosis by Death Receptor Following Trauma to the Developing Brain

Increase in expression of Fas and activation of caspase-8. Changes in Fas expression following trauma to the 7-day-old rat brain were determined at defined time points postinjury using RT-PCR. Western blotting, and immunohistochemistry. RT-PCR was performed in samples from the laterodorsal thalamus, the cingulate cortex, and the striatum of sham-operated rats

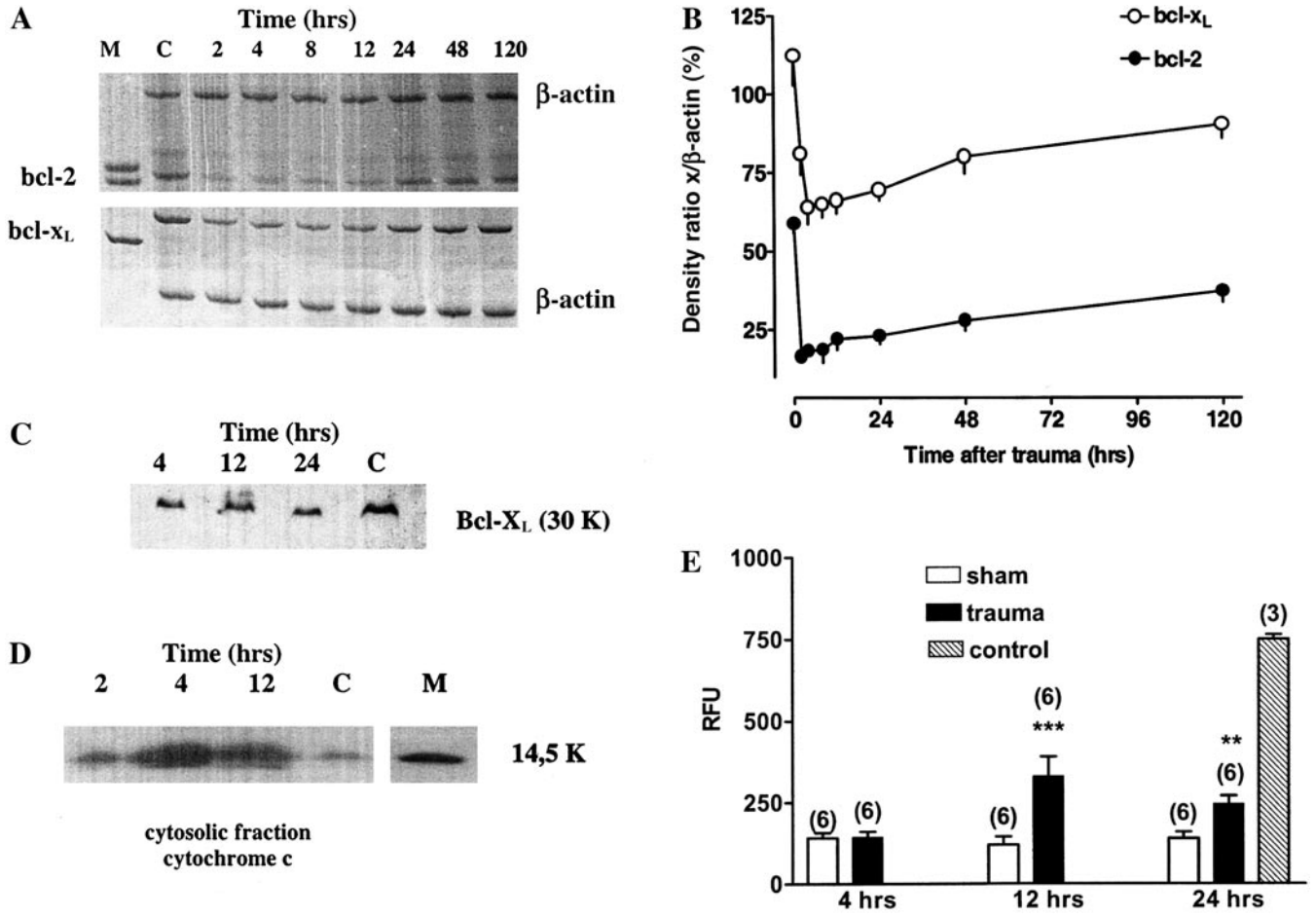

FIG. 2. Evidence implicating involvement of the intrinsic apoptotic pathway in neurodegeneration following trauma to the developing rat brain. (A) Bcl-2 and bcl-x_L mRNA expression in right thalamus (ipsilateral to trauma site) in a sham-operated rat at 0 h after trauma (C) and in rats subjected to head trauma at 2, 4, 8, 12, 24, 48, and 120 h after trauma. mRNA was reverse transcribed to cDNA, amplified by polymerase chain reaction using specific primers for bcl-2, bcl-x_L, and β-actin, and subjected to polyacrylamide gel electrophoresis and silver staining. There is an obvious decrease in mRNA levels for both bcl-2 and bcl-x_L. This is a representative gel from a series performed to analyze bcl-2 and bcl-x_L mRNA expression (see Results). In (B) the results of densitometric analysis of the gels from traumatized rats are presented in reference to β-actin. Data represent the ratio (%) of the density of the bcl-2 or bcl-x_L band to the β-actin band $\pm$ SEM. Two-way ANOVA revealed that trauma had a highly significant effect on the mRNA levels for bcl-2 [$F(7,44) = 40.9$, $P < 0.001$] and bcl-x_L [$F(7,44) = 31.71$, $P < 0.001$] in the thalamus. There was a highly significant effect of time (posttraumatic interval) on the mRNA levels for bcl-2 [$F(1,44) = 155.1$, $P < 0.001$] and bcl-x_L [$F(1,44) = 648.8$] in the thalamus as well, compared to sham-operated rats. (C) Western blot analysis of bcl-x_L immunoreactivity in brain extracts taken from the thalamus of a sham-operated rat (C) and rats traumatized on day 7, at 4, 12, and 24 h after trauma. There is a decrease in bcl-x_L immunoreactivity at 4 h after trauma. These blots are representative of a series performed on thalamus, striatum, and cortex. (D) Western blot analysis of cytochrome *c* immunoreactivity in the cytoplasmic fractions of brain extracts taken from the thalamus of a sham-operated rat (C) and rats traumatized on day 7, at 2, 4, and 12 h after trauma. There is an increase in cytochrome *c* immunoreactivity in the cytosolic fraction by 2 h after trauma. These blots are representative of a series performed to analyze cytosolic cytochrome *c*. (E) Caspase-9 activity in cytosolic protein extracts from thalamus of sham-operated rats and rats subjected to head trauma. Specimens were analyzed at 4, 12, and 24 h after trauma or sham surgery. Caspase-9-like activity was measured fluorometrically, using the specific substrate LEHD and by determining accumulation of free aminotrifluoromethyl coumarin. Data are expressed in relative fluorescence units (RFU) as means $\pm$ SEM after subtraction of the appropriate buffer controls. The numbers in parentheses represent the number of specimens in each group. Two-way ANOVA revealed that trauma had a highly significant effect on caspase-9 activity in the thalamus [$F(1,30) = 17.56$, $P < 0.001$]. Activity of caspase-9 was also dependent on time after trauma [$F(2,30) = 3.57$, $P < 0.05$]. Compared to sham-operated rats, there was a significant increase in caspase-9 activity in the thalamus in 7-day-old rats subjected to head trauma at 12 ($P < 0.001$) and 24 h ($P < 0.01$; Bonferroni / Dunn test) after trauma. The gray column depicts recombinant caspase-9 activity which served as control.

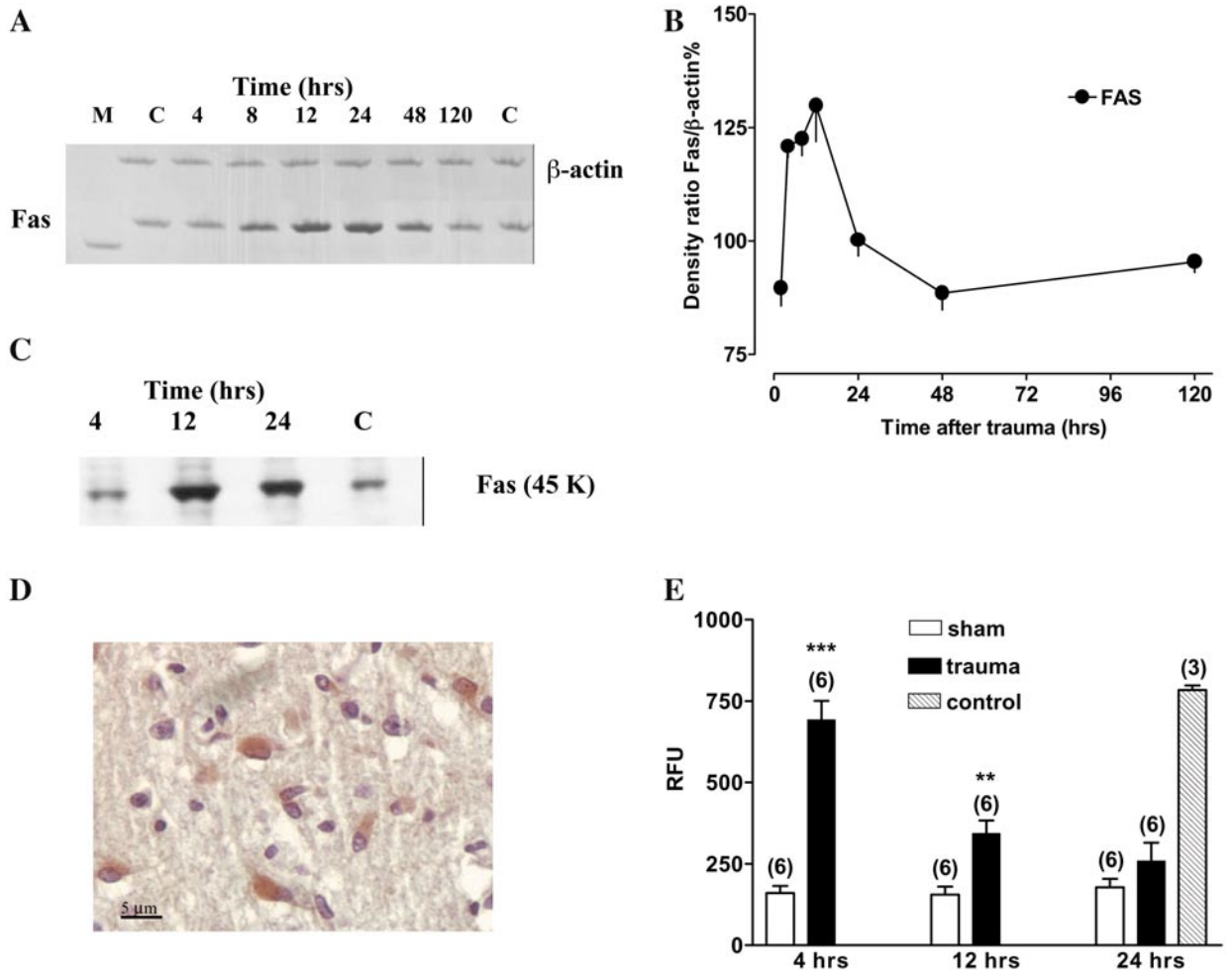

FIG. 3. Evidence implicating involvement of Fas receptor in apoptotic neurodegeneration following trauma to the developing rat brain. (A) Fas mRNA expression in the right thalamus in a sham-operated control rat (C) and in rats subjected to head trauma, at 4, 8, 12, 24, 48, and 120 h after trauma. mRNA was reverse transcribed to cDNA and amplified by polymerase chain reaction using specific primers for Fas and β-actin. There was an increase in mRNA levels for Fas at 4 h, peaking at 12 h after the insult and lasting up to 24 h. The β-actin band showed equal signal intensity in all columns, verifying cDNA integrity. In (B) the results of densitometric analysis of the gels (right thalamus) from traumatized rats are presented in reference to β-actin. Data represent the ratio (%) of the density of the Fas band to the β-actin band $\pm$ SEM. Comparison between sham-operated rats and rats subjected to brain trauma by ANOVA revealed that trauma had a highly significant effect on Fas mRNA levels in the thalamus [$F(1,44) = 804.5$, $P < 0.001$]. mRNA levels for Fas were also dependent on time after trauma [$F(7,44) = 54.39$, $P < 0.001$]. (C) Western blot analysis for Fas in brain extracts prepared from the thalamus of a sham-operated rat (C) and rats traumatized on day 7, at 4, 12, and 24 h after trauma. Representative blot of a series performed (thalamus, striatum, cortex), demonstrating an increase in Fas protein expression 4 h after trauma in the ipsilateral thalamus. (D) Light micrograph depicting Fas receptor expression on cortical neurons 24 h following trauma by means of immunohistochemistry, using a rabbit polyclonal antibody (M20). Binding (dark orange color) was visualized using a biotinylated secondary antibody in combination with the ABC method with DAB as a substrate. (E) Caspase-8 activity in cytosolic protein extracts from the right thalamus in rats subjected to head trauma compared to sham-operated rats. Specimens were analyzed at 4, 12, and 24 h after trauma or sham surgery. Caspase-8-like activity was measured fluorometrically using the specific substrate IETD and by determining accumulation of free aminotrifluoromethyl coumarin. Data are expressed in relative fluorescence units (RFU) as the mean ratios $\pm$ SEM of signal obtained in specimens from traumatized and sham-operated brains after subtraction of the appropriate buffer controls. The numbers in parentheses represent the number of specimens in each group. Two-way ANOVA revealed that trauma had a highly significant effect on caspase-8 activity in the thalamus [$F(1,30) = 63.27$, $P < 0.001$]. Activation of caspase-8 was dependent on time after trauma [$F(2,30) = 14.94$, $P < 0.001$]. Compared to sham-operated rats, there was an increase in caspase-8 activity in the thalamus in 7-day-old rats subjected to head trauma at 4 ($P < 0.001$) and 12 h ($P < 0.01$; Bonferroni/Dunn test) after trauma (D). The gray column depicts recombinant caspase-8 activity, which served as control.

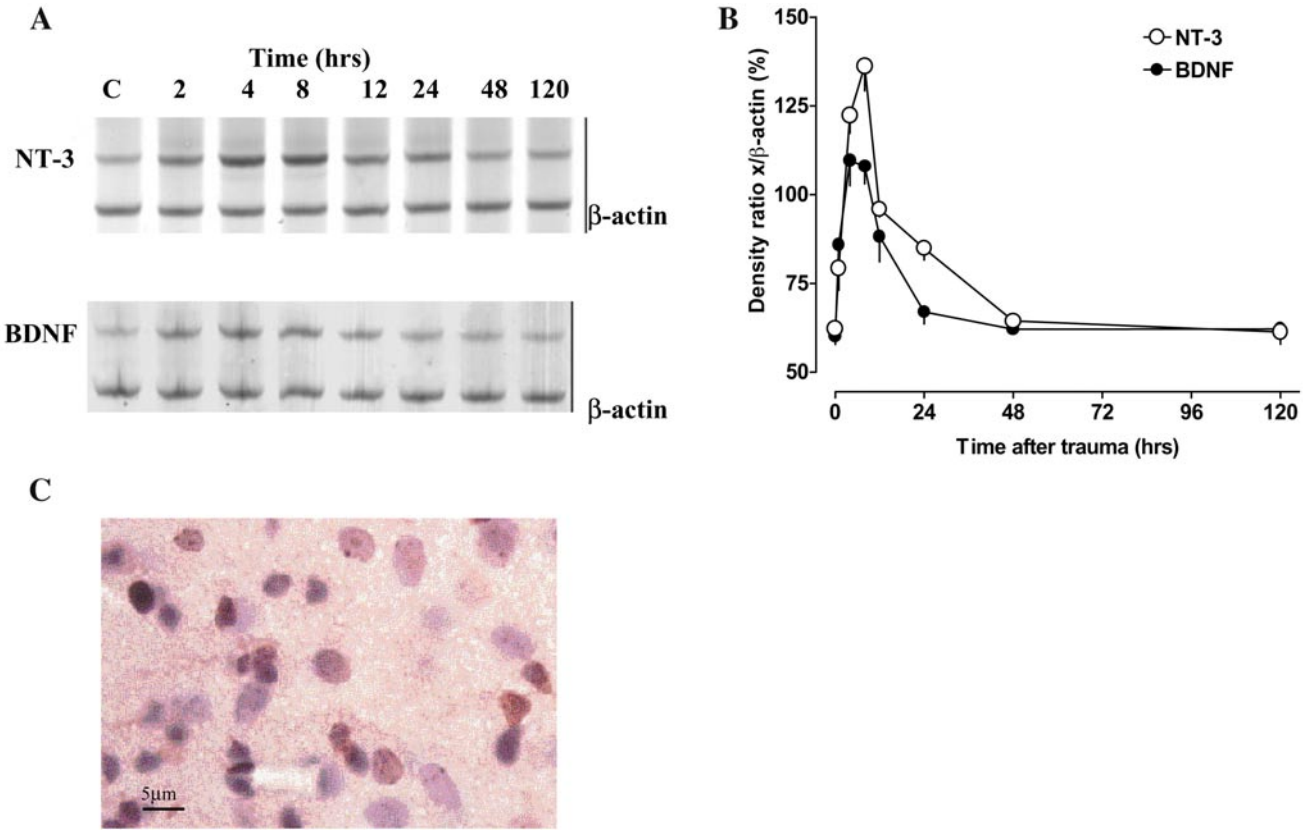

FIG. 4. Upregulation of brain-derived neurotrophic factor and neurotrophin-3 following trauma to the 7-day-old rat brain. (A) BDNF and NT-3 mRNA expression in right thalamus (ipsilateral to trauma site) in a sham-operated rat (C) at 0 h after surgery and in rats subjected to head trauma, at 2, 4, 8, 12, 24, 48, and 120 h after trauma. mRNA was reverse transcribed to cDNA and amplified by polymerase chain reaction using specific primers for BDNF, NT-3, and β-actin. There is an increase in mRNA levels for both neurotrophins at 4 h, with peaks between 4 and 8 h after the insult and decline to control values by 48 h after trauma. The β-actin band shows equal signal intensity in all columns, verifying cDNA integrity. In (B) the results of densitometric analysis of the gels from traumatized rats are presented in reference to β-actin. Data represent the ratio (%) of the density of the BDNF or NT-3 band to the β-actin band $\pm$ SEM at different time points after trauma. Two-way ANOVA revealed that trauma had a highly significant effect on BDNF and NT-3 mRNA levels in the thalamus compared to sham-operated rats [$F_{\text{BDNF}}(1,44) = 185.1$, $P < 0.001$; $F_{\text{NT-3}}(1,44) = 513.9$, $P < 0.001$]. mRNA levels for BDNF and NT-3 were also dependent on time after trauma [$F_{\text{BDNF}}(7,44) = 34.65$, $P < 0.001$; $F_{\text{NT-3}}(7,44) = 87.1$, $P < 0.001$). (C) Light micrograph showing BDNF expression in cortical neurons 24 h following trauma by means of immunohistochemistry, using a rabbit polyclonal antibody (N20). Binding (dark orange color) was visualized using a biotinylated secondary antibody in combination with the ABC method with DAB as a substrate.

and rats subjected to head trauma at the age of 7 days, at 0 ($n = 4$ per group), 2 ($n = 4$ per group), 4 ($n = 4$ per group), 8 ($n = 4$ per group), 12 ($n = 4$ per group), 24 ($n = 4$ per group), 48 ($n = 3$ per group), and 120 ($n = 3$ per group) h after trauma. Polyacrylamide gels were subjected to densitometric analysis, and density ratios (Fas in reference to β-actin) were statistically analyzed. Trauma triggered increase in Fas mRNA in the thalamus (Figs. 3A and 3B) ipsilateral to the trauma site. Fas mRNA levels showed significant elevation at 4 h which lasted up to 24 h with a peak at 8–12 h. They subsequently decreased to pretrauma levels (Fig. 3B). Two-way ANOVA revealed that trauma had a highly significant effect on Fas mRNA levels in the thalamus [$F(1,44) = 804.5$, $P < 0.001$]. mRNA levels for Fas were also dependent on time after trauma [$F(7,44) = 54.39$, $P < 0.001$]. In the contralateral side, increase in Fas mRNA levels was not significant. In Figs. 3A and 3B upregulation of Fas mRNA is shown in the thalamus; similar findings were obtained in the cingulate cortex and the striatum.

Protein levels of Fas were analyzed by means of Western blotting in brain extracts from thalamus, striatum, and cortex. Seven-day-old rats were examined at 4 ($n = 4$ per group), 12 ($n = 4$ per group), or 24 ($n = 4$ per group) h after trauma. Increased protein levels of

Fas were found in the ipsilateral thalamus at 4 h after trauma, with this increase being most pronounced at 12 and 24 h after trauma (Fig. 3C). Protein analysis in samples from striatum and cortex revealed similar results.

In the intact developing brain there is moderate physiological expression of Fas (Chema *et al.*, 1999; Felderhoff-Mueser *et al.*, 2000). We analyzed Fas immunoreactivity in paraffin-embedded brain sections in 7-day-old rats subjected to head trauma at 4 ($n = 3$), 12 ($n = 3$), and 24 h ($n = 3$) after trauma. Fas immunoreactivity increased particularly in the cortex and in the thalamus ipsilateral to the injury starting at 4 h after trauma (Fig. 3D). Fas immunostaining was also detected in the ventral, mediodorsal, and laterodorsal thalamus. Only moderate increase in Fas immunoreactivity was observed in the contralateral hemisphere. At 48 h, reduction of Fas immunoreactivity occurred in affected brain regions, possibly reflecting evacuation of cells that overexpressed the receptor.

To confirm activation of the extrinsic apoptotic pathway following trauma, caspase-8 activity was measured fluorometrically using the specific caspase-8 substrate IETD. Measurements of caspase-8 activity were performed in the thalamus in sham-operated rats and rats subjected to head trauma, at 4 ($n = 6$ per group), 12 ($n = 6$ per group), and 24 ($n = 6$ per group) h after trauma. Two-way ANOVA revealed that trauma had a highly significant effect on caspase-8 activity in the thalamus [$F(1,30) = 63.27$, $P < 0.001$]. Activation of caspase-8 was also dependent on time after trauma [$F(2,30) = 14.94$, $P < 0.001$]. Compared to sham-operated rats, there was an increase in caspase-8 activity in the thalamus in 7-day-old rats subjected to head trauma at 4 ($P < 0.001$) and 12 h ($P < 0.01$; Bonferroni/Dunn test) after trauma (Fig. 3E).

Trauma triggers transcription of neurotrophins. mRNA levels of BDNF and NT-3 were analyzed by RT-PCR in samples from the laterodorsal thalamus, the cingulate cortex, and the striatum of sham-operated rats and rats subjected to head trauma at the age of 7 days, at 0 ($n = 4$ per group), 2 ($n = 4$ per group), 4 ($n = 4$ per group), 8 ($n = 4$ per group), 12 ($n = 4$ per group), 24 ($n = 4$ per group), 48 ($n = 3$ per group), and 120 ($n = 3$ per group) h after trauma. Trauma triggered an increase in NT-3 and BDNF mRNA in the thalamus (Figs. 4A and 4B). This effect was evident at 2–4 h after trauma. Levels of BDNF and NT-3 demonstrated a peak at 8 h after trauma and returned to basal levels by 48 h (Figs. 4A and 4B). Two-way ANOVA revealed that trauma had a highly significant effect on BDNF and NT-3 mRNA levels in the thalamus [$F_{BDNF}(1,44) = 185.1$, $P < 0.001$; $F_{NT\text{-}3}(1,44) = 513.9$, $P < 0.001$]. mRNA levels for BDNF and NT-3 were also dependent on time after trauma [$F_{BDNF}(7,44) = 34.65$, $P < 0.001$; $F_{NT\text{-}3}(7,44) = 87.1$, $P < 0.001$]. In Figs. 4A and 4B upregulation of BDNF and NT-3 mRNA is shown in the thalamus; similar findings were obtained in the cingulate cortex and the striatum.

In addition, we analyzed BDNF immunoreactivity in paraffin-embedded brain sections in 7-day-old rats subjected to head trauma, at 4 ($n = 3$), 12 ($n = 3$), and 24 h ($n = 3$) after trauma. BDNF immunoreactivity was quite prominent in the cortex ipsilateral to the injury at 24 h after trauma (Fig. 4C). Immunostaining was also detected in the ventral, mediodorsal, and laterodorsal thalamus on the trauma side.

Treatment with z-VAD.FMK reduces trauma-induced apoptotic cell death. In a first step we wanted to determine whether icv injection of saline, vehicle, or z-VAD.FMK in sham-operated 7-day-old rats caused degenerative changes in the brains. For this purpose, saline (2 μl), DMSO (2 μl), or z-VAD.FMK (1 μg) dissolved in 1% DMSO was injected icv into sham-operated rats at 2 h after surgery. Histological analysis of the brains by means of DeOlmos silver staining revealed that injection of saline ($n = 5$), 1% DMSO ($n = 5$), or z-VAD.FMK ($n = 5$) into the lateral ventricle of sham-operated 7-day-old rats did not cause neurodegeneration at 24 h after surgery.

To assess the neuroprotective potential of caspase inhibition in traumatic brain injury in infant rats, the pancaspase inhibitor z-VAD.FMK was administered icv to 7-day-old rats in doses of 0.1 ($n = 6$), 0.5 ($n = 5$), 1 ($n = 5$), and 10 ($n = 5$) μg at 2 h after trauma and the brains were analyzed at 24 h after trauma by means of DeOlmos silver staining. Vehicle-treated rats ($n = 6$) received icv injection of 1% DMSO at 2 h after trauma. Estimation of numerical densities of degenerating cells was performed by means of disector stereology in 14 brain regions as described under Material and Methods. ANOVA revealed that treatment with z-VAD.FMK had a significant effect on severity of apoptotic brain damage following trauma ($F[5,30] = 30.06$, $P < 0.001$). Rats receiving a single dose of z-VAD.FMK displayed a reduction in cumulative scores for degenerating cells (Figs. 5A and 5B) compared to rats subjected to head trauma and icv injection of saline. Pairwise comparisons revealed that the minimal effective dose of z-VAD.FMK was 0.5 μg, with maximal neuroprotection achieved at 1 μg. Doses up to 10 μg were administered without further effect (Fig. 5B). This neuroprotective effect was evident in all brain regions analyzed (cortex, thalamus, striatum, hippocampus)

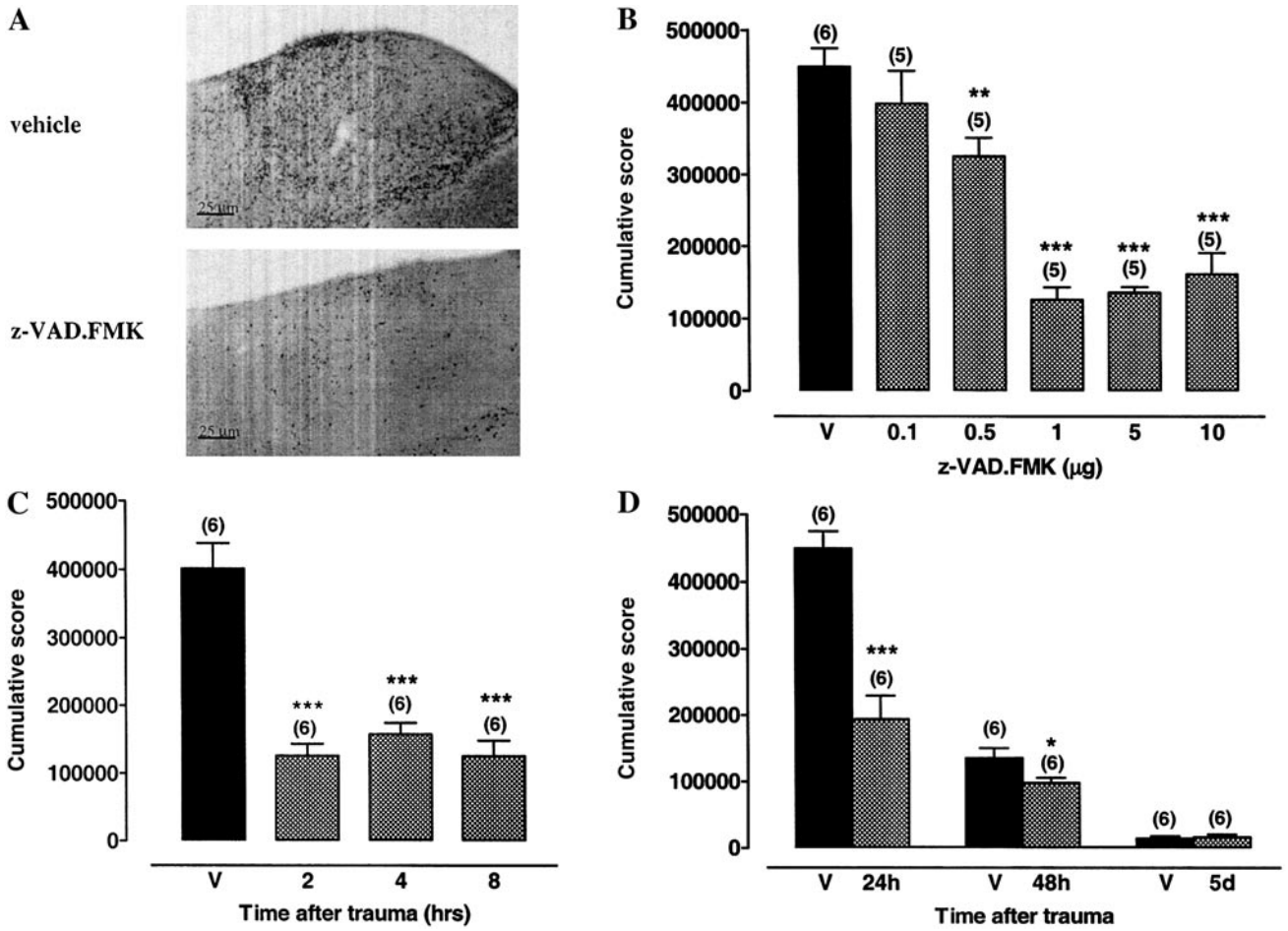

FIG. 5. Prevention of apoptotic cell death by the pancaspase inhibitor z-VAD.FMK. z-VAD.FMK was administered icv to 7-day-old rats at various time points after trauma. (A) Light micrographs depicting laterodorsal thalamic nuclei in the brains of 7-day-old rats treated icv with DMSO vehicle or z-VAD.FMK (1 μg in 2 μl DMSO) at 2 h after trauma and perfused at 24 h following trauma. In comparison to the vehicle-treated animal there is marked reduction in silver-positive cells in the z-VAD.FMK-treated rat. Original magnification $\times$80; DeOlmos cupric–silver staining. (B) Neuroprotective effect of z-VAD.FMK in infant traumatic brain injury. Seven-day-old rats received 0.1, 0.5, 1, 5, or 10 μg z-VAD.FMK (gray columns) or DMSO vehicle (V, dark column) icv at 2 h after trauma and were perfused at 24 h after trauma ($n = 6$ per group). In sections stained by the DeOlmos technique, the frontal, parietal, cingulate, and retrosplenial cortices; caudate nucleus; thalamus; dentate gyrus; and subiculum were subjected to morphometric analysis by the stereological disector method, estimating numerical densities of silver-positive cells. Each region was given a score of 1000 for every 1000 degenerating cells/mm^3, and the scores of 14 regions ipsilateral to the trauma side were added to a cumulative score. Columns represent cumulative scores $\pm$ SEM (numbers in parentheses represent the number of animals per group). ANOVA revealed that the effect of treatment with z-VAD.FMK was significant [$F(5,30) = 30.06$, $P < 0.0001$]. Pairwise comparisons revealed that the dose of 0.5 mg/kg z-VAD.FMK significantly reduced apoptotic neurodegeneration following trauma to the developing brain. $^{**}P < 0.01$; $^{***}P < 0.001$ compared to DMSO-treated rats, Student's t test. (C) Time window of neuroprotective effect of z-VAD.FMK in 7-day-old infant rats which received vehicle (V, dark column) or 1 μg z-VAD.FMK icv at 2, 4, or 8 h after trauma (gray columns). Columns represent mean cumulative severity scores $\pm$ SEM at 24 h after trauma (numbers in parentheses depict number of animals per group) at the side ipsilateral to the trauma. $^{***}P < 0.001$ compared to vehicle-treated rats (V), Student's t test. (D) Time course of apoptotic neurodegeneration following trauma in vehicle-treated (dark columns) and z-VAD.FMK (1 μg icv 2 h after trauma; gray columns)-treated rats. Columns represent mean cumulative severity scores $\pm$ SEM at 24 h, 48 h, and 5 days after trauma (numbers in parentheses depict number of animals per group) at the side ipsilateral to the trauma. There is no difference in cumulative scores between the two groups at 5 days after trauma, whereas a protective effect of z-VAD.FMK is evident at 24 ($^{***}P < 0.001$) and 48 h ($^{*}P < 0.05$, Student's t test) after trauma.

ipsilateral to the trauma side. A protective effect was also observed in the hemisphere contralateral to the injury.

To determine a time window of the neuroprotective effect of z-VAD.FMK, 7-day-old rats received icv injection of the compound at a dose of 1 μg at 2 ($n = 6$),

4 ($n = 6$), and 8 ($n = 6$) h and brains were analyzed at 24 h after trauma. Vehicle-treated rats ($n = 6$) received icv injection of DMSO at 2 h after trauma. Delayed administration of z-VAD.FMK up to 8 h following trauma resulted in lower scores for apoptotic brain damage compared to vehicle-treated rats (Fig. 5C).

In order to exclude the possibility that caspase inhibition might delay but not inhibit apoptosis, we injected z-VAD.FMK (1 μg in 2 μl) or DMSO (2 μl) 2 h after trauma i.c.v. into 7-day-old rats and analyzed their brains at 24 ($n = 6$ per group), 48 ($n = 6$ per group) h and 5 days ($n = 6$ per group) after trauma. A protective effect of z-VAD.FMK was still evident at 48 h after trauma in comparison to vehicle. At 5 days after trauma densities of degenerating cells in both vehicle and z-VAD.FMK-treated rats were equally low and did not significantly differ between groups (Fig. 5D).

Finally, to provide additional evidence that treatment with z-VAD.FMK offered lasting protection against traumatic brain injury, we subjected 7-day-old rats to brain trauma and injected icv the protective dose of 1 μg z-VAD.FMK ($n = 7$) or vehicle ($n = 7$) at 2 h after trauma. Sham-operated 7-day-old rats served as controls ($n = 6$). All animals were sacrificed 7 days after trauma or sham surgery without transcardial perfusion; the forebrains were hemisected and their weights taken. Trauma resulted in significant weight reduction of the right (traumatized) hemisphere in vehicle-treated rats compared to the nontraumatized left side. Treatment with z-VAD.FMK resulted also in a significant but less pronounced reduction in right hemispheric weights compared to vehicle-treated traumatized rats ($P < 0.0001$) and sham-operated rats ($P < 0.0017$; Table 2). Thus, time studies suggest lasting prevention of the neurodegenerative response to trauma by the pancaspase inhibitor and provide no evidence for postponement of that response.

TABLE 2
Hemispheric Weights

	Right (trauma side)	Left
Trauma + vehicle	0.3743 ± 0.0057***	0.4357 ± 0.0078
Trauma + z-VAD.FMK	0.4043 ± 0.0037***	0.4357 ± 0.0043
Sham operated	0.4367 ± 0.0049	0.4383 ± 0.0048

Note. Hemispheric weights (g) of rats treated with 1 μg z-VAD.FMK ($n = 7$) or vehicle ($n = 7$) at 2 h after trauma at the age of 7 days. Sham-operated 7-day-old rats served as controls ($n = 6$). All animals were sacrificed 7 days after trauma or sham surgery without transcardial perfusion; the forebrains were hemisected and weighed. Trauma resulted in significant weight reduction of the right (traumatized) hemisphere in vehicle-treated rats compared to the nontraumatized left side (***$P < 0.0001$) and to hemispheric weights of sham-operated rats (***$P < 0.0001$). Rats treated with z-VAD.FMK also displayed a significant reduction in right hemispheric weights compared to the left side and to sham-operated rats (***$P < 0.0001$). This weight reduction was less pronounced in the z-VAD.FMK-treated compared to the vehicle-treated group (**$P < 0.0017$).

DISCUSSION

Here we show that apoptotic neurodegeneration triggered by trauma in the developing brain is associated with activation of at least two distinct pathways. The first, the intrinsic pathway, is initiated by cytochrome *c* release into the cytoplasm and activation of caspase-9. The second, the extrinsic pathway, involves activation of caspase-8 and can be initiated by activation of death receptors. Here we provide evidence that one death receptor, the Fas receptor, is markedly upregulated in the context of infant brain trauma.

These molecular and biochemical changes appear to be pathogenetically linked to apoptotic neurodegeneration following trauma to the developing brain, since the pancaspase inhibitor z-VAD.FMK confers neuroprotection with a therapeutic time window of up to 8 h after trauma.

Cytochrome *c* immunoreactivity was elevated in the cytoplasmic fraction by 2 h after trauma, at a time point when no apoptotic cell death can be detected by histological methods in the brain regions analyzed. Thus, presence of cytochrome *c* in the cytoplasmic fraction precedes neurodegeneration, even in brain regions distant from the primary site of the impact. Involvement of the intrinsic apoptotic pathway has previously been reported in *in vivo* trauma models (Morita-Fujimura *et al.*, 1999; Raghupathi *et al.*, 2000; Keane *et al.*, 2001). How cytochrome *c* manages to cross the mitochondrial membrane is not understood. In all proposed models (Hengartner, 2000), members of the bcl-2 family play a key role in that they decrease mitochondrial membrane permeability and prevent release of cytochrome *c* into the cytoplasm (Nicholson, 2000). In the infant rat brain we demonstrate downregulation of the expression of bcl-2 and bcl-x_L by 0.5–2 h following trauma, which is expected to result in increased permeability of the mitochondrial membranes. Changes in the mRNA levels correlated with decreased protein levels. Reasons for decreased expression of antiapoptotic bcl-2 family proteins remain unclear. Transcription of antiapoptotic bcl-2 family

members is influenced by CREB, whose activity level is regulated by growth factors (Xing *et al.,* 1996). It has been shown that release of trophic factors and their trophic effects on developing neurons depend upon the level of neuronal activity (McCallister *et al.,* 1996; Liou & Fu, 1997). Spreading depression triggered by trauma disrupts physiological synaptic activity. This may lead to an impairment of neurotrophin-initiated survival signals and decrease in the transcription of survival genes. Our studies did not demonstrate downregulation in the expression of the neurotrophins BDNF and NT-3. In contrast, neurotrophin mRNA levels and immunoreactivity increased within hours after trauma, suggesting that neurotrophin upregulation may represent an endogenous compensatory mechanism to counteract neuronal destruction in the developing central nervous system and provide modes for regeneration and repair.

Previous studies have demonstrated Fas expression in the context of trauma to the adult brain and in infant hypoxia–ischemia (Nakashima *et al.,* 1999; Beer *et al.,* 2000; Felderhoff-Mueser *et al.,* 2000). Mice lacking functional Fas (lpr mice) have reduced infarct volumes following ischemic insults (Martin-Villalba *et al.,* 1999). Our data implicate the involvement of Fas in apoptotic cell death in infant rats subjected to brain trauma. Fas induction and protein expression were present in areas destined to undergo apoptosis, predominantly the ipsilateral cortex and the thalamic nuclei, and correlated with an increase in caspase-8 activity. These findings imply Fas receptor involvement in activation of caspase-8 after neonatal brain trauma but do not exclude the possibility that other death receptors and their ligands (TNF, TRAIL) may also contribute to activation of this extrinsic apoptotic pathway.

Cross talk between the extrinsic pathway and the mitochondria has been postulated (Hengartner, 2000). Activation of caspase-8 leads to proteolysis of the proapoptotic protein bid. Truncated bid enters the mitochondria and promotes cytochrome *c* release. Time course studies suggest that activation of caspase-8 occurs early (within 4 h) after trauma. Therefore, it is possible that caspase-8-mediated bid cleavage may constitute one additional mechanism to facilitate release of cytochrome *c* into the cytoplasm.

We further demonstrate that neuronal apoptosis following trauma can be effectively blocked by inhibition of caspases. The caspase inhibitor z-VAD.FMK significantly reduced ongoing cell death, even when administered in a delayed fashion up to 8 h following trauma. In adult animal models, caspase inhibition may confer neuroprotection in cerebral ischemia (Hara *et al.,* 1997; Endres *et al.,* 1998; Fink *et al.,* 1998; Himi *et al.,* 1998). Furthermore, early treatment of experimental pneumococcal meningitis with z-VAD.FMK was shown to have a beneficial effect, whereas delayed application of this compound did not result in substantial reduction of neuronal loss (Braun *et al.,* 1999).

In traumatic injury to the adult brain, z-VAD.FMK and the selective caspase-3 inhibitor z-DEVD.FMK can block neuronal death (Yakovlev *et al.,* 1997; Clark *et al.,* 2000). However, only a small amount of supporting data exists for the developing nervous system. In hippocampal and cortical neuronal cultures, the cell-permeable pancaspase inhibitor Boc-aspartyl(OMe)-fluoromethyl ketone (BAF) and the more selective caspase-8 inhibitor IETD-FMK (IETD) reduced Fas-induced apoptosis (Felderhoff-Mueser *et al.,* 2000). The only existing *in vivo* study on caspase inhibition in the immature brain demonstrated neuroprotection with the pancaspase inhibitor BAF in an infant model of hypoxic–ischemic injury (Cheng *et al.,* 1998). Our data indicate a beneficial effect of caspase inhibition in brain trauma for neuronal death occurring distant to the impact site. More importantly, the protective effect could be achieved even when the compound was administered 8 h after trauma, indicating relevance in the clinical setting.

One concern with regard to the use of caspase inhibitors has been that they may not prevent but may only postpone apoptotic neurodegeneration. Our findings, however, indicate that the extent of apoptosis following trauma to the developing brain at 48 h and at 5 days after trauma is not higher in rats treated with the caspase inhibitor in comparison to vehicle-treated controls. In fact, z-VAD.FMK-treated animals were still protected at 48 h after trauma. Thus, we find no evidence that apoptotic cell death is postponed due to peritraumatic inhibition of caspases. It is possible that slow recovery of levels of antiapoptotic proteins and the compensatory increase in levels of neurotrophins may provide modes for restoring cellular homeostasis and limiting neuronal loss.

Traumatic injury to the developing central nervous system has two major components, an acute excitotoxic component at the site of the insult and a delayed apoptotic component affecting the impact site as well as deeper brain structures. The number of brain cells affected by the apoptotic component is disproportionally larger than the number of cells degenerating by an excitotoxic mechanism (Bittigau *et al.,* 1999). Given our findings, targeting the downstream effectors of neuro-

nal apoptosis in the acute phase of the insult has therapeutic potential in the treatment of traumatic injury to the immature brain. Antiapoptotic therapies may give cells enough time to establish intrinsic protection systems and restore cellular homeostasis and function (Han & Holtzman, 2000). However, since apoptosis is also a physiological process in the developing brain, studies addressing the long-term functional effects following caspase inhibition appear to be potential targets for future research (Gillardon *et al.*, 1999).

ACKNOWLEDGMENTS

This study was supported by Grant 01K095151TPA3 from the Bundesministerium für Bildung und Forschung, a grant from the Dr. Emil-Alexander Huebner und Gemahlin Stiftung, and a grant from Humboldt University.

REFERENCES

Adelson, P. D., & Kochanek, P. M. (1998) Head injury in children. *J. Child Neurol.* **13,** 2–15.

Beer, R., Franz, G., Schopf, M., Reindl, M., Zelger, B., Schmutzhard, E., Poewe, W., & Kampfl, A. (2000) Expression of Fas and Fas ligand after experimental traumatic brain injury in the rat. *J. Cereb. Blood Flow Metab.* **20,** 669–677.

Bittigau, P., Sifringer, M., Pohl, D., Stadthaus, D., Ishimaru, M., Shimizu, H., Ikeda, M., Lang, D., Speer, A., Olney, J. W., & Ikonomidou, C. (1999) Apoptotic neurodegeneration following trauma is markedly enhanced in the immature brain. *Ann. Neurol.* **45,** 724–735.

Braun, J. S., Novak, R., Herzog, K. H., Bodner, S. M., Cleveland, J. L., & Tuomanen, E. I. (1999) Neuroprotection by a caspase inhibitor in acute bacterial meningitis. *Nat. Med.* **5,** 298–302.

Cheema, Z. F., Wade, S. B., Sata, M., Walsh, K., Sohrabji, F., & Miranda, R. C. (1999) Fas/Apo [apoptosis]-1 and associated proteins in the differentiating cerebral cortex: Induction of caspase-dependent cell death and activation of NF-kappaB. *J. Neurosci.* **19,** 1754–1770.

Cheng, Y., Deshmukh, M., D'Costa, A., Demaro, J. A., Gidday, J. M., Shah, A., Sun, Y., Jacquin, M. F., Johnson, E. M., & Holtzman, D. M. (1998) Caspase inhibitor affords neuroprotection with delayed administration in a rat model of neonatal hypoxic–ischemic brain injury. *J. Clin. Invest.* **101,** 1992–1999.

Chinnaiyan, A. M., O'Rourke, K., Tewari, M., & Dixit, V. M. (1995) FADD, a novel death domain-containing protein interacts with the death domain of Fas and initiates apoptosis. *Cell* **81,** 505–512.

Chomczynski, P., & Sacchi, N. (1987) Single-step method of RNA isolation by acid guanidinium thiocyanate–phenol–chloroform extraction. *Anal. Biochem.* **162,** 156–159.

Clark, R. S., Kochanek, P. M., Watkins, S. C., Chen, M., Dixon, C. E., Seidberg, N. A., Melick, J., Loeffert, J. E., Nathaniel, P. D., Jin, K. L., & Graham, S. H. (2000) Caspase-3, mediated neuronal death after traumatic brain injury in rats. *J. Neurochem.* **74,** 740–753.

DeOlmos, J. S., & Ingram, W. R. (1971) An improved cupric–silver method for impregnation of axonal and terminal degeneration. *Brain Res.* **33,** 523–529.

Diamond, P. T. (1996) Brain injury in the Commonwealth of Virginia: An analysis of Central Registry data 1988–1993. *Brain Injury* **10,** 414–419.

Endres, M., Namura, S., Shimizu-Sasamata, M., Waeber, C., Zhang, L., Gomez-Isla, T., Hyman, B. T., & Moskowitz, M. A. (1998) Attenuation of delayed neuronal death after mild focal ischemia in mice by inhibition of the caspase family. *J. Cereb. Blood Flow Metab.* **18,** 238–247.

Felderhoff-Mueser, U., Taylor, D. L., Greenwood, K., Kozma, M., Stibenz, D., Joashi, U. C., Edwards, A. D., & Mehmet, H. (2000) Fas/CD95/Apo-1 can function as a death receptor for neuronal cells in vitro and in vivo and is upregulated following cerebral hypoxic–ischemic injury to the developing rat brain. *Brain Pathol.* **10,** 17–29.

Fink, K., Zhu, J., Namura, S., Shimizu-Sasamata, M., Endres, M., Ma, J., Dalkara, T., Yuan, J., & Moskowitz, M. A. (1998) Prolonged therapeutic window for ischemic brain damage caused by delayed caspase activation. *J. Cereb. Blood Flow Metab.* **18,** 1071–1076.

Gillardon, F., Kiprianova, I., Sandkuhler, J., Hossmann, H. A., & Spranger, M. (1999) Inhibition of caspases prevents cell death of hippocampal CA1 neurons, but not impairment of hippocampal long-term potentiation following global ischemia. *Neuroscience* **93,** 1219–1222.

Goldstein, M. (1990) Traumatic brain injury: A silent epidemic. *Ann. Neurol.* **27,** 327.

Han, B. H., & Holtzman, D. M. (2000) BDNF protects the neonatal brain from hypoxic–ischemic injury in vivo via the ERK pathway. *J. Neurosci.* **20,** 5775–5781.

Hara, H., Friedlander, R. M., Gagliardini, V., Ayata, C., Fink, K., Huang, Z., Shimizu-Sasamata, M., Yuan, J., & Moskowitz, M. A. (1997) Inhibition of interleukin 1 beta converting enzyme family proteases reduces ischemic and excitotoxic neuronal damage. *Proc. Natl. Acad. Sci. USA* **94,** 2007–2012.

Hengartner, M. O. (2000) The biochemistry of apoptosis. *Nature* **407,** 770–776.

Himi, T., Ishizaki, Y., & Murota, S. (1998) A caspase inhibitor blocks ischaemia-induced delayed neuronal death in the gerbil. *Eur. J. Neurosci.* **10,** 777–781.

Ikonomidou, C., Qin, Y., Labruyere, J., Kirby, C., & Olney, J. W. (1996) Prevention of trauma-induced neurodegeneration in infant rat brain. *Pediatr. Res.* **39,** 1020–1027.

Keane, R. W., Kraydieh, S., Lotocki, G., Alonso, O. F., Aldana, P., & Dietrich, W. D. (2001) Apoptotic and antiapoptotic mechanisms after traumatic brain injury. *J. Cereb. Blood Flow Metab.* **21,** 1189–1198.

Koskiniemi, M., Kyykka, T., Nybo, T., & Jarho, L. (1995) Long-term outcome after severe brain injury in preschoolers is worse than expected. *Arch. Pediatr. Adolesc. Med.* **149,** 249–254.

Krammer, P. H. (2000) CD95′s deadly mission in the immune system. *Nature* **407,** 789–795.

Liou, J. C., & Fu, W. M. (1997) Regulation of quantal secretion from developing motoneurons by postsynaptic activity-dependent release of NT-3. *J. Neurosci.* **17,** 2459–2468.

Lohmann, J., Schickle, H., & Bosch, T. C. (1995) REN display, a rapid and efficient method for nonradioactive differential display and mRNA isolation. *Biotechniques* **18,** 200–202.

Martin-Villalba, A., Herr, I., Jeremias, I., Hahne, M., Brandt, R., Vogel, J., Schenkel, J., Herdegen, T., & Debatin, K. M. (1999) CD95 ligand (Fas-L/APO-IL) and tumor necrosis factor-related apopto-

sis-inducing ligand mediate ischemia-induced apoptosis in neurons. *J. Neurosci.* **19,** 3809–3817.

McCallister, A. K., Katz, L. C., & Lo, D. C. (1996) Neurotrophin regulation of cortical dendritic growth requires activity. *Neuron* **17,** 1057–1064.

Medema, J. P., Scaffidi, C., Kischkel, F. C., Shevchenko, A., Mann, M., Krammer, P. H., & Peter, M. E. (1997) FLICE is activated by association with the CD95 death-inducing signaling complex (DISC). *EMBO J.* **16,** 2794–2804.

Meier, P., Finch, A., & Evan, G. (2000) Apoptosis in development. *Nature* **407,** 796–801.

Morita-Fujimura, Y., Fujimura, M., Kawase, M., Chen, S. F., & Chan, P. H. (1999) Release of mitochondrial cytochrome c and DNA fragmentation after cold injury-induced brain trauma in mice: Possible role in neuronal apoptosis. *Neurosci. Lett.* **267,** 201–205.

Muzio, M., Chinnaiyan, A. M., Kischkel, F. C., O'Rouke, K., Shevchenko, A., Ni, J., Scaffidi, C., Bretz, J. D., Zhang, M., Gentz, R., Mann, M., Krammer, P. H., Peter, M. E., & Dixit, V. M. (1996) FLICE, a novel FADD-homologous ICE/CED-3-like protease, is recruited to the CD95 (Fas/APO-1) death-inducing signaling complex. *Cell* **85,** 817–827.

Nakashima, K., Yamashita, K., Uesugi, S., & Ito, H. (1999) Temporal and spatial profile of apoptotic cell death in transient intracerebral mass lesion of the rat. *J. Neurotrauma* **16,** 143–151.

Nicholson, D. W. (2000) From bench to clinic with apoptosis-based therapeutic agents. *Nature* **407,** 810–816.

Pohl, D., Bittigau, P., Ishimaru, M. J., Stadthaus, D., Hubner, C., Olney, J. W., Turski, L., & Ikonomidou, C. (1999) *N*-Methyl-d-aspartate antagonists and apoptotic cell death triggered by head trauma in developing rat brain. *Proc. Natl. Acad. Sci. USA* **96,** 2508–2513.

Raghupathi, R., Graham, D. I., & McIntosh, T. K. (2000) Apoptosis after traumatic brain injury. *J. Neurotrauma* **17,** 927–938.

Rich, T., Allen, R. L., & Wyllie, A. H. (2000) Defying death after DNA damage. *Nature* **407,** 777–783.

Savill, J., & Fadok, V. (2000) Corpse clearance defines the meaning of cell death. *Nature* **407,** 784–788.

Shi, S., Cote, R., & Taylor, C. (1997) Antigen retrieval immunohistochemistry: Past, present and future. *J. Histochem. Cytochem.* **45,** 327–343.

West, M. J., & Gundersen, H. J. G. (1990) Unbiased stereological estimation of the number of neurons in the human hippocampus. *J. Comp. Neurol.* **296,** 1–22.

Xing, J., Ginty, D. D., & Greenberg, M. E. (1996) Coupling of the RAS–MAPK pathway to gene activation by RSK2, a growth factor-regulated CREB kinase. *Science* **273,** 959–963.

Yakovlev, A. G., Knoblach, S. M., Fan, L., Fox, G. B., Goodnight, R., & Faden, A. I. (1997) Activation of CPP32-like caspases contributes to neuronal apoptosis and neurological dysfunction after traumatic brain injury. *J. Neurosci.* **17,** 7415–7424.

Yuan, J., & Yankner, B. A. (2000) Apoptosis in the nervous system. *Nature* **407,** 802–809.

Proc. Natl. Acad. Sci. USA
Vol. 96, pp. 2508–2513, March 1999
Pharmacology

N-Methyl-D-aspartate antagonists and apoptotic cell death triggered by head trauma in developing rat brain

(traumatic head injury/apoptosis/necrosis/excitotoxicity/neurodegeneration)

D. POHL*, P. BITTIGAU*, M. J. ISHIMARU†, D. STADTHAUS*, C. HÜBNER*, J. W. OLNEY†, L. TURSKI‡, AND C. IKONOMIDOU*§

*Department of Pediatric Neurology, Charité-Virchow Clinics, Children's Hospital, Humboldt University School of Medicine, Augustenburger Platz 1, D-13353 Berlin, Germany; †Department of Psychiatry, Washington University School of Medicine, 4940 Children's Place, St. Louis, MO 63110; and ‡Eisai London Research Laboratories, Bernard Katz Building, University College London, Gower Street, London WC1E 6BT, United Kingdom

Communicated by Martin Lindauer, University of Würzburg, Würzburg, Germany, December 21, 1998 (received for review February 11, 1998)

ABSTRACT **Morbidity and mortality from head trauma is highest among children. No animal model mimicking traumatic brain injury in children has yet been established, and the mechanisms of neuronal degeneration after traumatic injury to the developing brain are not understood. In infant rats subjected to percussion head trauma, two types of brain damage could be characterized. The first type or primary damage evolved within 4 hr and occurred by an excitotoxic mechanism. The second type or secondary damage evolved within 6–24 hr and occurred by an apoptotic mechanism. Primary damage remained localized to the parietal cortex at the site of impact. Secondary damage affected distant sites such as the cingulate/retrosplenial cortex, subiculum, frontal cortex, thalamus and striatum. Secondary apoptotic damage was more severe than primary excitotoxic damage. Morphometric analysis demonstrated that the *N*-methyl-D-aspartate receptor antagonists 3-(2-carboxypiperazin-4-yl)-propyl-1-phosphonate and dizocilpine protected against primary excitotoxic damage but increased severity of secondary apoptotic damage. 2-Sulfo-α-phenyl-*N*-*tert*-butyl-nitrone, a free radical scavenger, did not affect primary excitotoxic damage but mitigated apoptotic damage. These observations demonstrate that apoptosis and not excitotoxicity determine neuropathologic outcome after traumatic injury to the developing brain. Whereas free radical scavengers may prove useful in therapy of head trauma in children, *N*-methyl-D-aspartate antagonists should be avoided because of their propensity to increase severity of apoptotic damage.**

Although children under 6 years of age sustain traumatic brain injury more frequently than any other age group (1), there has been a dearth of research focusing on traumatic brain injury to the developing brain. Consequently, very little progress has been made toward understanding the mechanisms and developing neuroprotective measures for traumatic brain damage in children. Current therapy is symptomatic and consists of control and support of cardiovascular and respiratory systems, hemodynamic stabilization, control of intracranial pressure, and prophylactic anticonvulsant treatment (2).

Clinical experience and experimental observations in animals suggest that brain damage resulting from severe head injury can be classified into primary, which occurs at impact and appears immediately or shortly after injury, and secondary, which occurs distant to the impact and may not appear until several hours after injury (3, 4). It is assumed that injured neurons have a potential for recovery and that neurodegeneration triggered by traumatic impact is a dynamic and time-related process (5). According to this viewpoint, early diagnosis and medical support are crucial for the prevention of additional brain damage after head injury.

The publication costs of this article were defrayed in part by page charge payment. This article must therefore be hereby marked "*advertisement*" in accordance with 18 U.S.C. §1734 solely to indicate this fact.

PNAS is available online at www.pnas.org.

Studies focusing on the adult brain have shown that the damage associated with head trauma is triggered by an excitotoxic mechanism involving glutamate (6, 7). Accordingly, drugs that block glutamate receptors ameliorate both primary and secondary damage in adult head injury models (7). Neuronal death may also occur by an apoptotic programmed and genomically controlled mechanism (8, 9). No study has addressed involvement of apoptotic cell death in traumatic damage in the developing brain. Therefore, we have developed morphometric methods for detecting primary and secondary damage after traumatic head injury in infant rats by using a modified contusion device initially described by Allen (10) for the spinal cord and by Feeney *et al.* (11) for the brain. Using this experimental approach, we report that mechanical trauma to the developing brain causes primary excitotoxic (nonapoptotic) damage to the cortex and secondary delayed damage that is apoptotic to the cingulate/retrosplenial cortex, frontal cortex, parietal cortex, subiculum, thalamus, and striatum. We describe the type of neurodegenerative response to head trauma in the infant rat brain in terms of its topography, time course, age dependency, and response to neuroprotective treatment and critically evaluate potential implications for the therapy of head trauma in children.

MATERIALS AND METHODS

Traumatic Brain Injury and Contusive Device. Wistar rat pups (Bundesinstitut für gesundheitlichen Verbraucherschutz und Veterinärmedizin, Berlin, Germany) were anesthetized with halothane and placed in a mold fashioned to fit the contours of the skull and holding it in the desired attitude. The anesthesia was induced in 4% halothane and maintained in 1.5% halothane in balanced room air (12, 13) until the end of the procedure. A skin incision was made to expose the skull surface. The contusing device consisted of a hollow stainless steel tube 40 cm long, perforated at 1-cm intervals to prevent air compression. The device was kept perpendicular to the surface of the skull and guided a falling weight onto a circular footplate (2.0 mm in diameter) resting upon the surface of the parietal bone. A force of 160 g×cm produced by a 10-g weight was selected to produce brain contusion. The following coordinates in relation to lambda were used for stereotaxic positioning of the footplate onto the exposed parietal bone: 2 mm anterior and 2 mm lateral at the age of 3 days; 3 mm anterior and 2 mm lateral at the age of 7 days; 3.5 mm anterior and 2.5 mm lateral at the ages of 10 and 14 days and 4 mm anterior and 3 mm lateral at the age of 30 days. The contusion force was delivered unilaterally to the right side of the skull. The experiments were performed in accordance with the

Abbreviations: CPP, 3-(2-carboxypiperazin-4-yl)-propyl-1-phosphonate; MK-801, dizocilpine; NMDA, *N*-methyl-D-aspartate; SPBN, 2-sulfo-α-phenyl-*N*-*tert*-butyl-nitrone; N_v, numerical density; T_n, total number of cells; TUNEL, terminal deoxynucleotidyltransferase-mediated UTP end labeling.

§To whom reprint requests should be addressed. e-mail: hrissanthi.ikonomidou@charite.de.

German and United States Animal Welfare Acts and the National Institutes of Health Guide for the Care and Use of Laboratory Animals.

Morphometry. For morphological analysis rats were anesthetized with an overdose of chloral hydrate and perfused through the heart and ascending aorta for 15 min with a solution of paraformaldehyde (1%) and glutaraldehyde (1.5%) in pyrophosphate buffer (for combined light and electron microscopy) or paraformaldehyde (4%) in phosphate buffer [for terminal deoxynucleotidyltransferase-mediated UTP end labeling (TUNEL) or DeOlmos cupric silver staining].

Light Microscopy on Plastic Sections and Electron Microscopy. Brains were sliced in 1-mm-thick slabs, fixed in osmium tetroxide, dehydrated in alcohols, and embedded in araldite. For light microscopy, transverse serial sections, 1–10 μm, were cut and stained with methylene blue/azure II. Subsequently, ultrathin sections were cut and stained with uranyl acetate/lead citrate and examined by electron microscopy.

TUNEL Staining. To visualize nuclei with DNA cleavage, serial coronal sections (70 μm) of the entire brain were cut on a vibratome and residues of peroxidase-labeled digoxigenin nucleotide were catalytically added to DNA fragments by terminal deoxynucleotidyltransferase (ApopTag, Oncor Appligene, Heidelberg, Germany). Subsequently, the sections were counterstained with methyl green. Nuclei displaying DNA cleavage had a dark brown appearance and were surrounded by green-colored cytoplasm.

DeOlmos Cupric Silver Staining. To visualize degenerating cells, coronal sections of the whole brain were stained with silver nitrate and cupric nitrate by the method of DeOlmos and Ingram (14). Degenerating cells had a distinct dark appearance due to the silver impregnation.

Methylene Blue/Azure II Staining. To visualize normal cells, serial coronal sections of the entire brain were stained with methylene blue/azure II. Normal cells were identified by the presence of the typical nuclei with clear nucleoplasm and distinct nucleolus surrounded by homogenous cytoplasm.

Quantitation of the Excitotoxic Damage in the Parietal Cortex. Thirty minutes and 2, 4, 6, and 24 hr after traumatic injury the number of degenerating cells undergoing excitotoxic death within the parietal cortex was determined in methylene blue/azure II-stained sections. For this purpose the volume of the damage in the parietal cortex was determined by means of a video enhanced image analysis system (IMAGE 1.54; National Institutes of Health). Subsequently, mean numerical density (N_v) of degenerating cells in parietal cortex was determined by using an unbiased stereological disector technique (15) under blinded conditions. The total number (T_n) of degenerating cells was then determined by multiplying N_v with volume. The degenerating cells undergoing excitotoxic death were identified by the presence of pyknotic nuclei surrounded by massively swollen cytoplasm (edematous degeneration) or by darkening of the cytoplasm and presence of intracytoplasmic vacuoles (vacuolar condensation) (16).

Quantitation of the Distant Damage in the Brain. The distant damage was quantified in TUNEL or DeOlmos cupric silver-stained sections in the frontal, parietal, cingulate, retrosplenial cortex, caudate (mediodorsal), thalamus (laterodorsal, mediodorsal and ventral nucleus), and subiculum by the method of stereological disector, estimating mean N_v of degenerating cells. An unbiased counting frame (0.05 mm $\times$ 0.05 mm; disector height, 0.07 mm) and a high aperture objective were used for the sampling. The N_v for each brain region was determined with 8–10 disectors under blinded conditions. Furthermore, to assess the severity of the distant damage for every 1,000 degenerating cells per mm^3, a score 1 was given (1,000 cells per mm^3 = 1), and the scores from 13 regions ipsilateral and 13 regions contralateral to the trauma were added to give a cumulative severity score for the brain. The 13 regions within which quantitative analysis of degenerating cell densities was performed were layers II and IV of the frontal, parietal, cingulate, and retrosplenial cortices; caudate nucleus; laterodorsal, mediodorsal and ventral thalamic nuclei; and subiculum.

To determine the total number of cells undergoing apoptotic death within the brain 24 hr after trauma, the numbers of degenerating cells within a total of 26 regions per brain (13 regions ipsilateral and 13 regions contralateral to trauma) were individually calculated by means of disector techniques and stereological volumetry and summed to give a total number of cells undergoing apoptotic death 24 hr after trauma.

Drugs and Treatment Regimen. To determine whether *N*-methyl-D-aspartate (NMDA) antagonists mitigate primary damage in the brain induced by head trauma in developing rats, 3-(carboxypiperazin-4-yl)-propyl-1-phosphonate (CPP; Tocris), a competitive NMDA antagonist, and dizocilpine (MK-801; RBI), a noncompetitive NMDA antagonist, were used. CPP was administered i.p. in a dose of 30 mg/kg 30 min before and 20 and 70 min after trauma, and dizocilpine was given i.p. in a dose of 1 mg/kg 30 min before traumatic injury. High-dose and antecedent treatment regimen were selected to ensure that CPP and dizocilpine were reaching the brain in relevant concentrations (17, 18) before the excitotoxic injury was maximally expressed at the survival time of 4 hr. The effect of 2-sulfo-α-phenyl-*N*-*tert*-butylnitrone (SPBN; Aldrich), a free-radical scavenger, on primary damage was studied as well. SPBN was administered i.p. in a dose of 60 mg/kg 1 hr before traumatic injury.

To determine whether NMDA antagonists protect against the distant damage in the brain induced by head trauma in developing rats CPP was administered i.p. to 7-day-old rats in a dose of 15 mg/kg 60, 110, and 160 min and 9 and 17 hr after trauma. Dizocilpine was given i.p. in a dose of 0.5 mg/kg every 4 hr for 24 hr beginning 1 hr after trauma. This treatment regimen was chosen to give relevant concentrations of antagonists in the brain to interact with NMDA receptors (17, 18). The ability of SPBN to prevent the delayed damage when administered i.p. in a dose of 60 mg/kg 1 and 13 hr after trauma was also tested in 7-day-old rats.

To determine whether NMDA antagonists alone might cause neuropathologic changes in the brains of nontraumatized 7-day-old rats, sham-controls received i.p. injections of CPP in a dose of 15 mg/kg 60, 110, and 160 min and 9 and 17 hr or dizocilpine in a dose of 0.5 mg/kg every 4 hr for 24 hr, and the brains were removed at 24 hr after sham-surgery. In addition we tested whether SPBN alone might interfere with physiological apoptosis by using i.p. administration of 60 mg/kg 1 and 13 hr after sham-surgery in 7-day-old rats. The treatment regimen was chosen to ensure that SPBN was present in relevant concentrations in the brain (19).

Statistics. Statistical analysis of the data was performed by means of analysis of variance followed by Student's *t* test.

RESULTS

Excitotoxic Degeneration at the Site of Traumatic Injury. Shortly after head trauma neurons in parietal cortex subjacent to the site of impact began showing changes that by electron microscopic analysis were identical to those induced in developing brain by glutamate (16). Edematous swelling of neuronal dendrites and cell bodies and disruption of intracytoplasmic organelles were the earliest changes. These changes were followed by clumping of nuclear chromatin and nuclear pyknosis. Analysis of the time course of excitotoxic damage in the parietal cortex revealed a gradual progression of its size between 30 min and 4 hr after trauma with a peak at 4 hr (Table 1). Little or no signs of excitotoxic damage were seen in the brain 24 hr after head trauma (Table 1).

Delayed Apoptotic Degeneration at Distant Sites. TUNEL-positive nuclei started to appear in retrosplenial/cingulate cortex and dorsolateral thalamus 6 hr after trauma, and their numbers were increased at 16 and 24 hr. At 24 hr, the density of TUNEL-positive cells at the distant sites was similar to the density

Table 1. Time course of excitotoxic damage in the parietal cortex in rats subjected to traumatic head injury at the age of 7 days and the effect of NMDA antagonists dizocilpine and CPP and the radical scavenger SPBN on the extent of the damage 4 hr after head trauma

Survival time, hr	T_n	% of maximum	Dizocipline, T_n	CPP, T_n	SPBN, T_n
0.5	1,568 ± 215	9.56			
2	8,118 ± 1,023	49.50			
4	16,400 ± 2,435	100	2,329 ± 506* (14.2%)	6,224 ± 942* (37.95%)	15,100 ± 3,971 (92.07%)
6	14,599 ± 2,842	89.02			
24	210 ± 24	1.28			

Total number of degenerating cells (T_n) in parietal cortex was assessed in methylene blue/azure II-stained sections by multiplying mean numerical density (N_V) with the volume of cortex damage. Cells undergoing excitotoxic death were identified by the presence of pyknotic nuclei surrounded by swollen cytoplasm (edematous degeneration) or by darkening of the cytoplasm and presence of intracytoplasmic vacuoles (vacuolar condensation). Shown are means ± SEMs of T_n of degenerating cells in the parietal cortex on the site ipsilateral to head injury in 6–15 rats. Dizocilpine was administered in the dose of 1 mg/kg i.p. 30 min before head trauma, CPP was given i.p. in the dose of 30 mg/kg i.p. 30 min before and 20 and 70 min after trauma, and SPBN was given in the dose of 60 mg/kg i.p. 30 min before trauma. *, $P < 0.001$; Student's t test.

of degenerating cells detected by silver staining (Fig. 1). The degeneration did occur bilaterally and reached its maximal severity 24 hr after trauma (see Fig. 3). At all survival times studied, 6, 16, 24, and 48 hr and 5 days, the distant damage was more severe in the hemisphere ipsilateral to the site of traumatic injury (Table 2 and Fig. 2). In most severely affected areas such as retrosplenial cortex, subiculum, parietal cortex, cingulate cortex, and laterodorsal thalamus the density of degenerating cells 24 hr after head trauma was up to 23%–33% of the total cell density (Table 2). The extent of the damage in the caudate and ventral thalamus reached only 2% of the entire cell population in these regions (Table 2). The density of spontaneously degenerating cells in sham rats was up to 0.74%–1.67% of the total cell density in the frontal, cingulate, parietal, and retrosplenial cortex, suggesting that physiological programmed cell death was ongoing and that the brain regions with highest inherent apoptosis were matching those with the highest sensitivity to apoptotic degeneration after traumatic injury (Table 2). Because degenerating neurons dying by a nonapoptotic process can be TUNEL-positive (20), we examined the degenerating cells in the cingulate cortex and dorsolateral thalamus by electron microscopy to determine whether the mechanism of cell death was apoptotic. The first detectable ultrastructural changes in cells undergoing delayed degeneration consisted of clumping of nuclear chromatin and mild to moderate condensation of the entire cell. Nuclear chromatin became transformed into flocculent densities that joined together to form one or more large electron-dense spherical balls. In early stages the nuclear envelope separated into fragments that floated randomly about the cytoplasm. In the absence of an intact continuous nuclear membrane, the cell became unpartitioned with nucleoplasmic contents freely intermingling with cytoplasmic contents. The large chromatin masses migrated often toward

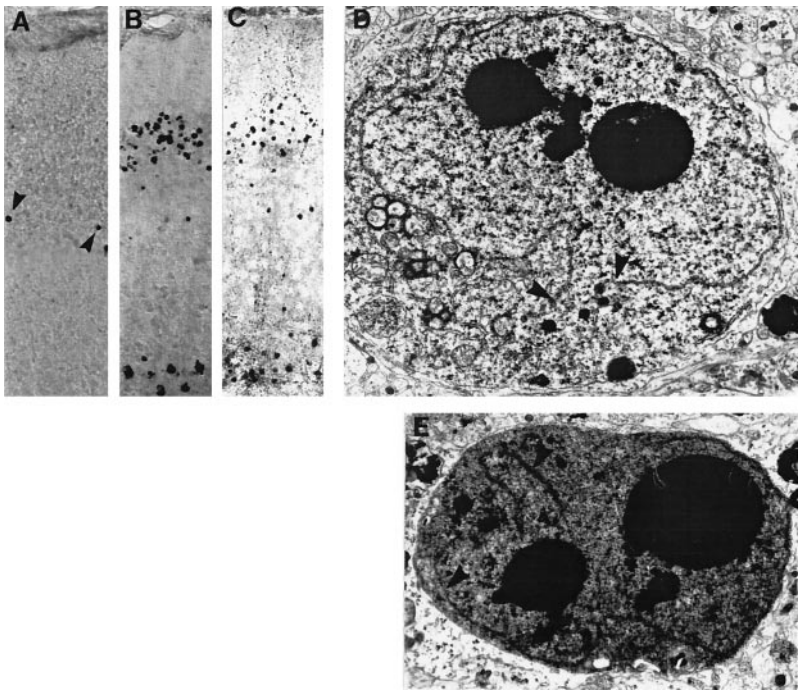

FIG. 1. Apoptotic cell death in the cingulate cortex of an 8-day-old nontraumatized rat (*A*) and a rat subjected to head trauma on postnatal day 7 and sacrificed 24 hr (*B* and *C*) or 16 hr (*D* and *E*) later. In *A* and *B*, the apoptotic cells are detected by TUNEL staining and in *C* apoptotic cells are detected by DeOlmos cupric silver staining. In *D* and *E,* the cell death process is shown by electron microscopy to have the hallmark morphological characteristics of apoptosis. (*A*) In the nontraumatized control brain, an occasional cell is TUNEL-positive (arrowheads), indicating that it is undergoing physiological (programmed) cell death that occurs normally in scattered distribution in the developing brain. (*B* and *C*) A much more robust display of degeneration is detected in the cingulate cortex of traumatized brains, and the pattern of degeneration revealed by TUNEL staining (*B*) is the same as revealed by DeOlmos silver staining (*C*). (*D* and *E*) Electron microscopic evaluation of the cingulate cortex 16 hr after head trauma reveals that the type and sequence of morphological changes meet the classical criteria for apoptosis and are identical to the changes in neurons undergoing physiological cell death in the developing brain (20, 21). The neuron in *D* is showing very early signs of apoptotic cell death, which consist of the formation of electron-dense spherical chromatin masses in the nucleus and a discontinuity in the nuclear membrane (arrowheads), signifying breakdown of the membrane boundary that normally partitions the nucleus from the cytoplasm. In this very early stage, the cell shows only mild condensation, and cytoplasmic organelles appear essentially normal except for some peculiar coated vesicles of undetermined origin. As the apoptotic process evolves (*E*), the nuclear membrane decomposes into fragments (arrowheads) that float randomly about, the contents of the nucleoplasm and cytoplasm freely intermix, and the entire cell becomes uniformly condensed. In later stages, apoptotic bodies containing both cytoplasmic and nucleoplasmic materials are formed and these are extruded into the neuropil (data not shown). Finally, both the main cell mass and the apoptotic bodies are transformed into shrunken amorphous masses of debris and are phagocytized. (Magnification: *A–C*, ×100; *D*, ×10,500; E, ×9,750.)

Table 2. Numerical density (N_V) of cells in frontal, parietal, cingulate, and retrosplenial cortex; mediodorsal, laterodorsal, and ventral thalamus; caudate; and subiculum in rats subjected to traumatic head injury at the age of 7 days

	Sham			Trauma			
Position	Normal cells, N_V normal	Degenerating cells, N_V spontaneous	%	Degenerating cells, N_V ipsilateral	%	Degenerating cells, N_V contralateral	%
Frontal cortex II	0.1897 ± 0.0045	0.0032 ± 0.0003	1.67	0.0198 ± 0.0038*	10.45	0.0101 ± 0.0021*	5.35
Frontal cortex IV	0.1212 ± 0.0103	0.0002 ± 0.00003	0.16	0.0051 ± 0.0010†	4.20	0.0045 ± 0.0010†	3.74
Parietal cortex II	0.2239 ± 0.0134	0.0022 ± 0.0006	0.96	0.0689 ± 0.0081‡	30.77	0.0137 ± 0.0019*	6.12
Parietal cortex IV	0.1360 ± 0.0063	0.0003 ± 0.00008	0.26	0.0852 ± 0.0017†	6.26	0.0009 ± 0.0002*	0.69
Cingulate II	0.1958 ± 0.0113	0.0030 ± 0.0004	1.54	0.0515 ± 0.0088†	26.32	0.0091 ± 0.0017*	4.67
Cingulate IV	0.1281 ± 0.0061	0.0002 ± 0.00003	0.13	0.0098 ± 0.0011‡	7.62	0.0012 ± 0.0003*	0.91
Retrosplenial II	0.2159 ± 0.0139	0.0016 ± 0.0003	0.74	0.0538 ± 0.0080‡	24.93	0.0026 ± 0.0003*	1.21
Retrosplenial IV	0.1230 ± 0.0109	0.0004 ± 0.00007	0.33	0.0415 ± 0.0057‡	33.71	0.0008 ± 0.0001*	0.67
Caudate	0.2225 ± 0.0111	0.0006 ± 0.0001	0.29	0.0048 ± 0.00009†	2.16	0.0029 ± 0.0061*	1.31
Mediodorsal thalamus	0.1683 ± 0.0064	0.0002 ± 0.00004	0.14	0.0015 ± 0.00003‡	0.88	0.0010 ± 0.0002*	0.59
Laterodorsal thalamus	0.1339 ± 0.0131	0.0004 ± 0.00006	0.30	0.0307 ± 0.0072‡	22.95	0.0020 ± 0.0005*	1.53
Ventral thalamus	0.1129 ± 0.0026	0.0001 ± 0.00003	0.11	0.0023 ± 0.0005†	2.04	0.0014 ± 0.0004*	1.22
Subiculum	0.1681 ± 0.0082	0.0004 ± 0.00006	0.22	0.0520 ± 0.0063‡	30.93	0.0033 ± 0.0006†	1.99

Assessment of cell densities were performed 24 hr after head trauma or sham surgery in DeOlmos cupric silver or methylene blue/azure II-stained sections of the whole brain. N_V values of normal and silver-accumulating cells were determined by using the unbiased disector technique and are shown as means ± SEMs × 10^6 cells per mm^3 in 6–16 rats. II and IV stand for cortical layers II and IV.
*, $P < 0.05$; †, $P < 0.01$; ‡, $P < 0.001$; Student's t test.

the periphery of the cell and in some cases the cell divided into separate independent bodies consisting of a contingent of cytoplasm and one or more nuclear chromatin balls. This type and sequence of changes are unequivocally apoptotic in that they are identical to those seen in neurons undergoing apoptosis in physiologically developing brain (20) and meet all the criteria set for diagnosing apoptosis (22). It is of interest that 16 hr after trauma, cells in both early and late stages of apoptosis were detected (Fig. 1), which indicates that 16 hr after trauma the process of cell suicide was still progressing.

Extent of Excitotoxic and Apoptotic Cell Death in the Rat Brain After Head Trauma. The evolution of brain damage after head trauma in developing rats is a highly dynamic process. To determine which type of damage, excitotoxic or apoptotic, was more devastating, we chose to compare the numbers of cells dying an excitotoxic or apoptotic cell death at the respective times of their maximal expression. From the time course studies, it was known that excitotoxic degeneration is most prominent at 4 hr after trauma (Table 1). Apoptotic cell death reached its maximum at 24 hr after trauma (Fig. 3.). Estimation of numbers of degenerating cells in the brains of 7-day-old rats subjected to head trauma revealed that at 24 hr after trauma (the time of maximal expression of apoptotic cell death) 2,241,986 ± 336,297 cells (n = 9) were dying an apoptotic death as opposed to 16,400 ± 2,435 cells (n = 12) dying an excitotoxic death at 4 hr after trauma (the point of maximal expression of excitotoxic cell death). This indicates that apoptotic, rather than nonapoptotic, cell death determines neuropathologic outcome after head trauma in the brain of rats at the age of 7 days.

Age Dependency of the Delayed Apoptotic Degeneration. To determine whether susceptibility to apoptotic cell death is dependent upon age, we subjected 3-, 7-, 10-, 14-, and 30-day-old rats to head trauma and evaluated the damage quantitatively 24

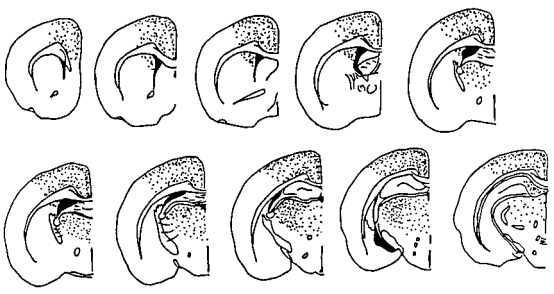

FIG. 2. Distribution pattern of degenerating cells (dots) as shown by DeOlmos cupric silver staining in the brains of developing rats traumatized on postnatal day 7 and sacrificed 24 hr later.

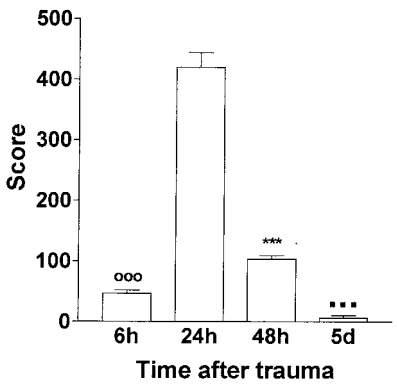

FIG. 3. Time course and severity of delayed disseminated apoptotic death observed in the brains of developing rats traumatized on postnatal day 7 and sacrificed 6, 24, or 48 hr or 5 days later. For quantification purposes, each brain was given a score that was based on determined densities of degenerating cells within 13 regions ipsilateral and 13 regions contralateral to the trauma. Depicted are means ± SEMs in 6–16 animals. Delayed damage was more severe at 24 hr compared with 6 hr (○○○, $P < 0.001$) and 48 hr (***, $P < 0.001$) after trauma. Damage severity continued to decline and was significantly less at 5 days compared with 48 hr after trauma (■■■, $P < 0.001$; Student's t test.).

hr after injury by using the DeOlmos cupric-silver staining. Three- and 7-day-old rats demonstrated the highest vulnerability (Fig. 4). In 10-day- and 14-day-old rats, the severity of distant damage had markedly decreased. At 30 days of age damage was limited to the site of impact and no distant lesions were found (Fig. 4).

Effects of Neuroprotective Drugs on Excitotoxic Degeneration in the Parietal Cortex. Quantitative evaluation 4 hr after trauma of the brains of 7-day-old rats treated with dizocilpine revealed reduction of the extent of excitotoxic damage in the parietal cortex by 86%. CPP reduced excitotoxic damage in the parietal cortex by 62%, whereas SPBN elicited no significant neuroprotective effect (Table 1).

Effects of Neuroprotective Drugs on Apoptotic Degeneration in the Brain. Quantitative evaluation of the brains 24 hr after head trauma revealed that the apoptotic degeneration was more severe in rats treated with dizocilpine than in those subjected to vehicle (Fig. 5). Severity of the apoptotic degeneration in the brains of 7-day-old rats subjected to head trauma reached a mean cumulative score of 382 ± 26 ($n = 26$), whereas that in rats treated with dizocilpine was 780 ± 28 ($n = 13$), demonstrating increase of the damage by 104%. Degeneration in the brains of rats subjected to head trauma and to the treatment with CPP reached a mean cumulative score of 826 ± 37 ($n = 8$) revealing increase in the extent of the damage by 116% (Fig. 5). Highest increases in the extent of apoptotic degeneration was noted in the cingulate cortex ipsilateral (71%) and contralateral (15%), laterodorsal thalamus ipsilateral (56%) and contralateral (6%), frontal cortex ipsilateral (32%) and contralateral (20%), and retrosplenial cortex contralateral (18%) to trauma after treatment with dizocilpine. In the brains of rats subjected to head trauma and treatment with CPP, highest increases were noted in the cingulate cortex contralateral (81%), frontal cortex ipsilateral (69%) and contralateral (44%), subiculum ipsilateral (63%) and contralateral (27%), retrosplenial cortex contralateral (20%), and laterodorsal thalamus contralateral (7%) to the traumatic injury.

NMDA antagonists gave rise to apoptotic degeneration in the brains of 7-day-old sham-operated rats, indicating that they interfered with physiological apoptosis at this age. An apoptotic response to NMDA antagonists was noted in cortical layers II and IV, thalamic nuclei, the caudate, and in the subiculum. Mean cumulative scores for apoptotic damage caused by CPP and dizocilpine in sham-operated rats were 184 ± 6 ($n = 6$) and 236 ± 5 ($n = 6$), respectively. In 7-day-old rats subjected to head trauma and subsequent treatment with NMDA antagonists the severity of apoptotic cell death was higher (by 27% after treatment with dizocilpine and 37% after treatment with CPP) than the expected additive apoptotic response triggered by trauma or the NMDA antagonists alone (Fig. 5).

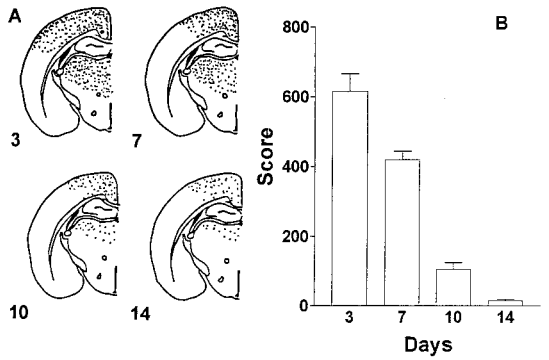

FIG. 4. (*A*) Distribution of degenerating cells (dots) as shown by the DeOlmos cupric silver staining in the brains of developing rats subjected to head trauma on postnatal days 3, 7, 10, or 14. Morphological analysis was performed 24 hr after traumatic injury. (*B*) Severity of delayed posttraumatic cell death in relation to age. Rats were given a score 1 for every 1,000 degenerating cells per mm^3 (1,000 cells per mm^3 = 1) and the scores from 13 regions ipsilateral and 13 regions contralateral to the trauma were added to give a cumulative severity score for the brain. Depicted are the means ± SEMs in 6–16 rats. Three-day-old rats ($n = 11$) were more severely affected than 7-day-old rats ($P < 0.0008$; $n = 16$), 7-day-old rats more severely than 10-day-old rats ($P < 0.0001$; $n = 6$), and 10-day-old more severely than 14-day-old rats ($P < 0.0014$; $n = 6$; Student's t test).

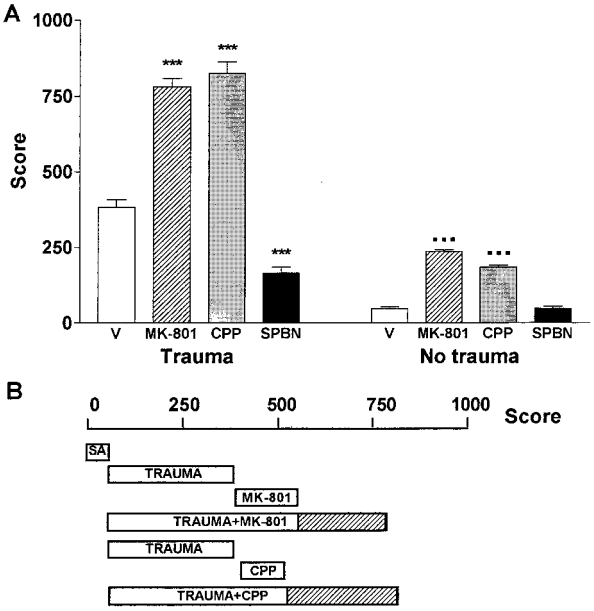

FIG. 5. Potentiation by NMDA antagonists of apoptotic cell death in the brains of rats subjected to head trauma or sham surgery on postnatal day 7 and sacrificed 24 hr later (*A*). Dizocilpine was administered at the dose of 0.5 mg/kg i.p. 60 min after trauma or sham surgery and subsequently every 4 hr. CPP was injected i.p. at the dose of 15 mg/kg at 60 min, 110 min, and 160 min and then at 9 hr and 17 hr after trauma or sham surgery. SPBN was administered i.p. at the dose of 60 mg/kg at 1 and 13 hr after trauma or sham surgery. Nontraumatized rats received the drugs according to the same schedule. Densities of degenerating cells were calculated in 13 brain regions ipsilateral and 13 regions contralateral to trauma and the brains were given a cumulative score that reflects severity of the damage. Dizocilpine ($P < 0.001$) and CPP ($P < 0.001$) potentiated delayed apoptotic damage, whereas SPBN significantly ameliorated apoptotic cell death ($P < 0.001$) compared with vehicle-treated (V) traumatized rats. Surprisingly, both dizocilpine ($P < 0.001$) and CPP ($P < 0.001$) caused a significant amount of apoptosis in the brains of sham-operated 7-day-old rats compared with vehicle-treated (V) sham-operated rats. The severity of apoptotic degeneration caused by head trauma and subsequent treatment with dizocilpine or CPP was higher than the expected additive effect of the apoptotic responses to head trauma or treatment with NMDA antagonists alone. To illustrate this, in *B* the mean scores for apoptotic damage caused by each treatment condition are presented as horizontal bars. SA represents the mean score for spontaneous apoptosis in the brains of vehicle-treated sham rats. Shaded areas represent the amount of damage that reflects potentiation by dizocilpine and CPP of the trauma-triggered component of apoptotic degeneration in the brains of 7-day-old rats. ***, $P < 0.001$ vs. vehicle-treated rats; ■■■, $P < 0.001$ vs. vehicle- treated rats; Student's t test.

In contrast, analysis of cumulative severity scores revealed that SPBN reduced the severity of apoptotic damage in the brain after head trauma in 7-day-old rats by 57% (Fig. 5). Rats subjected to the treatment with SPBN had mean cumulative severity score of 165 ± 20 ($n = 13$) only (Fig. 5). SPBN did not affect physiological apoptosis in the brain of 7-day-old sham-operated rats (Fig. 5).

DISCUSSION

The damage triggered by head trauma in the brain of developing rats has two major components, an acute component at the impact site that by ultrastructural criteria is excitotoxic and nonapoptotic and a delayed component at sites distant to the impact that fulfills ultrastructural criteria for apoptosis. The apoptotic damage that occurs in multiple locations in the brain

affects a larger number of neurons than excitotoxic damage and is likely to make a greater contribution to posttraumatic deficits.

Excitotoxic damage, known to occur in the brain after deleterious insults such as ischemia, trauma, or seizures (status epilepticus), has remained a main focus of research over the past two decades (23, 24). Although apoptosis has been identified as an additional to excitotoxicity mechanism leading to neurodegeneration, our findings show that in the developing rat brain after traumatic injury apoptotic cell death carries higher impact than excitotoxic cell death in determining neuropathologic outcome.

The NMDA antagonists CPP and dizocilpine protect against the excitotoxic but increase the apoptotic component of traumatic brain injury. Because the extent of excitotoxic damage induced by head trauma is minor in comparison to the extent of apoptotic damage, the net effect of NMDA antagonist treatment is a clear-cut worsening of neuropathologic outcome after trauma to the developing brain.

Apoptotic damage triggered by head trauma in the developing brain presumably does not occur as a secondary manifestation causally linked to the primary excitotoxic damage at the impact site because if this were the case, blocking the excitotoxic reaction at the impact site by NMDA antagonists should diminish instead of enhance distant damage. Head trauma may trigger apoptosis either by activating a mechanism that normally promotes programmed cell death or by compromising a mechanism that normally suppresses it. Distant apoptotic damage after head trauma is most severe in areas that show highest densities of spontaneous apoptotic cells in sham rats, such as the cingulate, frontal, parietal, and retrosplenial cortex. This fact suggests that the widespread apoptotic cell death triggered by head trauma in the infant rat brain may be due in part to interference with the programmed cell death process that occurs during a critical developmental period. Regardless which mechanism might explain how trauma elicits apoptotic damage, the fact that this damage is augmented by treatment with NMDA antagonists raises the possibility that glutamate acting via NMDA receptors suppresses programmed cell death in the developing brain. NMDA antagonists may therefore compromise this mechanism, thereby making neurons overly prone to show an apoptotic response to trauma.

Our studies demonstrate that vulnerability to apoptotic cell death in the rat brain is highest in the first two postnatal weeks and decreases thereafter. Although it is uncertain how the rodent and human compare regarding the time window of vulnerability to posttraumatic brain damage, it is possible that humans may be at risk for this type of damage during early childhood, and this signifies that it may be detrimental to use NMDA antagonists in the therapeutic management of pediatric head trauma. Furthermore, such conclusions call into question the practice of administering NMDA antagonists such as ketamine during the stabilization period immediately after head trauma in young children (25, 26). On the other hand, the fact that the delayed pattern of brain damage continued to evolve over 24 hr after head trauma in developing rats suggests that there may be a wide time-window for therapeutic intervention.

The present findings suggest that a free-radical scavenger, SPBN, may have therapeutic value in mitigating delayed apoptotic degeneration triggered by head trauma. These observations are in line with reports on protective action and wide therapeutic time window of SPBN in adult head trauma and ischemia models (27). Treatment with SPBN is beneficial only because apoptosis represents the predominant form of neurodegeneration after head trauma in developing rats. SPBN did not protect against excitotoxic damage, suggesting that it would be useless in a neurodegeneration with a predominant excitotoxic component. Our results call for the necessity to better understand and define the relative contributions of excitotoxicity and apoptosis to the pathogenesis of neurodegenerative syndromes before making a decision on the mode of treatment. Nonetheless, determining relative contributions of these two mechanisms of cell death is of crucial importance also because certain antiexcitotoxic regimen, when used in syndromes with predominant apoptotic component, may elicit unexpected deleterious side effects.

If such conclusions apply to human brain, then they call for careful selection of neuroprotective measures depending on the cell death type predominating in a specific neurodegenerative disorder.

This work was supported by Grant 01KO95151TPA3 from the Bundesministerium für Bildung und Forschung (BMBF).

1. Diamond, P. T. (1996) *Brain Injury* **10,** 413–419.
2. Greenberg, J. (1993) *Handbook of Head and Spine Trauma* (Dekker, New York).
3. Adams, J. H. (1992) in *Greenfield's Neuropathology,* eds. Adams, J. H. & Duchen, L. W. (Arnold, London), pp. 106–152.
4. Stein, S. C. & Spettell, C. M. (1995) *Pediatr. Neurosurg.* **23,** 299–304.
5. Povlishock, J. T. (1993) in *Neuroregeneration*, ed. Gorio, A. (Raven, New York), pp. 185–216.
6. Faden, A. I., Demediuk, P., Panter, S. S. & Vink, R. (1989) *Science* **244,** 798–800.
7. Bernert, H. & Turski, L. (1996) *Proc. Natl. Acad. Sci. USA* **93,** 5235–5240.
8. Crowe, M. J., Bresnahan, J. C., Shuman, S. L., Masters, J. N. & Beattie, M. S. (1997) *Nat. Med.* **3,** 73–76.
9. Yakovlev, A. G., Knoblach, S. M., Fan, L., Fox, G. B., Goodnight, R. & Faden, A. I. (1997) *J. Neurosci.* **17,** 7415–7424.
10. Allen, A. R. (1911) *J. Am. Med. Assoc.* **57,** 878–880.
11. Feeney, D. M., Boyeson, M. G., Linn, R. T., Murray, H. M. & Dail, W. G. (1981) *Brain Res.* **211,** 67–77.
12. Rice, J. E., Vannucci, R. C. & Brierley, J. B. (1981) *Ann. Neurol.* **9,** 131–141.
13. Cheng, Y., Gidday, J. M., Yan, Q., Shah, A. R. & Holtzman, D. M. (1997) *Ann. Neurol.* **41,** 521–529.
14. DeOlmos, J. S. & Ingram, W. R. (1971) *Brain Res.* **33,** 523–529.
15. Cruz-Orive, L. M. & Weibel, E. R. (1990) *Am. J. Physiol.* **258,** L148–L156.
16. Olney, J. W. & Ho, O. L. (1970) *Nature (London)* **227,** 609–610.
17. Lehmann, J., Schneider, J., McPherson, S., Murphy, D. E., Bernard, P., Tsai, C., Bennett, D. A., Pastor, G., Steel, D. J., Boehm, C., *et al.* (1987) *J. Pharmacol. Exp. Ther.* **240,** 737–746.
18. Turski, L., Bressler, K., Rettig, K.-J., Löschmann, P.-A. & Wachtel, H. (1991) *Nature (London)* **349,** 414–418.
19. Carney, J. M., Starke-Reed, P. E., Oliver, C. N., Landum, R. W., Cheng, M. S., Wu, J. F. & Floyd, R. A. (1991) *Proc. Natl. Acad. Sci. USA* **88,** 3633–3636.
20. Ishimaru, M. J., Ikonomidou, C., Dikranian, K. & Olney, J. W. (1997) *Soc. Neurosci. Abst.* **23,** 895.
21. Olney, J. W. & Ishimaru, M. J. (1997) in *Cell Death in Diseases of the Nervous System*, eds. Koliatsos, V. E. & Ratan, R. (Humana, Totowa, NJ), pp. 167–197.
22. Wyllie, A. H., Kerr, J. F. R. & Currie, A. R. (1980) *Int. Rev. Cytol.* **68,** 251–306.
23. Ikonomidou, C. & Turski, L. (1995) *Crit. Rev. Neurobiol.* **8,** 487–497.
24. Bullock, R. (1995) *Ann. N.Y. Acad. Sci.* **767,** 272–278.
25. Gremmelt, A. & Braun, U. (1995) *Anaesthesist* **44,** S559–S565.
26. Cunitz, G. (1995) *Anaesthesist* **44,** 369–391.
27. Hensley, K., Carney, J. M., Stewart, C. A., Tabatabaie, T., Pye, Q. & Floyd, R. A. (1997) *Int. Rev. Neurosci.* **40,** 299–317.

clear coactivators in the conventional manner. The allosteric ligand activation and the phosphorylation work synergistically to promote receptor-mediated gene function. Finally, DA reinforces P action through a direct ligand-independent activation of the PR (*1*) as well as indirectly through activation of DARPP-32. It is implicit that cross-talk between these two pathways is important for integration of the multitude of signals that modulate reproductive behavior.

References and Notes

1. S. K. Mani, J. M. C. Allen, J. H. Clark, J. D. Blaustein, B. W. O'Malley, *Science* **265**, 1246 (1994); E. M. Apostolakis *et al.*, *J. Neurosci.* **16**, 4823 (1996).
2. J. P. Lydon *et al.*, *Genes Dev.* **9**, 2266 (1995).
3. S. K. Mani *et al.*, *Mol. Endocrinol.* **10**, 1728 (1996).
4. P. Greengard *et al.*, *Brain Res. Rev.* **26**, 274 (1998); H. C. Hemmings Jr., P. Greengard, H. Y. L. Tung, P. Cohen, *Nature* **310**, 503 (1984); K. R. Williams, H. C. Hemmings Jr., M. B. LoPresti, W. H. Konigsberg, P. Greengard, *J. Biol. Chem.* **261**, 1890 (1986); P. Greengard, P. B. Allen, A. C. Nairn, *Neuron* **23**, 435 (1999).
5. Ovariectomized female rats were prescreened for sexual receptivity (*6*) by subcutaneous (sc) administration of EB (2 μg) followed by P (100 μg) 48 hours later. Stereotaxic surgery was performed on sexually receptive rats (*6*) and mice (*3*), which were then used in experiments to compare the effects of P, D_1 agonist, and serotonin. Behavioral testing was performed during the dark phase of the reversed light/dark cycle as described (*3, 6*). The experimental observer was blind to the treatment conditions and mouse genotypes.
6. S. K. Mani *et al.*, *Endocrinology* **135**, 1409 (1994).
7. G. Pollio, P. Xue, A. Zanisi, A. Nicolin, A. Maggi, *Mol. Brain Res.* **19**, 135 (1993); S. Ogawa, U. E. Olazabal, D. W. Pfaff, *J. Neurosci.* **14**, 1766 (1994).
8. A. A. Fienberg *et al.*, *Science* **281**, 838 (1998).
9. EB-induced hypothalamic cytosol PRs in mice carrying the wild-type gene encoding DARPP-32 (+/+) and the null mutation (−/−) were assayed by one-point binding analysis as described previously (*3*). The following PR concentrations (in fmol/mg of protein) were obtained: vehicle (+/+) = 2.5 ± 1.2; vehicle (−/−) = 2.6 ± 0.87; EB (+/+) = 8.75 ± 1.5; EB (−/−) = 8.4 ± 1.8. Each value is the mean ±SEM of six independent determinations.
10. A. C. Nairn and S. Shenolikar, *Curr. Opin. Neurobiol.* **2**, 296 (1992).
11. P. B. Allen *et al.*, in preparation.
12. Mice homozygous for the I-1 and DARPP-32 targeted mutations were generated by cross-breeding the two mutant lines. Resulting double heterozygotes were then crossed to yield mouse lines homozygous for each mutation and also the corresponding wild-type controls. Additional wild-type and double mutant mice were then generated by inbreeding wild types and double mutants.
13. Rats were decapitated and the brains removed. The hypothalamus was dissected from coronal sections submerged in oxygenated ice-cold artificial cerebrospinal fluid without Ca^{2+} or Mg^{2+}, and the tissues were processed for cAMP and PKA assays. Sample processing and cAMP assays were performed according to the procedures of Moore *et al.* (*20*). PKA assays using Kemptide (Leu-Arg-Arg-Ala-Ser-Leu-Gly) as a substrate were carried out with 5 μg of protein as described (*21*). The amount of cAMP and PKA activity in each sample was normalized to the total amount of protein in the homogenate. Preincubation of protein extracts with the PKA-specific peptide inhibitor Walsh peptide demonstrated a concentration-dependent inhibition of substrate phosphorylation (a substrate:inhibitor ratio of 1:10 = 85% inhibition; 1:100,000 = 15%), confirming that the phosphorylation of the substrate peptide was specific to PKA.
14. P. M. Wise, N. Rance, C. Barraclough, *Endocrinology* **108**, 2186 (1981); I. Vathy and A. M. Etgen, *J. Neuroendocrinol.* **1**, 383 (1989); J. G. Kohlert, R. K. Rowe, R. L. Meisel, *Horm. Behav.* **32**, 143 (1997).
15. F. Kimura, M. Kawakami, H. Nakano, S. M. McCann, *Endocrinology* **106**, 631 (1980).
16. R. E. Whalen and A. H. Lauber, *Neurosci. Biobehav. Rev.* **10**, 47 (1986); L. Kow, C. V. Mobbs, D. W. Pfaff, *Neurosci. Biobehav. Rev.* **18**, 1 (1994); C. Beyer and G. Gonzalez-Mariscal, *Ann. N.Y. Acad. Sci.* **474**, 270 (1986).
17. Mice were killed by exposure of the head to microwave irradiation for 900 ms, for which a Muromachi Microwave Applicator (Stoelting, Wood Dale, IL) set at 1.5 power was used. The brains were isolated from the crania, and 1-mm coronal sections bracketing the hypothalamic area were prepared with the aid of a mouse brain matrix (Activational Systems, Ann Arbor, MI), following the stereotaxic coordinates of Franklin and Paxinos (*22*). The microdissection of the hypothalamus was performed as described (*23*), and the tissues were stored at −80°C until processed. Frozen samples were processed and immunoblotted for phospho–DARPP-32 and total DARPP-32 (*24*). Phospho–DARPP-32 and total DARPP-32 bands were quantified by densitometry with the use of a Phosphoimager:SF (Molecular Dynamics). The phospho–DARPP-32 values were normalized for the amount of total DARPP-32 present in the samples, and data were represented as percent of vehicle controls. The linear range of signals for densitometry was obtained by exposing the chemiluminescent membranes to x-ray film for varying periods of time. The linearity of measurements was confirmed by calibrating the values obtained to a standard range of phospho–DARPP-32 concentrations in striatal tissues under conditions of basal and D_1 activation. The exposure conditions that yielded linear measurements for phospho–DARPP-32 were obtained by comparison of phospho–DARPP-32 signals in hypothalamic tissue extracts with those obtained from signals in striatal tissue measurements.
18. J. M. Meredith *et al.*, *J. Neurosci.* **18**, 10189 (1998).
19. R. F. Power, S. K. Mani, J. Codina, O. M. Conneely, B. W. O'Malley, *Science* **254**, 1636 (1991).
20. A. N. Moore, M. N. Waxham, P. K. Dash, *Proc. Natl. Acad. Sci. U.S.A.* **271**, 14214 (1996).
21. E. D. Roberson and J. D. Sweatt, *J. Biol. Chem.* **271**, 30436 (1996).
22. K. B. J. Franklin and G. Paxinos, in *The Mouse Brain in Stereotaxic Coordinates* (Academic Press, San Diego, CA, 1997).
23. J. P. O'Callaghan, K. L. Lavin, Q. Chess, D. H. Clouet, *Brain Res. Bull.* **11**, 31 (1983).
24. G. L. Snyder, G. Fisone, P. Greengard, *J. Neurochem.* **63**, 1766 (1994); A. Nishi, G. L. Snyder, P. Greengard, *J. Neurosci.* **17**, 8147 (1997).
25. Statistical analysis was done by either of the following two methods as appropriate. For each significant analysis of variance (ANOVA), post-hoc comparisons were made using Dunn's method for comparison of all groups versus the control group or the Tukey-Kramer method for multiple comparisons. Instat (Graph Pad, San Diego, CA) was used for statistical analyses.
26. Supported by U.S. Public Health Service grants MH57442 (S.K.M.), MH49662 and NS 35457 (P.K.D.), MH40899 and DA10044 (P.G.), and HD74095 (B.W.O.). We thank P. Ingrassia and J. Ellsworth for excellent assistance.

3 June 1999; accepted 22 December 1999

Ethanol-Induced Apoptotic Neurodegeneration and Fetal Alcohol Syndrome

Chrysanthy Ikonomidou,[1] Petra Bittigau,[1] Masahiko J. Ishimaru,[2] David F. Wozniak,[3] Christian Koch,[1] Kerstin Genz,[1] Madelon T. Price,[3] Vanya Stefovska,[1] Friederike Hörster,[1] Tanya Tenkova,[3] Krikor Dikranian,[3] John W. Olney[3]*

The deleterious effects of ethanol on the developing human brain are poorly understood. Here it is reported that ethanol, acting by a dual mechanism [blockade of *N*-methyl-D-aspartate (NMDA) glutamate receptors and excessive activation of $GABA_A$ receptors], triggers widespread apoptotic neurodegeneration in the developing rat forebrain. Vulnerability coincides with the period of synaptogenesis, which in humans extends from the sixth month of gestation to several years after birth. During this period, transient ethanol exposure can delete millions of neurons from the developing brain. This can explain the reduced brain mass and neurobehavioral disturbances associated with human fetal alcohol syndrome.

Intrauterine exposure of the human fetus to ethanol causes a neurotoxic syndrome (*1*) termed fetal alcohol effects (FAE) or fetal alcohol syndrome (FAS), depending on severity. The most disabling features of FAE/FAS are neurobehavioral disturbances ranging from hyperactivity and learning disabilities to depression and psychosis (*2, 3*). It is thought that the brain is particularly sensitive to the neurotoxic effects of ethanol during the period of synaptogenesis, also known as the brain growth spurt period, which occurs postnatally in rats but prenatally (during the last trimester of gestation) in humans (*4–6*). Thus, ethanol treatment of neonatal rats causes reproducible effects relevant to FAE/FAS, including a generalized loss

[1]Department of Pediatric Neurology, Charité, Virchow Clinics, Humboldt University, Augustenburger Platz 1, 13353 Berlin, Germany. [2]Medical Research Institute, Tokyo Medical and Dental University, 2-3-10 Kandasurugadai, Chiyodku, Tokyo, Japan. [3]Department of Psychiatry, Washington University School of Medicine, 4940 Children's Place, St. Louis, MO 63110, USA.

*To whom correspondence should be addressed.

of brain mass and a specific loss of cerebellar and hippocampal neurons (*7, 8*). However, these circumscribed losses cannot account for the overall loss of brain mass, and the mechanism(s) underlying ethanol's injurious effects on the developing brain remain a mystery.

Having recently found (*9*) that transient blockade of NMDA glutamate receptors during the period of synaptogenesis causes widespread apoptotic neurodegeneration in the infant rat brain, we decided to evaluate ethanol, a known NMDA antagonist (*10*), for its ability to trigger apoptotic neurodegeneration in the developing rat brain. A 20% solution of ethanol in normal saline was administered to 7-day-old Sprague-Dawley rats in two separate treatments, 2 hours apart, each treatment delivering 2.5 g/kg subcutaneously (sc); control rats were treated with saline only. The brains were examined histologically 24 hours after the first treatment. In the brains of saline-treated rats, both silver staining and TUNEL (terminal deoxynucleotidyl transferase–mediated deoxyuridine triphosphate nick-end labeling) (*11–13*) revealed a very light pattern of neurodegeneration attributable to physiological cell death (PCD), the apoptotic process by which biologically redundant neurons are deleted from the developing brain. In the brains of ethanol-treated rats, these stains revealed a very dense and widely distributed pattern of neurodegeneration, a pattern that overlapped with but was more extensive than that (*9*) induced by other NMDA antagonists (Fig. 1, A to H). As assessed by electron microscopy, the ethanol-induced cell death process clearly met ultrastructural criteria (*14, 15*) for apoptosis (Fig. 1L).

Quantitative evaluation (*16, 17*) revealed that the densities of degenerating neurons in saline-treated rats varied from 0.13 to 1.55% of the total neuronal density in brain regions examined (Table 1). This represents the rate of spontaneous apoptosis (PCD) that occurs naturally in the rat brain at postnatal day 8 (P8). In contrast, the densities of degenerating neurons in ethanol-treated pups ranged from 5 to 30% of the total neuronal densities in the same brain regions. The mean number (±SEM) of degenerating neurons in selected regions of the forebrain (*16*) was 12,567,726 ± 1,008,195 for the ethanol-treated rats (n = 6), compared to

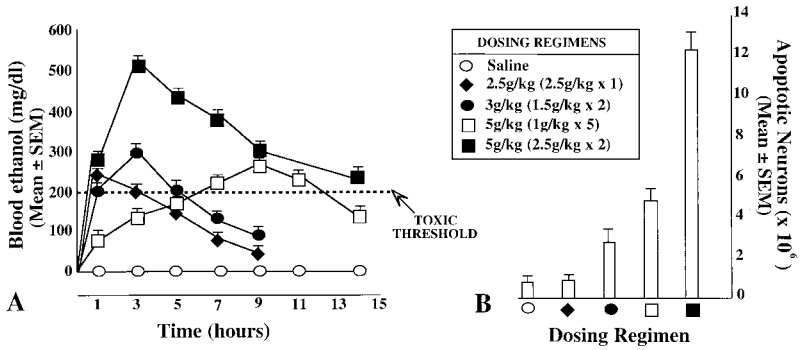

Fig. 2. Ethanol was administered to P7 rats by several dosing regimens. The total dose ranged from 0 to 5 g/kg sc and was administered either in a single injection or in multiple injections spaced 2 hours apart. (**A**) Blood ethanol curves associated with each of several dosing regimens. (**B**) Severity of apoptotic neurodegeneration associated with each dose–blood ethanol curve. The histographic values in (B) represent total numbers of apoptotic neurons (means ± SEM, n = 6 per group) in the forebrains of saline- and ethanol-treated rats. Severity of degeneration was established using silver-stained sections and by counting argyrophilic profiles in 13 brain regions, as described (*16*). Many blood ethanol curves not shown were generated; those shown were selected because each is representative of a type of curve required to trigger a certain amount of apoptotic neurodegeneration. The data show that the severity of apoptotic degeneration does not correlate with total dose, but rather with the rate at which the dose is given and the length of time the blood ethanol level remains elevated above a toxic threshold in the range of 200 mg/dl. Dosing regimens that produced blood ethanol concentrations that did not exceed 200 mg/dl for more than 2 hours did not increase the rate of apoptotic neurodegeneration significantly above the spontaneous rate in saline-treated rats. If blood ethanol concentrations exceeded 200 mg/dl for 4 hours, apoptotic neurodegeneration was significantly increased, and if concentrations exceeded 200 mg/dl for more than 4 hours, the degenerative response became progressively more severe in proportion to the length of time the concentrations exceeded 200 mg/dl.

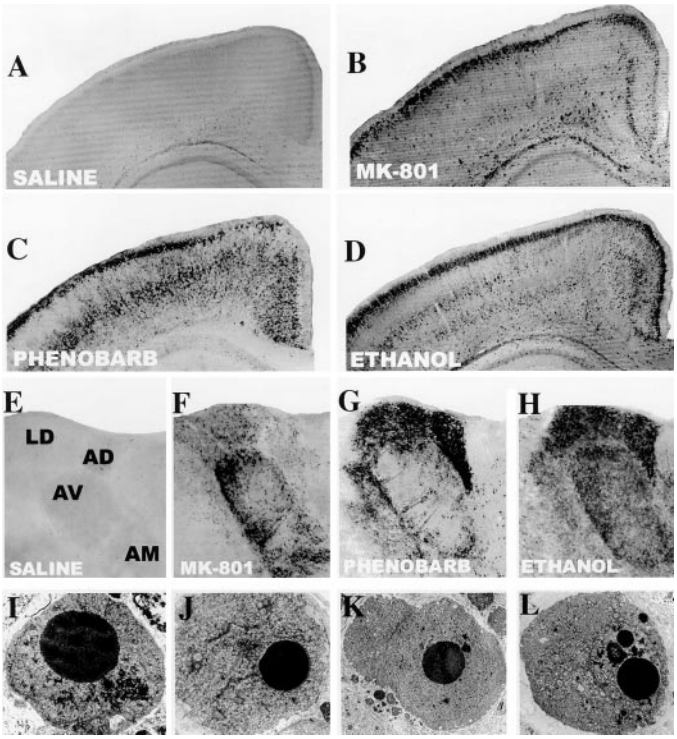

Fig. 1. (**A** to **D**) Low-magnification (25×) light microscopic overviews of silver-stained (*11–13*) transverse sections from the parietal and cingulate cortex of P8 rats treated 24 hours previously with saline, MK-801 (NMDA antagonist), phenobarbital, or ethanol. Degenerating neurons (small dark dots) are abundantly present in several brain regions after treatment with MK-801, phenobarbital, or ethanol, but are only sparsely present after saline treatment. Note that MK-801 and phenobarbital both affect neurons superficial to the cortical surface, whereas the middle cortical layers are affected very prominently by phenobarbital and are relatively spared by MK-801. The ethanol pattern resembles a combination of the MK-801 and phenobarbital patterns. (**E** to **H**) Light micrographs (55×) depicting the anterior thalamus at the level of the laterodorsal (LD), anterodorsal (AD), anteroventral (AV), and anteromedial (AM) nuclei, respectively. Note that MK-801 affects the LD, AV, and AM nuclei but not the AD nucleus, whereas phenobarbital affects the LD and AD nuclei very prominently but almost entirely spares the AV and AM nuclei. The ethanol pattern includes all four nuclei, as would be expected if it acts by a dual mechanism involving blockade of NMDA receptors plus activation of $GABA_A$ receptors. (**I** to **L**) Electron micrographs (1800×) illustrating that apoptotic neurodegeneration induced by MK801 (J), phenobarbital (K), or ethanol (L) has the same ultrastructural appearance as PCD (I), an apoptotic phenomenon that occurs spontaneously in the developing brain. As we have recently described (*9, 14*), in both spontaneous and induced apoptosis, the earliest signs are the formation of spherical chromatin masses and flocculent densities in the nucleus while the nuclear envelope remains intact and cytoplasmic organelles are relatively unaltered; this is followed in the middle and late stages by fragmentation of the nuclear envelope, intermixing of nucleoplasmic and cytoplasmic contents, and progressive condensation of the entire cell. All four examples shown here have a similar appearance, as they are all in the middle stage of apoptotic neurodegeneration.

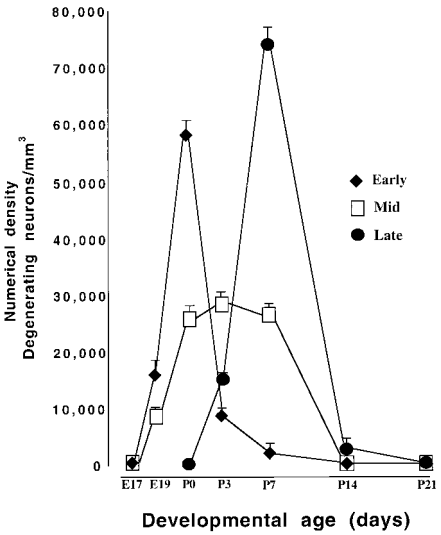

Fig. 3. Age dependency of ethanol-induced apoptosis in the brains of developing rats. Immature rats were exposed at different developmental ages (E17 to P21) to saline or ethanol (2.5 g/kg sc at 0 and 2 hours; total dose 5 g/kg), and 24 hours later we used the stereological disector method (*16, 17*) to assess the numerical densities of degenerating neurons in DeOlmos silver-stained sections of various brain regions. To determine the apoptotic degeneration that could be attributed to ethanol, we subtracted the mean numerical density count for the saline-treated rats ($n = 6$) in a given brain region from the mean numerical density count for the ethanol-treated rats ($n = 6$) in the same brain region. In each brain region there was a time window during which neurons showed vulnerability to ethanol-induced apoptosis, and the timing of this vulnerability period was different for different brain regions. However, each region displayed a temporal profile that fit into an early-, middle-, or late-stage category. Neuronal populations showing the early-stage profile (ventromedial hypothalamus, mediodorsal and ventral thalamus) began to display a significant response to ethanol on day E19, which reached a peak at P0 and rapidly declined thereafter. Neurons showing the middle-stage profile (subiculum, hippocampus, caudate, and laterodorsal and anteroventral thalamus) began to show a response on E19, which reached a peak at P3 and gradually declined to zero by P14. Those showing the late-stage profile (frontal, parietal, temporal, cingulate, and retrosplenial cortices) exhibited a degenerative response that began on day P3, peaked at P7, was markedly diminished at P14, and was absent at P21. Each of the curves presented here pertains to a single brain region that is representative of a response pattern: ventromedial hypothalamus, early stage; laterodorsal thalamus, middle stage; and frontal cortex, layer II, late stage.

835,360 ± 101,079 for the saline-treated group ($n = 6$).

In additional experiments with P7 rats, we administered ethanol by various dosing regimens and compared the severity of the apoptotic response (*16*) with the blood ethanol curves produced by each regimen. We found that the apoptotic response induced by ethanol cannot be predicted by the dose, but rather depends on how rapidly the dose is administered and on how long the blood ethanol levels are elevated above a toxic threshold in the range of 180 to 200 mg/dl (Fig. 2). Maintaining blood ethanol concentrations at or above 200 mg/dl for four consecutive hours was the minimum condition for triggering neurodegeneration. If ethanol concentrations remained above 200 mg/dl for more than 4 hours, the degenerative response became progressively more severe and more widespread in proportion to the length of time that the concentrations remained above this level.

To determine how the apoptotic response to ethanol might differ as a function of developmental age, we administered either saline or ethanol (2.5 g/kg sc at 0 and 2 hours; total dose 5 g/kg) to pregnant rats on embryonic day 17 (E17) or E19 or to their offspring on P0, P3, P14, or P21; after 24 hours, we

Table 1. Rate of apoptotic neurodegeneration in 15 brain regions of P8 rats 24 hours after treatment with saline, ethanol, diazepam, or MK801.

Brain region	Saline		Ethanol*: Degenerating cell density as percentage of total cell density (mean ± SEM)	Diazepam*: Degenerating cell density as percentage of total cell density (mean ± SEM)	MK801*: Degenerating cell density as percentage of total cell density (mean ± SEM)
	Numerical density, total cells (mean/mm^3 ± SEM)	Degenerating cell density as percentage of total cell density (mean ± SEM)			
CA1 hippocampus	220,050 ± 4,584	0.85 ± 0.11	17.35 ± 1.36	8.00 ± 1.31	3.35 ± 0.67
Subiculum	198,124 ± 8,205	0.59 ± 0.04	16.48 ± 1.60	13.47 ± 2.75	10.70 ± 1.72
Caudate	242,534 ± 11,140	0.29 ± 0.04	8.07 ± 0.50	3.97 ± 0.92	4.77 ± 0.85
Laterodorsal thalamus	133,945 ± 13,148	0.30 ± 0.05	18.33 ± 2.72	11.79 ± 1.99	11.91 ± 2.21
Mediodorsal thalamus	199,335 ± 6,398	0.40 ± 0.01	5.02 ± 1.17	5.51 ± 1.34	2.39 ± 0.34
Septum	107,143 ± 9,510	0.31 ± 0.05	10.31 ± 0.79	5.82 ± 0.38	3.30 ± 0.81
Pallidum	214,286 ± 21,087	0.13 ± 0.03	5.43 ± 0.81	3.50 ± 0.19	2.09 ± 0.19
Frontal cortex layer II	219,432 ± 4,541	1.55 ± 0.18	24.62 ± 2.28	7.47 ± 0.96	22.65 ± 1.93
Frontal cortex layer IV	142,120 ± 10,323	0.20 ± 0.05	4.91 ± 0.34	3.89 ± 0.95	1.43 ± 0.18
Parietal cortex layer II	223,900 ± 13,434	1.08 ± 0.28	25.38 ± 2.03	10.69 ± 2.42	26.13 ± 2.51
Parietal cortex layer IV	156,078 ± 6,323	0.22 ± 0.05	5.70 ± 0.55	3.84 ± 0.73	1.72 ± 0.26
Cingulate cortex layer II	218,932 ± 11,239	1.54 ± 0.21	26.73 ± 2.72	9.36 ± 0.27	15.49 ± 1.79
Cingulate cortex layer IV	148,100 ± 6,125	0.13 ± 0.03	13.72 ± 0.87	11.81 ± 1.54	3.22 ± 0.85
Retrosplenial cortex layer II	235,948 ± 13,857	0.89 ± 0.07	29.87 ± 1.60	13.38 ± 1.17	11.49 ± 1.82
Retrosplenial cortex layer IV	143,250 ± 10,857	0.33 ± 0.08	11.70 ± 0.98	5.47 ± 1.29	5.95 ± 0.42

*In all brain regions, the rate of apoptosis was significantly higher ($P < 0.001$) in rats treated with ethanol (2.5 g/kg × 2) ($n = 7$), diazepam (30 mg/kg × 1) ($n = 6$), or MK801 (0.5 mg/kg × 3) ($n = 6$) than in rats treated with saline ($n = 5$). For all comparisons (ethanol, diazepam, or MK801 versus saline), the P values exceeded the Bonferroni corrected levels ($P = 0.05/45 = 0.0011$).

compared the neurodegenerative response in the fetal or infant brains with the response in P7 rats. To assess the degenerative response to ethanol, we compared the density of degenerating neurons in various brain regions of saline-treated rats with the density of degenerating neurons in the same brain regions of ethanol-treated rats. We found that there is a time window from E19 to P14 when various neurons in the forebrain show transient sensitivity to ethanol-induced neurodegeneration, and within this period, which coincides with the synaptogenesis period, different neuronal populations display transient sensitivity at different times. Three response patterns were observed (Fig. 3).

To assess whether the apoptotic response to ethanol is associated with a loss of brain mass, we administered saline or ethanol (2.5 g/kg sc at 0 and 2 hours; total dose 5 g/kg) to infant rats on P7 and found, when the experiment was terminated at P12, that the brain weights (whole brain or forebrain and cerebellum weighed separately) of the ethanol-treated rats were significantly lower than those of the saline-treated rats (Fig. 4).

Because ethanol triggered apoptosis in some brain regions that are not typically affected by NMDA antagonists, we attempted to identify other possible mechanisms to explain ethanol's effects in these brain regions. In a series of experiments (*18*), we were unable to demonstrate an appreciable apoptotic response to agents that act as either agonists or antagonists at dopamine receptors, block kainic acid or muscarinic cholinergic receptors, or block voltage-gated ion channels. However, a robust apoptotic response

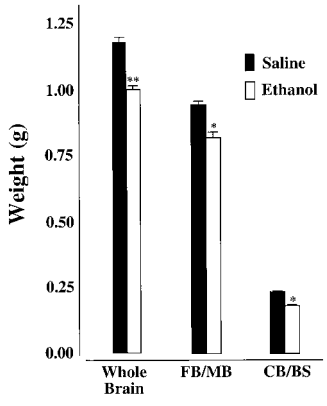

Fig. 4. On day P12, the brains of rats that were treated with saline ($n = 6$) or ethanol ($n = 6$) on day P7 were weighed to obtain a whole brain weight, then were dissected at the level of the pons into two portions, one including the forebrain (FB) and midbrain (MB) and the other including the cerebellum (CB) and brainstem (BS). Sampling and weighing of the brains were performed in a blinded manner. The weights for the ethanol-treated brains (whole or in parts) were significantly lower than those for the saline-treated brains ($^*P < 0.05$, $^{**}P < 0.01$; Student's t test).

was triggered by benzodiazepines and barbiturates, "GABAergic" agents that either mimic or potentiate the action of GABA at $GABA_A$ receptors. The agents tested were diazepam [10 to 30 mg/kg intraperitoneally (ip) at 0 hours, $n = 6$], clonazepam (0.5 to 4 mg/kg ip at 0 hours, $n = 6$), pentobarbital (10 mg/kg ip at 0 and 4 hours, $n = 6$), and phenobarbital (50 to 75 mg/kg ip at 0 hours, $n = 6$). These agents, in a dose-dependent manner, triggered widespread cell death in the infant rat brain, which was apoptotic as assessed by ultrastructural analysis (Fig. 1K). The pattern of degeneration was similar for each GABAergic agent, but this pattern differed in several major respects from that induced by NMDA antagonists (Fig. 1, A to H). However, superimposing one pattern on the other resulted in a composite pattern closely resembling that induced by ethanol. We also studied the window of vulnerability to the proapoptotic actions of diazepam and phenobarbital, and we determined that it coincides with the period of synaptogenesis.

Our results show that exposure of the developing rat brain to ethanol for a period of hours during a specific developmental stage (synaptogenesis) predictably induces an apoptotic neurodegenerative reaction that deletes large numbers of neurons from several major regions of the developing brain. Of ethanol's many actions in the brain, it appears that two—its blocking action at NMDA glutamate receptors and its positive modulatory action at $GABA_A$ receptors—are primarily responsible for its proapoptotic effects. In addition, the developmental period during which the immature brain is vulnerable to the proapoptotic action of NMDA antagonists, GABAergic agents, and ethanol is the same: For all three, it coincides with the synaptogenesis period.

In humans, as noted earlier, the period of synaptogenesis occurs prenatally, during the last 3 months of gestation (*6*). If a pregnant mother imbibes ethanolic beverages for several hours in a single drinking episode, she could expose her third-trimester fetus to blood ethanol levels equivalent to those required to trigger apoptotic neurodegeneration in the immature rat brain (200 mg/dl lasting 4 hours or more).

From a clinical perspective, it is important to recognize that both NMDA antagonists and $GABA_A$ agonists are frequently used as sedatives, tranquilizers, anticonvulsants, or anesthetics in pediatric and/or obstetric medicine. These agents also are drugs of abuse. Because the human brain growth spurt spans not only the last trimester of pregnancy but several years after birth (*6*), the developing human brain may be exposed to these agents by medical professionals or by drug-abusing pregnant mothers. Also relevant is our observation that within the synaptogenesis period, different neuronal populations have different temporal patterns of response to the apoptosis-inducing effects of these drugs. Thus, depending on the timing of exposure, different combinations of neuronal groups will be deleted, which signifies that this is a neurodevelopmental mechanism that can contribute to a wide spectrum of neuropsychiatric disturbances.

References and Notes

1. K. L. Jones and D. W. Smith, *Lancet* **ii**, 999 (1973); ———, C. N. Ulleland, A. P. Streissguth, *Lancet* **i**, 1267 (1973); S. K. Clarren, A. C. Alvord, S. M. Sumi, A. P. Streissguth, D. W. Smith, *J. Pediatr.* **92**, 64 (1978); V. W. Swayze *et al*., *Pediatrics* **99**, 232 (1977).
2. S. K. Clarren and D. W. Smith, *N. Engl. J. Med.* **298**, 1063 (1978); K. A. Kerns, A. Don, C. A. Mateer, A. P. Streissguth, *J. Learn. Disab*. **30**, 685 (1977); K. K. Sulik, M. C. Johnston, M. A. Webb, *Science* **214**, 936 (1981); C. Famy, A. P. Streissguth, A. S. Unis, *Am. J. Psychiatr*. **155**, 552 (1998).
3. M. J. Eckardt *et al*., *Alcohol. Clin. Exp. Res*. **22**, 998 (1998); C. L. Faingold, P. N'Gouemo, A. Riaz, *Prog. Neurobiol*. **55**, 509 (1998); D. W. Sapp and H. H. Yeh, *J. Pharmacol. Exp. Ther.* **284**, 768 (1998).
4. C. R. Goodlett and J. R. West, in *Maternal Substance Abuse and the Developing Nervous System*, I. Zagon and T. Slotkin, Eds. (Academic Press, San Diego, CA, 1992), pp. 45–75.
5. J. R. West, *Alcohol Drug Res*. **7**, 423 (1987).
6. J. Dobbing and J. Sands, *Early Hum. Dev*. **3**, 79 (1979).
7. J. R. West, K. M. Hamre, M. D. Cassell, *Alcohol. Clin. Exp. Res*. **10**, 190 (1986).
8. C. Bauer-Moffett and J. Altman, *Brain Res*. **119**, 249 (1977); C. R. Goodlett, B. L. Marcussen, J. R. West, *Alcohol* **7**, 107 (1990); A. E. Ryabinin, M. Cole, F. E. Bloom, M. C. Wilson, *Alcohol. Clin. Exp. Res*. **19**, 784 (1995).
9. C. Ikonomidou *et al*., *Science* **283**, 70 (1999).
10. D. M. Lovinger, G. White, F. F. Weight, *Science* **243**, 1721 (1989); P. L. Hoffman, C. S. Rabe, F. Moses, B. Tabakoff, *J. Neurochem.* **52**, 1937 (1989).
11. Twenty-four hours after saline or ethanol treatment, the immature rats were deeply anesthetized and perfused with aldehyde fixative, and the brains were studied with the use of three histological methods: TUNEL, DeOlmos silver impregnation, and electron microscopy. The TUNEL method, first described by Gavrieli *et al*. (*12*), detects a DNA fragmentation process that occurs typically in cells that are dying by an apoptotic mechanism. Thus, it is useful for marking neurons that are undergoing experimentally induced apoptosis or neurons in the normal brain that are undergoing PCD. We have found (*9, 14*) that DeOlmos silver impregnation (*13*) also stains neurons undergoing either experimentally induced apoptosis or PCD, and that it reveals in the normal brain the same pattern of cells dying by PCD that is revealed by TUNEL. The DeOlmos silver method is more favorable for quantitative purposes because it more uniformly penetrates thick histological sections. Because neither TUNEL nor the DeOlmos method is specific for apoptosis (they are positive for apoptosis but also for at least some nonapoptotic cell death processes), it is necessary to establish the apoptosis diagnosis by ultrastructural analysis, using as a reference standard the ultrastructural appearance of neurons undergoing PCD in the normal developing rat brain (*14*).
12. Y. Gavrieli, Y. Sherman, S. A. Ben-Sasson, *J. Cell Biol*. **119**, 493 (1992).
13. J. S. DeOlmos and W. R. Ingram, *Brain Res.* **33**, 523 (1971).
14. M. J. Ishimaru *et al*., *J. Comp. Neurol*. **408**, 461 (1999).
15. A. H. Wyllie, J. F. R. Kerr, A. R. Currie, *Int. Rev. Cytol*. **68**, 251 (1980).
16. In the normal developing brain, after neurons have differentiated, migrated, and are undergoing synaptogenesis, spontaneous apoptotic neurodegeneration (PCD) occurs at a relatively low rate, about 1% of the total neuronal population (*9*). To determine whether ethanol treatment induced a rate of apoptotic neu-

rodegeneration exceeding the spontaneous rate in a given brain region, we used an unbiased stereological disector method (*17*) to quantify the numerical density (neurons/mm^3) of normal neurons in 70-μm Nissl-stained sections, or of degenerating neurons in 70-μm sections stained by the DeOlmos silver method (*13*). A total of 8 to 10 disectors (0.05 mm by 0.05 mm, disector height 0.07 mm) were used to sample each brain region. Counts were performed in a blinded manner. To establish the absolute numbers of degenerating neurons, we identified boundaries of individual brain regions [thalamus, dentate gyrus, CA1 hippocampus, subiculum, caudate, septum, hypothalamus, amygdala, and frontoparietal, cingulate, retrosplenial, temporal, and pyriform/entorhinal cortices, according to G. Paxinos, I. Tork, L. H. Tecott, K. L. Valentino, *Atlas of the Developing Rat Brain* (Academic Press, New York, 1991)] in Nissl-stained sections. We used an image analysis system (IMAGE 1.54, National Institutes of Health) to facilitate volume determinations for each brain region. Multiplication of the volume of a given region by the numerical density of degenerating neurons in that region provided an estimate of total numbers of neurons deleted from each brain region by ethanol treatment. The regional values were summed to give a total for each brain, and from these totals, means (±SEM) were calculated separately for the brains in the ethanol- and saline-treated groups.

17. M. J. West, *Neurobiol. Aging* **14**, 275 (1993); H. J. G. Gundersen, T. F. Bendtsen, L. Korbo, M. J. West, *APMIS* **96**, 379 (1988).

18. In addition to GABAergic agents, we tested 6-nitro-7-sulfamoylbenzo[f]quinoxaline-2,3-dione (NBQX), an antagonist of non-NMDA glutamate receptors, at a dose of 20 mg/kg ip given at 0, 75, and 150 min and at 8 hours (n = 5); scopolamine hydrobromide, an antagonist of cholinergic muscarinic receptors, at a dose of 0.3 mg/kg ip given at 0, 4, and 8 hours (n = 5); haloperidol, an antagonist of dopamine receptors, at a dose of 10 mg/kg ip given at 0 and 8 hours (n = 5); and L-dopa, an agent that increases the availability of dopamine at dopamine receptors, administered at 50, 100, or 200 mg/kg ip together with benserazide (dopamine decarboxylase inhibitor) at 14, 28, or 56 mg/kg ip (n = 5 per dose). Finally, because NMDA receptor–activated ion channels are highly permeable to Ca^{2+} ions, we tested whether blockade of calcium influx via other routes (i.e., voltage-dependent Ca^{2+} channels) may also cause apoptotic neurodegeneration in the brain. For this purpose we treated P7 rats with the Ca^{2+} channel blockers nimodipine (50 mg/kg ip at 0 and 8 hours; n = 6) or nifedipine (10 mg/kg ip at 0 and 8 hours; n = 6). We examined the brains histologically 24 hours after each of these treatments. None of these agents reproduced the apoptosis-inducing action of NMDA antagonists.

19. Supported in part by Deutsche Forschungsgemeinschaft grant Ik2/2-1, Humboldt University grant 98-649, National Institute for Mental Health Research Scientist Award MH 38894 (J.W.O.), National Institute on Aging grant AG 11355, National Institute on Drug Abuse grant DA 05072, National Eye Institute grant EY 08089, and a National Alliance for Research on Schizophrenia and Depression Established Investigator Award (J.W.O.).

3 August 1999; accepted 21 December 1999

Evidence for DNA Loss as a Determinant of Genome Size

Dmitri A. Petrov,[1]* Todd A. Sangster,[2] J. Spencer Johnston,[3] Daniel L. Hartl,[2] Kerry L. Shaw[2]

Eukaryotic genome sizes range over five orders of magnitude. This variation cannot be explained by differences in organismic complexity (the *C* value paradox). To test the hypothesis that some variation in genome size can be attributed to differences in the patterns of insertion and deletion (indel) mutations among organisms, this study examines the indel spectrum in *Laupala* crickets, which have a genome size 11 times larger than that of *Drosophila*. Consistent with the hypothesis, DNA loss is more than 40 times slower in *Laupala* than in *Drosophila*.

Wide variation in eukaryotic genome size is a pervasive feature of genome evolution. Large differences in haploid DNA content (*C* value) are found within protozoa (5800-fold range), arthropods (250-fold), fish (350-fold), algae (5000-fold), and angiosperms (1000-fold) (*1*). This variation is called the *C* value paradox (*2*, *3*) because genome size is not correlated with the structural complexity of organisms or with the estimated number of genes. Despite much progress in the study of genomes, the *C* value paradox remains largely unresolved.

Drosophila species, which have small genomes, spontaneously lose DNA at a much higher rate than mammalian species, which have large genomes (*4*–*7*). Although many mechanisms can affect genome size—including polyploidy, fixation of accessory chromosomes or large duplications (*8*), and expansions of satellite DNA or transposable elements (*9*)—the *Drosophila* findings suggest that some differences in haploid genome size may result from variation in the rate of spontaneous loss of nonessential DNA (*4*). Here, we test this hypothesis by examining the indel spectrum in Hawaiian crickets (*Laupala*), which have a genome size ~11-fold larger than that of *Drosophila* (*10*). Specifically, we test the prediction of a lower rate of DNA loss in *Laupala* than in *Drosophila*, corresponding to the large difference in genome size.

Sequences unconstrained by natural selection exhibit patterns of substitution, reflecting the underlying spectra of spontaneous mutations (*11*). As pseudogene surrogates we chose nontransposing copies of non-LTR (long terminal repeat) retrotransposable elements (*4*, *12*). Transposition of non-LTR elements usually results in a 5′-truncated copy that is unable to transpose because of lack of a promoter and lack of the capacity to encode functional proteins (*13*, *14*); these "dead-on-arrival" (DOA) elements are essentially pseudogenes.

We identified a new non-LTR element in *Laupala*, here designated *Lau1*, by means of polymerase chain reaction (PCR) with degenerate primers to conserved regions of the non-LTR reverse transcriptase (*15*). Evolution of unconstrained DOA elements can be distinguished from that of the constrained, active elements via phylogenetic analysis of nucleotide sequences of individual DOA elements (*4*, *12*). Substitutions in a transpositionally active lineage are represented in multiple DOA elements generated by transposition of the active copy, whereas substitutions in each DOA lineage are unique (barring parallel mutations) because of the inability of DOA elements to transpose. This implies that, in a gene tree of non-LTR sequences from closely related species, the active lineages map to internal branches (identified through substitutions shared among elements), whereas DOA lineages map to terminal branches (identified through unique substitutions). Some DOA lineages may also map to internal branches, because elements from different species may be identical by descent (IBD) because of transmission of the same (allelic) DOA copy from a common ancestor (*7*, *12*). Nevertheless, as long as the number of active lineages is small and the sampling is dense, substitutions in the terminal branches will correspond primarily to the DOA element evolution (*12*).

If the terminal branches of the *Lau1* gene tree (Fig. 1) represent unconstrained evolution of DOA elements, we predict the absence of purifying selection operating along these branches. Confirming this prediction, point substitutions in terminal branches map with equal frequencies to all three codon positions (G test; P = 0.64). In addition, the terminal branches feature numerous element-specific indels (48 deletions and 18 insertions in 49 terminal branches). The internal branches show evidence of relaxed selection as well, which suggests that many elements in our sample are IBD through inheritance of ancestral allelic DOA copies. The substitutions in the internal branches are found at equal fre-

[1]Harvard University Society of Fellows, [2]Department of Organismic and Evolutionary Biology, Harvard University, Cambridge, MA 02138, USA. [3]Department of Entomology, Texas A&M University, College Station, TX 77843, USA.

*To whom correspondence should be addressed. E-mail: dpetrov@oeb.harvard.edu

Antiepileptic drugs and apoptotic neurodegeneration in the developing brain

Petra Bittigau*, Marco Sifringer*, Kerstin Genz*, Ellen Reith*, Dana Pospischil*, Suresh Govindarajalu*, Mark Dzietko*, Stefanie Pesditschek*, Ingrid Mai†, Krikor Dikranian‡, John W. Olney‡, and Chrysanthy Ikonomidou*§

*Department of Pediatric Neurology, Children's Hospital, Charite-Virchow Clinics, Humboldt University, Augustenburger Platz 1, 13353 Berlin, Germany; †Department of Clinical Pharmacology, Humboldt University, Schumannstrasse 20/21, 10117 Berlin, Germany; and ‡Department of Psychiatry, Washington University School of Medicine, 4940 Children's Place, St. Louis, MO 63110

Communicated by Martin Lindauer, University of Würzburg, Munich, Germany, September 9, 2002 (received for review March 18, 2002)

Epilepsy is the most common neurological disorder of young humans. Each year 150,000 children in the United States experience their first seizure. Antiepileptic drugs (AEDs), used to treat seizures in children, infants, and pregnant women, cause cognitive impairment, microcephaly, and birth defects. The cause of unwanted effects of therapy with AEDs is unknown. Here we reveal that phenytoin, phenobarbital, diazepam, clonazepam, vigabatrin, and valproate cause apoptotic neurodegeneration in the developing rat brain at plasma concentrations relevant for seizure control in humans. Neuronal death is associated with reduced expression of neurotrophins and decreased concentrations of survival-promoting proteins in the brain. β-Estradiol, which stimulates pathways that are activated by neurotrophins, ameliorates AED-induced apoptotic neurodegeneration. Our findings present one possible mechanism to explain cognitive impairment and reduced brain mass associated with prenatal or postnatal exposure of humans to antiepileptic therapy.

survival | epilepsy | rat | neurotrophins

A seizure is a sudden change in behavior caused by synchronous, rhythmic firing of neurons in the brain. Between 2% and 4% of all children in Europe and the United States experience at least one seizure before the age of 5 years (1). Epilepsy, a brain disorder characterized by recurrent seizures, affects 1–2% of humans worldwide and shows its highest incidence in the first year of life (1).

Antiepileptic drugs (AEDs) are used to prevent or interrupt seizures. They act via three mechanisms: (*i*) limitation of sustained repetitive neuronal firing via blockade of voltage-dependent sodium channels; (*ii*) enhancement of γ-aminobutyric acid (GABA)-mediated inhibition; and (*iii*) blockade of glutamatergic excitatory neurotransmission (2–5). Phenytoin decreases neuronal firing through use-dependent blockade of voltage-gated sodium channels. Barbiturates and benzodiazepines enhance inhibition in the brain by allosterically modulating permeability of the chloride channel coupled to the GABA type A receptor. Vigabatrin decreases GABA breakdown by blocking the GABA-degrading enzyme GABA transaminase, and valproate influences GABA synthesis and breakdown, leading to an increase of GABA concentrations in the brain. Valproate also interferes with glutamate-mediated excitation and limits sustained repetitive neuronal firing through voltage- and use-dependent blockade of sodium channels (2–5).

AEDs are among the most common causes of fetal malformations, developmental delay, and microcephaly (6–11). Increasing maternal blood levels and combinations of AEDs impose an increased risk for harm to human infants (11). AEDs may also exert unfavorable effects on human intellect when given to treat seizures in infants and toddlers. Therapy with barbiturates during the first 3 years of life may cause cognitive impairment that persists into adulthood (12–16). Although neurotoxic effects of AEDs have been recognized since the 1970s, the underlying mechanisms are not understood.

In the immature rodent brain, suppression of synaptic neurotransmission via blockade of glutamate *N*-methyl-D-aspartate receptors or activation of GABA type A receptors may trigger apoptotic neurodegeneration (17, 18). Because depression of synaptic neurotransmission is the common denominator in the action of AEDs, we investigated whether common AEDs may cause apoptotic neurodegeneration in the developing brain and what the underlying pathogenetic mechanisms are. Furthermore, we attempted to identify measures that will prevent AED neurotoxicity.

Materials and Methods

***In Vivo* Experiments.** Wistar rats (Bundesinstitut für gesundheitlichen Verbraucherschutz und Veterinärmedizin, Berlin), 0–30 days old, received i.p. administration of AEDs, β-estradiol, or vehicle (normal saline) and were allowed to survive for up to 48 h after injection.

The following drugs and doses were administered: phenytoin (Desitin, Hamburg, Germany), 10–50 mg/kg; phenobarbital (Desitin), 20–100 mg/kg; pentobarbital (Sigma), 5 and 10 mg/kg; diazepam (Ratiopharm, Ulm, Germany), 5–30 mg/kg; clonazepam (Desitin), 0.5–4 mg/kg; valproate (Sigma), 50–400 mg/kg; and vigabatrin (Aventis, Bad Soden, Germany), 50, 100, or 200 mg/kg twice daily on 3 consecutive days. Flumazenil (Hoffman–La Roche) was administered in hourly intervals for 5 h at the dose of 2 mg/kg, beginning 15 min after administration of diazepam (30 mg/kg) or clonazepam (4 mg/kg). β-Estradiol (Sigma) was administered three times at the dose of 300 μg/kg every 8 h.

Intracerebroventricular injections of U0126 (Calbiochem) or wortmannin (Calbiochem) were performed in pups subjected to brief halothane anesthesia by using a Hamilton syringe with a 27-gauge needle. The location was 1 mm rostral, 1.5 mm lateral to bregma, and 2 mm deep to skull surface. Drugs were dissolved in 10% DMSO and phosphate buffer and administered in a volume of 1 μl over 2 min. Control pups received i.c.v. injection of vehicle.

To exclude the possibility that hypoxia might contribute to histological changes detected in the brains, oxygen saturations were measured every 30 min over a period of 4 h after injection of the drugs by pulse oximetry.

At the end of the observation period, animals received an overdose of chloralhydrate (150 mg/kg). Before perfusion fixation, a 200-μl blood sample was obtained from the left ventricle for measurement of drug-plasma concentrations. Rats were perfused through the heart and ascending aorta for 15 min with a solution containing paraformaldehyde (1%) and glutaraldehyde (1.5%) in pyrophosphate buffer (for combined light and electron microscopy) or paraformaldehyde (4%) in cacodylate buffer (for terminal deoxynucleotidyltransferase-mediated dUTP end labeling or De-Olmos cupric silver staining).

Histology. To visualize degenerating cells, coronal sections of the whole brain were stained with silver nitrate and cupric nitrate (19).

Abbreviations: AED, antiepileptic drug; GABA, γ-aminobutyric acid; BDNF, brain-derived neurotrophic factor; NT-3, neurotrophin 3; P*n*, postnatal day; ERK, extracellular signal-related protein kinase.

§To whom correspondence should be addressed. E-mail: hrissanthi.ikonomidou@charite.de.

Table 1. Phenytoin, phenobarbital, and valproate increase the rate of apoptosis in the brain of 7-day-old rats

	Vehicle		Phenytoin	Phenobarbital	Valproate
Brain region	Numerical density of total cells, mean/mm^3 ± SEM	Degenerating cells as % of total cells, mean ± SEM	Degenerating cells as % of total cells, mean ± SEM	Degenerating cells as % of total cells, mean ± SEM	Degenerating cells as % of total cells, mean ± SEM
CA1 HC	220,050 ± 4,584	0.85 ± 0.11	2.63 ± 0.43*	2.09 ± 0.45*	1.97 ± 0.40*
DG	284,127 ± 23,089	0.37 ± 0.06	1.21 ± 0.14***	1.54 ± 0.11***	1.32 ± 0.20**
Subiculum	198,124 ± 8,205	0.59 ± 0.04	2.28 ± 0.31***	3.79 ± 0.41***	7.30 ± 0.51***
Caudate	242,534 ± 11,140	0.29 ± 0.04	0.58 ± 0.04**	1.81 ± 0.29***	2.17 ± 0.16***
Thal LD	133,945 ± 13,148	0.30 ± 0.05	2.62 ± 0.37***	9.94 ± 0.96***	15.90 ± 3.53***
Thal MD	199,335 ± 6,398	0.40 ± 0.01	1.86 ± 0.34**	3.33 ± 0.79***	6.39 ± 1.57**
Thal V	132,907 ± 2,634	0.76 ± 0.05	0.72 ± 0.20ns	1.39 ± 0.21*	4.47 ± 0.97**
Hth VM	134,500 ± 2,343	0.90 ± 0.01	2.16 ± 0.15***	2.72 ± 0.51***	6.88 ± 0.90**
Fr II	219,432 ± 4,541	1.55 ± 0.18	5.19 ± 0.38***	4.23 ± 0.32***	4.64 ± 0.14***
Fr IV	142,120 ± 10,323	0.20 ± 0.05	2.57 ± 0.21***	1.46 ± 0.21***	3.33 ± 0.55***
Par II	223,900 ± 13,434	1.08 ± 0.28	6.07 ± 0.64***	4.01 ± 0.50***	4.22 ± 0.19***
Par IV	156,078 ± 6,323	0.22 ± 0.05	3.31 ± 0.33***	1.54 ± 0.29**	2.36 ± 0.49**
Cing II	218,932 ± 11,239	1.54 ± 0.21	3.59 ± 0.56**	4.80 ± 0.45***	3.01 ± 0.51**
Cing IV	148,100 ± 6,125	0.13 ± 0.03	2.85 ± 0.32***	1.15 ± 0.69*	6.01 ± 0.81***
Rspl II	235,948 ± 13,857	0.89 ± 0.07	2.16 ± 0.07***	1.78 ± 0.19***	1.40 ± 0.14**
Rspl IV	143,250 ± 10,857	0.33 ± 0.08	3.06 ± 0.22***	1.38 ± 0.21*	4.52 ± 0.64***

Rats received vehicle, phenytoin (50 mg/kg), phenobarbital (75 mg/kg), or valproate (400 mg/kg) and were killed 24 h later on P8. Using an optical disector method the numerical densities of total cells (cells per mm^3) and degenerating cells (degenerating cells per mm^3) in 16 brain regions of vehicle- ($n = 6$), phenytoin- ($n = 6$), phenobarbital- ($n = 6$), and valproate-treated rats ($n = 6$) were estimated. In column 2, mean numerical total cell densities ± SEM in 8-day-old rats are shown. The extent of apoptosis in vehicle-, phenytoin-, phenobarbital-, and valproate-treated rats is shown as the ratio of degenerating cell density to total cell density and is presented as % ± SEM. *, $P < 0.05$; **, $P < 0.01$; ***, $P < 0.001$, Student's t test. CA1 HC, CA1 hippocampus; DG, dentate gyrus; Thal, thalamus; LD, laterodorsal; MD, mediodorsal; V, ventral; Hthal VM, ventromedial hypothalamus; Fr, frontal cortex; Par, parietal cortex; Cing, cingulate cortex; Rspl, retrosplenial cortex; II, IV, cortical layers 2 and 4.

To visualize nuclei with DNA cleavage, serial coronal paraffin sections (10 μm) of the entire brain were cut on a microtome and residues of peroxidase-labeled digoxigenin nucleotides were catalytically added to DNA fragments by terminal deoxynucleotidyltransferase (TdT Frag EL, DNA Fragmentation Detection Kit, Calbiochem-Novabiochem).

For light microscopy on plastic sections and electron microscopy brains were sliced in 1-mm thick slabs, fixed in osmium tetroxide, dehydrated in alcohols, and embedded in araldite. Ultrathin sections were cut and stained with uranyl acetate/lead citrate.

Quantitation. Quantitation of damage was performed in silver-stained sections by estimating mean numerical densities (N_v) of degenerating cells (20). An unbiased counting frame (0.05 mm × 0.05 mm; disector height 0.07 mm) and a high aperture objective were used for the sampling. Counts were performed in a blinded manner. N_v values from 16 brain regions (Table 1) were summed to give a total score for degenerating neurons for each brain.

RT-PCR Studies and Western Blotting. Total cellular RNA was isolated from snap-frozen tissue by acidic phenol/chloroform extraction and DNase treatment (Hybaid, Roche Diagnostics); 500 ng of RNA was reverse-transcribed with Moloney murine leukemia virus reverse transcriptase (Promega) and oligo(dT)$_{16}$ primer (Roche Diagnostics) in 25 μl of reaction mixture. cDNA (1 μl) was amplified by PCR in 30 cycles, subjected to PAGE, subsequent silver staining, and densitometric analysis with the image analysis program BIODOCANALYZE (Whatman Biometra).

Primers for brain-derived neurotrophic factor (BDNF) [GenBank accession no. D10938; sense, 5′-CGACGTCCCTGGCTGGACACTTTT-3′ (positions 2296–2318); and antisense 5′-AGTAAGGGCCCGAACATACGATTGG-3′ (positions 2762–2786)], primers for neurotrophin 3 (NT-3) [GenBank accession no. M34643,; sense, 5′-GGTCAGAATTCCAGCCGATGATTGC-3′ (positions 308–332); and antisense 5′-CAGCGCCAGCCTACGAGTTTGTTGT-3′ (positions 767–791)], and primers for β-actin [GenBank accession no. V01217; sense, 5′-CCCTAAGGCCAACCGTGAAAAGATG-3′ (positions 1663–1687); and antisense 5′-GAACCGCTCATTGCCGATAGTGATG-3′ (positions 2535–2559)], were used.

For Western blotting analysis of brain tissue, animals were killed, and brains were removed, microdissected, and then immediately snap-frozen in liquid nitrogen.

Tissue was then homogenized at 4°C in a Tris·HCL buffer (50 mM, pH 7.6). Homogenate was centrifuged at 15,000 × g for 20 min, and the supernatant was used as the cytosolic fraction.

Total cellular proteins (30 μg/lane cytosolic fraction) were separated on a 10% SDS-polyacrylamide gel and electrotransferred onto nitrocellulose membranes (Hybond ECL, Amersham Pharmacia). The membranes were incubated overnight at 4°C with the following antibodies: antiphospho-raf (1:2,000), antiphospho-ERK1/2 (1:2,000), antiphospho-AKT (1:2,000), anti-ERK1/2 phosphorylation state independent (1:2,000), or anti-AKT phosphorylation state independent (1:2,000) (Cell Signaling Technology, Beverly, MA). After incubation with secondary antibody conjugated to horseradish peroxidase (anti-mouse, 1:1,000 dilution), immunoreactive proteins were detected by the enhanced chemiluminescence system (ECL, Amersham Pharmacia) and serial exposures were made to radiographic film (Hyperfilm ECL, Amersham Pharmacia). Densitometric analysis of the blots was performed with the image analysis program TINA 2.09g.

Results

To determine whether AEDs exert neurotoxic effects in the developing rat brain, we injected rats i.p. with phenytoin, phenobarbital, pentobarbital, diazepam, clonazepam, vigabatrin, or valproate on postnatal day 7 (P7) and analyzed their brains 24 h later.

In the brains of vehicle-treated rats, either silver or terminal deoxynucleotidyltransferase-mediated dUTP end labeling revealed a light pattern of neurodegeneration attributable to programmed cell death (21) (Table 1).

Phenytoin (10–50 mg/kg) produced widespread neurodegeneration on P7 (Fig. 1, Table 1). By electron microscopy it was determined that the cells degenerating in the brains of phenytoin-treated rats displayed ultrastructural changes similar to those described in neurons undergoing programmed cell death (21). A

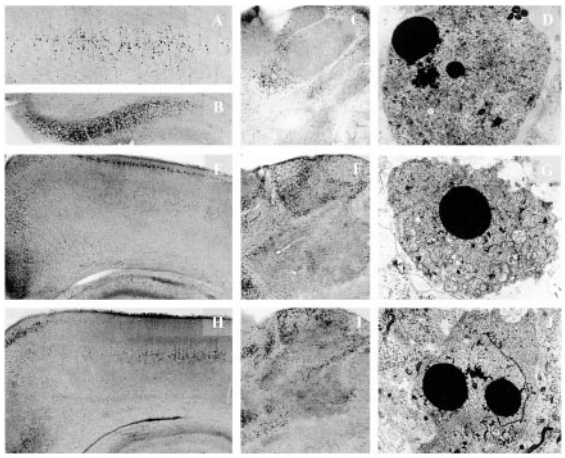

Fig. 1. Light microscopic overviews of silver-stained transverse sections and electron micrographs depicting neurodegenerative changes in the brains of P8 rats after treatment with phenytoin (*A–D*), diazepam (*E–G*), or valproate (*H–J*). (*A–C*) Layer IV of the parietal cortex (*A*, ×40), the subiculum (*B*, ×40), and the thalamus (*C*, ×25) of P8 rats treated 24 h previously with phenytoin (50 mg/kg). (*E* and *F*) Low-magnification (×25) light microscopic overviews of silver-stained sections from the parietal and cingulate cortices (*E*) and the thalamus (*F*) of P8 rats treated 24 h previously with diazepam (30 mg/kg). (*H* and *I*) Low-magnification (×25) light microscopic overviews of silver-stained sections from the parietal and cingulate cortices (*H*) and the thalamus (*I*) of P8 rats treated 24 h previously with valproate (200 mg/kg). Degenerating neurons (small dark dots) are sparsely present after treatment with saline in those same brain regions but abundantly present after treatment with phenytoin, diazepam, or valproate. (*D*, *G*, and *J*) Electron micrographs (×1,800) illustrating late stages of apoptotic neurodegeneration within the thalamus 24 h after administration of phenytoin (*D*), diazepam (*G*), or valproate (*J*) to rats on P7.

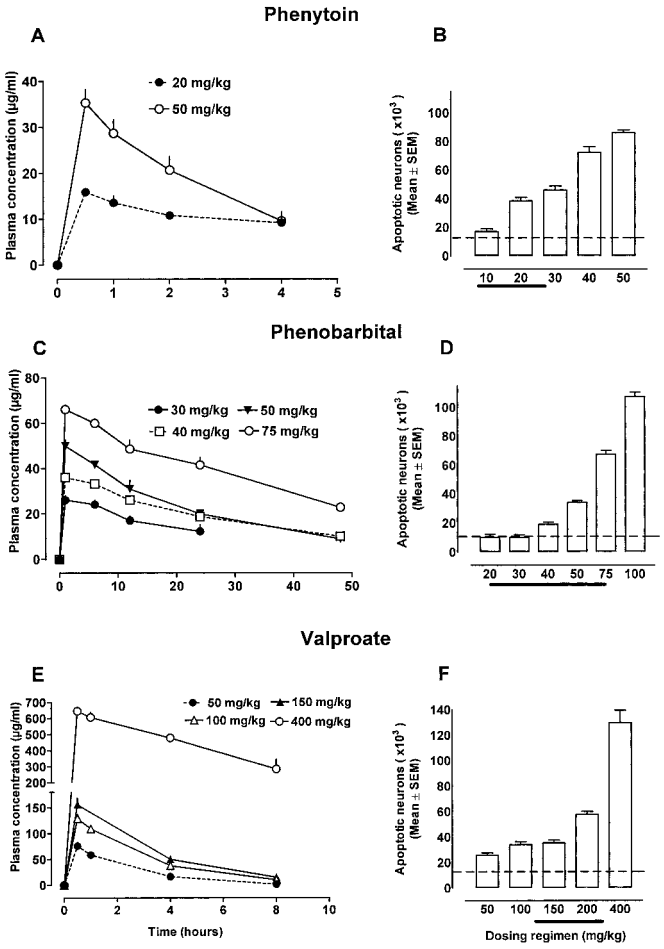

Fig. 2. Phenytoin (10–50 mg/kg), phenobarbital (30–75 mg/kg), or valproate (50–400 mg/kg) were administered to P7 rats. (*A*, *C*, and *E*) Phenytoin, phenobarbital, and valproate plasma concentrations associated with each of the several dosing regimens. Dotted lines represent threshold levels for triggering an apoptotic response. (*B*, *D*, and *F*) Severity of apoptotic neurodegeneration associated with each dose-plasma concentration curve. Severity of degeneration was established as described in *Materials and Methods*. Histographic values in *B*, *D*, and *F* represent cumulative scores for apoptotic brain damage (means ± SEM, $n = 6$ per group) in the forebrains of treated rats. Dotted lines in *B*, *D*, and *F* represent the mean score for apoptotic neurons in saline-treated rats. ANOVA revealed a significant effect of treatment with phenytoin [$F(1,50) = 703.8$, $P < 0.0001$], phenobarbital [$F(1,60) = 555.1$, $P < 0.0001$], and valproate [$F(1,50) = 356.0$, $P < 0.0001$] with multiple comparisons showing that the doses of 20 mg/kg phenytoin, 40 mg/kg phenobarbital, and 50 mg/kg valproate significantly increased apoptosis. Thick lines at the *x* coordinate indicate reported ED_{50} doses of the corresponding drug in various rodent seizure models. ED_{50} is defined as the dose that blocks seizures in 50% of tested animals.

proapoptotic effect of phenytoin has been described in the developing mouse cerebellum (22).

Phenytoin's neurotoxic action in the forebrain was dose-dependent. The threshold dose was 20 mg/kg, which resulted in phenytoin plasma concentrations ranging between 10 and 15 μg/ml over 4 h (Fig. 2).

Phenobarbital (20–100 mg/kg) and diazepam (5–30 mg/kg) caused widespread apoptotic neurodegeneration in the brains of rats on P7 (Fig. 1, Table 1). By electron microscopy (Fig. 1) it was determined that the cells degenerating in the brains of phenobarbital- or diazepam-treated rats fulfilled ultrastructural criteria for apoptosis. Neurotoxic effects were reproduced by pentobarbital (5 or 10 mg/kg) and clonazepam (0.5–4 mg/kg) in 7-day-old rats. Administration of the benzodiazepine receptor antagonist flumazenil prevented apoptotic neurodegeneration induced by diazepam (data not shown).

The threshold doses for triggering apoptotic brain damage were 40 mg/kg for phenobarbital, 10 mg/kg for diazepam, and 0.5 mg/kg for clonazepam (Fig. 2). These doses caused sedation but no hypoxia or cardiorespiratory compromise in 7-day-old rats. When concentrations of phenobarbital were maintained at 25–35 μg/ml over a 12-h period significant apoptotic neurodegeneration occurred (Fig. 2).

Valproate (50–400 mg/kg on P7) or vigabatrin (50, 100, or 200 mg/kg twice daily on 3 consecutive days starting on P5) elicited apoptotic neurodegeneration in the developing rat brain in a dose-dependent manner (Figs. 1 and 2, Table 2). The threshold dose for valproate was 50 mg/kg (Fig. 2) and resulted in a peak valproate plasma concentration of 80 μg/ml, which rapidly declined within 8 h. The threshold dose for vigabatrin was 100 mg/kg given twice daily on 3 consecutive days.

To investigate whether a combination of AEDs with different modes of action may result in a more profound neurodegenerative response compared with monotherapy, we administered diazepam (5 mg/kg) in combination with phenobarbital (20 mg/kg) or phenytoin (20 mg/kg) to rats on P7. This combination resulted in profound apoptotic neurodegeneration with the combination of diazepam and phenobarbital being most detrimental (Fig. 3). Oxygen saturations remained above 90% in pups treated with phenobarbital and diazepam.

To determine whether treatment with AEDs causes a persistent reduction in brain weight, we administered a single dose of phenytoin (50 mg/kg, $n = 6$), phenobarbital (75 mg/kg, $n = 6$), or valproate (300 mg/kg, $n = 6$) to P7 rats and measured unperfused hemispheric brain weights after 8 days. A single treatment with phenytoin on P7 led to a significant decrease in mean hemispheric weight of 9.2% (0.3958 ± 0.008 g vs. 0.4363 ± 0.03 g in vehicle-

Table 2. Phenobarbital, valproate, and vigabatrin trigger an increased rate of apoptosis in the rat brain on P0, P3, or P7

Numerical density of degenerating neurons, means/mm³ ± SEM

	P0				P3				P7					
Brain region	Vehicle	Phenobarbital	Fold ↑	Valproate	Fold ↑	Vehicle	Phenobarbital	Fold ↑	Valproate	Fold ↑	Vehicle	Phenobarbital	Fold ↑	Valproate	Fold ↑	Vigabatrin	Fold ↑
CA1 HC	3,789 ± 305	5,867 ± 892	1.6	5,333 ± 893	1.4	4,576 ± 756	6,318 ± 715	1.4	4,877 ± 243	1.1	1,863 ± 242	4,599* ± 990	2.5	4,335* ± 880	2.3	1,968 ± 340	1.1
DG	4,796 ± 716	5,333 ± 337	1.1	8,533** ± 892	1.8	2,745 ± 420	3,095 ± 538	1.1	3,365 ± 208	1.2	1,045 ± 170	4,376*** ± 313	4.2	3,750** ± 568	3.5	1,905** ± 142	1.8
Subiculum	3,996 ± 459	9,600*** ± 587	2.4	26,755** ± 5,635	6.7	3,663 ± 760	12,374** ± 2,611	3.4	6,832* ± 844	1.9	1,168 ± 172	7,509*** ± 812	6.4	14,463*** ± 1,010	12.4	3,448* ± 890	3.0
Caudate	8,349 ± 915	8,400 ± 1,168	1.0	11,467* ± 447	1.4	4,359 ± 740	5,125 ± 226	1.2	4,960 ± 198	1.1	703 ± 97	4,310*** ± 388	6.1	5,263*** ± 388	7.5	1,028* ± 99	1.5
Hypothal vm	23,186 ± 2,309	24,000 ± 2,800	1.0	25,066 ± 2,361	1.1	1,835 ± 270	6,498*** ± 715	3.5	7,131*** ± 880	3.9	1,209 ± 14	3,658** ± 686	3.0	9,254** ± 1,211	7.6	4,686** ± 851	3.9
Thal ld	2,428 ± 423	11,733*** ± 1,687	4.8	11,945** ± 2,115	4.9	3,172 ± 756	23,265** ± 4,583	7.3	10,104** ± 1,599	3.2	402 ± 67	13,310*** ± 962	33.0	10,150*** ± 2,433	25.2	1,486*** ± 147	3.7
Thal md	18,824 ± 2,078	19,333 ± 2,264	1.0	30,667* ± 4,088	1.6	926 ± 85	8,406*** ± 1,476	9.6	9,554*** ± 1,281	10.3	768 ± 20	6,578*** ± 1,574	8.6	12,738** ± 2,731	16.6	3,886*** ± 610	5.1
Thal v	10,787 ± 693	19,733*** ± 1,470	1.8	21,333*** ± 892	2.0	1,156 ± 205	4,138** ± 663	3.6	2,920*** ± 230	2.5	1,003 ± 66	1,847* ± 279	1.8	5,941** ± 1,289	5.9	1,600** ± 140	1.6
Fr II	0	0 (–)		0 (–)		5,672 ± 750	10,123** ± 822	1.8	5,932 ± 419	1.1	3,398 ± 395	9,282*** ± 702	2.7	10,182*** ± 307	3.0	5,016* ± 512	1.5
Par II	0	0 (–)		0 (–)		5,291 ± 905	8,088 ± 914	1.5	7,741 ± 527	1.5	2,421 ± 602	8,978*** ± 1,170	3.7	9,448*** ± 425	3.9	5,397** ± 526	2.3
Cing II	0	0 (–)		0 (–)		9,242 ± 1,200	11,308 ± 748	1.2	10,595 ± 1,028	1.2	3,369 ± 445	10,509*** ± 985	3.2	6,570** ± 1,117	2.0	5,853** ± 344	1.7
Cing IV	0	0 (–)		0 (–)		3,065 ± 518	4,127 ± 395	1.4	4,001 ± 415	1.3	196 ± 44	1,700*** ± 132	8.67	1,693** ± 282	8.63	2,223** ± 511	11.3
Rspl II	0	0 (–)		0 (–)		5,320 ± 445	6,104 ± 276	1.2	7,467* ± 692	1.4	2,089 ± 159	4,200** ± 448	2.0	3,303** ± 330	1.6	2,647 ± 366	1.3
Rspl IV	0	0 (–)		0 (–)		2,104 ± 482	2,575 ± 240	1.2	2,857 ± 370	1.4	476 ± 115	1,975** ± 193	4.1	3,006*** ± 809	6.3	1,079*** ± 55	2.3

At these ages rat pups received vehicle, 75 mg/kg phenobarbital i.p., or 400 mg/kg valproate at 0 h and were killed at 24 h. Vigabatrin was administered at the dose of 400 mg/kg on 3 subsequent days, starting on P5, and the pups were perfused on P8 (24 h after the last dose). Using an optical disector method (20), the numerical densities of degenerating neurons (degenerating neurons per mm³) in 14 brain regions of vehicle and drug-treated pups were estimated. Shown are mean numerical densities of degenerating neurons ± SEM ($n = 6$). Effects of phenobarbital, valproate, and vigabatrin on the rate of apoptosis at each age are presented as ratios of mean numerical densities of degenerating cells in drug-treated vs. age-matched vehicle-treated rats (expressed as fold ↑). Note that both phenobarbital and valproate do not trigger apoptosis in brain regions displaying no physiological apoptosis and that vulnerability to their proapoptotic action depends on developmental age. *, $P < 0.05$; **, $P < 0.01$; ***, $P < 0.001$, Student's t test. Abbreviations are as in Table 1.

Fig. 3. (*A*) Combinations of AEDs elicit neurotoxic effects. Diazepam (DZ, 5 mg/kg), phenobarbital (PHB, 20 mg/kg), and phenytoin (DPH, 20 mg/kg) were administered alone or in combination to P7 rats. Severity of degeneration was established as described in *Materials and Methods*. Histographic values represent cumulative scores for apoptotic damage (means ± SEM, $n = 6$ per group) in the forebrains of treated rats on P8. Dotted line represents the mean apoptotic score in saline-treated rats. Whereas these doses of AEDs alone elicited no or minimal neurotoxic response, their combination resulted in severe apoptotic neurodegeneration (***, $P < 0.001$ compared with DZ- and PHB-treated rats; ††, $P < 0.01$ compared with DPH-treated rats, Student's t test). (*B*) β-Estradiol (Estr) ameliorates apoptotic response to phenobarbital (PHB) and phenytoin in P7 rats. Saline or β-estradiol (300 μg/kg) were administered s.c. to P6 rats in three injections 8 h apart. Pups received i.p. injection of phenobarbital (50 mg/kg) or phenytoin (30 mg/kg) on P7 and the brains were analyzed on P8. Histographic values represent cumulative scores for brain damage (means ± SEM, $n = 6$ per group) in the forebrains of treated rats on P8. The scores illustrate that there are fewer apoptotic neurons in the brains of β-estradiol-treated rats compared with saline-treated rats (***, $P < 0.001$ for phenobarbital; *, $P < 0.05$ for phenytoin, Student's t test). (*C*) β-Estradiol increases protein levels for p-ERK1/2 and p-AKT but does not alter total protein levels in the thalamus of rats treated with phenobarbital (50 mg/kg) or phenytoin (50 mg/kg). Immunoblotting was performed with antiphospho-ERK1/2, antiphospho-AKT, ERK1/2 (phosphorylation state independent), or AKT (phosphorylation state independent) antibodies. Blots are representative of a series of four blots for each antibody and each treatment condition.

treated rats, $P < 0.05$). Phenobarbital treatment also resulted in a significant decrease in hemispheric weight of 8% (0.4012 ± 0.008 g, $P < 0.05$). Similarly, valproate treatment resulted in a decrease of hemispheric weight of 15% compared with control rats (0.3698 ± 0.01g, $P < 0.001$).

To determine how the apoptotic response to AEDs might differ as a function of developmental age, we administered either saline, phenobarbital (75 mg/kg), or valproate (400 mg/kg) to postnatal rats on P0, P3, P7, P14, and P20. These experiments revealed (Table 2) that there is a time window from P0 to P14 when various neuronal populations in the forebrain show transient sensitivity to phenobarbital and valproate, and within this period, different neuronal populations display transient sensitivity at different times (Table 2).

Neurotrophins provide trophic support to developing neurons and their withdrawal may lead to neuronal death (23). We tested

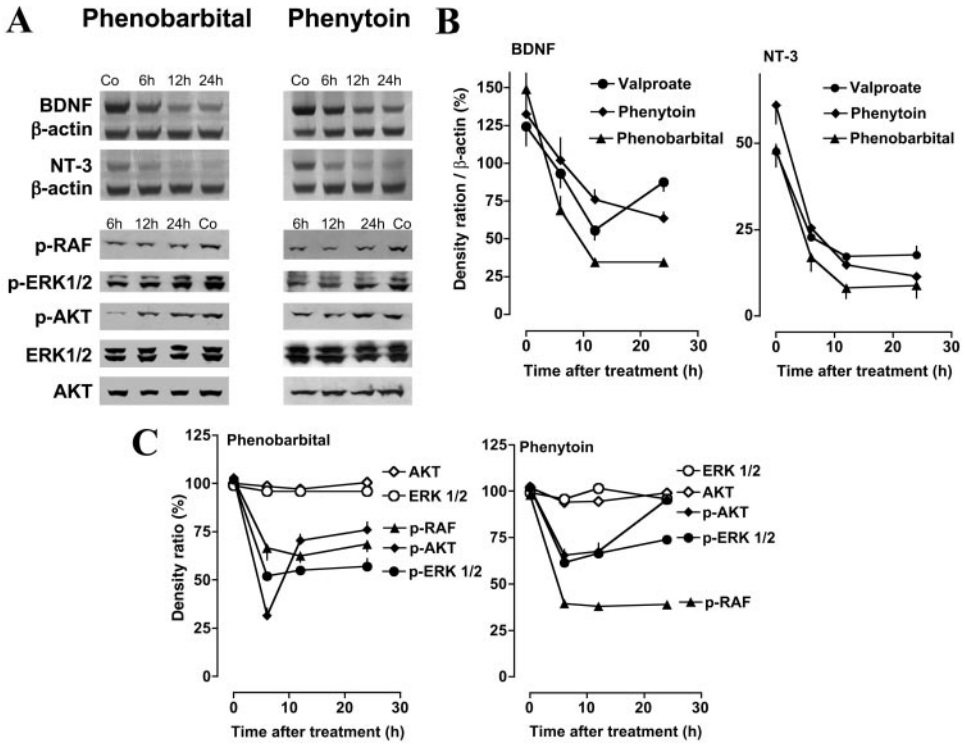

Fig. 4. (*A*) Phenobarbital and phenytoin decrease mRNA levels for BDNF and NT-3 and decrease phosphorylation of c-RAF, ERK1/2, and AKT in the neonatal brain. P7 pups received i.p. injection of phenobarbital (50 mg/kg), phenytoin (40 mg/kg), or vehicle (Co). Brain tissue from the thalamus was dissected at the various times indicated. Decreased density of the BDNF- and NT-3-specific bands is evident at 6, 12, and 24 h after administration of AEDs. Immunoblotting was performed with antiphospho-RAF, antiphospho-ERK1/2, antiphospho-AKT, ERK1/2 (phosphorylation state independent), or AKT (phosphorylation state independent) antibodies. There is a decrease in the levels of p-RAF, p-ERK1/2, and p-AKT at 6 h after injection of AEDs, whereas ERK1/2 and AKT (phosphorylation independent) are unaffected. (*B*) Quantitation of suppression by AEDs of mRNA levels for BDNF and NT-3 in the thalamus of infant rats. P7 pups received injection of phenobarbital (50 mg/kg, $n = 9$), phenytoin (50 mg/kg, $n = 9$), valproate (200 mg/kg, $n = 9$), or vehicle ($n = 9$) and were killed at 6, 12, or 24 h after treatment ($n = 3$ per group). mRNA levels for BDNF, NT-3, and β-actin were analyzed by means of PAGE and densitometrically quantitated. Values represent mean normalized ratios of the BDNF and NT-3 bands to β-actin ($n = 3$ per point $\pm$ SEM). ANOVA revealed that there was a significant effect of treatment with AEDs on BDNF [$F(1,12)_{\text{valproate}} = 29.79$, $P < 0.0001$; $F(1,12)_{\text{phenytoin}} = 5.492$, $P < 0.05$; $F(1,12)_{\text{phenobarbital}} = 838.2$, $P < 0.0001$] and NT-3 [$F(1,12)_{\text{valproate}} = 283.9$, $P < 0.0001$; $F(1,12)_{\text{phenytoin}} = 167.3$, $P < 0.0001$; $F(1,12)_{\text{phenobarbital}} = 109.2$, $P < 0.0001$] levels. (*C*) Quantitation of suppression by AEDs of protein levels of p-RAF, p-ERK1/2, and p-AKT in the thalamus of infant rats. P7 pups received injection of phenobarbital (50 mg/kg, $n = 16$), phenytoin (50 mg/kg, $n = 16$), or vehicle ($n = 16$) and were killed at 0, 6, 12, or 24 h after treatment ($n = 4$ per group). Protein levels for p-RAF, p-ERK1/2, p-AKT, ERK1/2, and AKT were analyzed by Western blotting and densitometrically quantitated. Values represent the mean normalized values of the densities of p-RAF, p-ERK1/2, p-AKT, ERK1/2, and AKT bands compared with the density of the respective band at 0 h (percent; $n = 4$ per point $\pm$ SEM). ANOVA revealed that there was a significant effect of treatment with AEDs on p-RAF [$F(1,24)_{\text{phenobarbital}} = 115.9$, $P < 0.0001$; $F(1,24)_{\text{phenytoin}} = 3{,}206$, $P < 0.0001$], p-ERK1/2 [$F(1,24)_{\text{phenobarbital}} = 477.4$, $P < 0.0001$; $F(1,24)_{\text{phenytoin}} = 478.7$, $P < 0.0001$] and p-AKT [$F(1,24)_{\text{phenobarbital}} = 254.3$, $P < 0.0001$; $F(1,24)_{\text{phenytoin}} = 96.69$, $P < 0.0001$] levels. ERK1/2 and AKT levels were not affected by treatment.

whether and how AEDs affect expression of the neurotrophins BDNF and NT-3 in the cingulate cortex, hippocampus, and thalamus in P7 rats. Phenobarbital (50 mg/kg), valproate (200 mg/kg), and phenytoin (40 mg/kg) reduced mRNA levels for BDNF and NT-3, as revealed by RT-PCR analysis, in all three areas. This down-regulation was evident within 6 h and still present at 24 h after administration of the AEDs (Fig. 4).

Western blot analysis revealed decreased levels of the active, phosphorylated isoforms of the serine-threonin kinase AKT (p-AKT, protein kinase B), and the members of the mitogen-activated protein kinase pathway c-RAF and extracellular signal-related protein kinase ERK1/2 (p-ERK1/2), which mediate intracellular signaling after activation of receptor tyrosine kinases by growth factors (Fig. 4) (24).

To confirm that reduction of levels of phosphorylated forms of ERK1/2 and AKT may cause neurodegeneration in the developing rat brain, we injected the mitogen-activated protein kinase kinase inhibitor U0126 (2 nmol), the phosphatidylinositol 3-kinase inhibitor wortmannin (2 nmol), or vehicle into the right cerebral ventricle of P7 rats and analyzed the brains 24 h later for signs of degeneration. These doses of U0126 and wortmannin have been shown to reduce p-ERK1/2 and p-AKT levels in the brains of P7 rats (25). Both compounds induced a significant neurodegenerative response in brain areas surrounding the right cerebral ventricle, i.e., septum and caudate nucleus.

The female hormone estrogen has neuroprotective properties in models of *in vitro* and *in vivo* neurodegeneration. These properties result from activation of estrogen receptors and cross-talking of estrogen with intracellular signaling pathways that are activated by neurotrophins, such as mitogen-activated protein kinase and phosphatidylinositol 3-AKT pathways (26). In an attempt to identify measures that will counteract neurotoxicity of AEDs and taking into consideration that AEDs impair neurotrophin-activated signaling, we investigated whether stimulation of these same pathways by β-estradiol may ameliorate phenobarbital- and phenytoin-induced apoptotic neurodegeneration.

β-Estradiol (total of three injections at 300 μg/kg every 8 h starting 10 h before the injection of phenobarbital or phenytoin) or vehicle were injected s.c. to P7 rats followed by phenobarbital (50 mg/kg) or phenytoin (30 mg/kg) on P7.

The numerical densities of degenerating cells in 16 evaluated brain regions were significantly lower in β-estradiol-pretreated pups in comparison to P7 pups who received phenobarbital, phenytoin, and vehicle (Fig. 3*B*). Analysis of protein levels for p-AKT and p-ERK1/2 revealed higher levels for p-AKT and p-ERK1/2 after β-estradiol treatment (Fig. 3*C*).

Discussion

Here we report that major AEDs cause sensitive neurons to undergo apoptotic death in the developing rat forebrain. These findings apply to compounds that block voltage-gated sodium channels, enhance GABAergic inhibition, or block glutamate-mediated excitation. Neurotoxicity of AEDs is age-dependent and is associated with impairment of neurotrophin-mediated, survival-promoting signals in the brain. The combination of AEDs with different modes of action results in a substantially higher apoptotic response compared with monotherapy.

Proapoptotic threshold doses and plasma concentrations of AEDs are not higher than their reported anticonvulsant doses in rodent seizure models. ED_{50} doses range between 5 and 25 mg/kg

for phenytoin (27, 28), 5 and 15 mg/kg for diazepam, and 0.4 and 0.6 mg/kg for clonazepam (28–31). We found that phenobarbital plasma concentrations between 25 and 35 μg/ml over a 12-h period triggered apoptotic neurodegeneration in infant rats. Such plasma concentrations are easily achieved when phenobarbital is given to human infants for management of seizures or status epilepticus and in the course of long-term antiepileptic treatment (32, 33). Reported ED_{50} doses for vigabatrin in rodent seizure models range between 200 and 1,000 mg/kg (34, 35). The threshold neurotoxic dose of valproate (50 mg/kg) was even lower than the reported effective anticonvulsant doses in rodents (133–250 mg/kg). Valproate's high neurotoxicity probably relates to the fact that it acts via several different mechanisms to elicit its anticonvulsant action (3, 4).

We find that AEDs depress an endogenous neuroprotective system in the brain that is crucial for neuronal survival during development (23, 36). Phenytoin, phenobarbital, and valproate depressed synthesis of the neurotrophins BDNF and NT-3 and reduced levels of the active phosphorylated forms of c-RAF, ERK1/2, and AKT. Such changes reflect impairment of survival-promoting signals and an imbalance between neuroprotective and neurodestructive mechanisms in the brain, which, during a developmental period of ongoing programmed neuronal death, will promote apoptotic neurodegeneration (37). In support of this hypothesis, administration of the mitogen-activated protein kinase kinase inhibitor U0126 and the phosphatidylinositol 3-kinase inhibitor wortmannin induced neurodegeneration in the developing rat forebrain. Furthermore, β-estradiol, at doses that increased levels of phosphorylated ERK1/2 and AKT, ameliorated AED neurotoxicity. These findings conform with the hypothesis that depression of the mitogen-activated protein kinase and the phosphatidylinositol 3-AKT pathways by AEDs contributes to the induction of neuronal apoptosis in the developing brain.

The vulnerability period to the proapoptotic effect of AEDs coincides with the brain growth spurt period, which in the rat spans the first 2 postnatal weeks of life (38). In humans, the comparable period begins in the third trimester of gestation and extends to several years after birth. Apoptotic neurodegeneration triggered by AEDs during this critical stage of development can at least partly account for reduced head circumference and impaired intellectual skills observed in prenatally or postnatally exposed humans (6–16). The observation that combinations of AEDs cause more pronounced neurotoxic effects offers one possible explanation for the increased risk for cognitive impairment associated with AED polytherapy (11). It remains open whether other mechanisms, not explored in the context of this study, such as impairment of migration or proliferation of neuronal progenitors as well as disturbance of synaptogenesis, may also account for neurological deficits seen in humans exposed prenatally or postnatally to AEDs.

Our results raise the interesting hypothesis that burst firing may play a role in neuronal survival during critical stages of development. Furthermore, they raise concerns with regard to current clinical practice using AEDs for seizure control in young humans and call for the design of novel AEDs and/or adjunctive neuroprotective therapies that will enable pregnant women, infants, and young children to be safely treated for epilepsy. In addition, measures that promote neurotrophin signaling in the brain may offer a novel adjunctive neuroprotective approach. The finding that β-estradiol ameliorated phenobarbital and phenytoin neurotoxicity is encouraging in that respect. Because the brain growth spurt period in humans begins in the third trimester of gestation, preterm infants, which are prematurely deprived of maternal β-estradiol and are frequently treated with AEDs (especially phenobarbital), are expected to be at high risk for AED neurotoxicity. β-Estradiol replacement therapy in premature infants has been introduced in some centers with the goal to improve bone mineralization (39) and, so far, no adverse side effects have been observed. Based on our findings, we advocate that maintaining *in utero* β-estradiol plasma levels may be one safe and effective measure to protect premature infants from AED neurotoxicity.

This work was supported by Deutsche Forschungsgemeinschaft Grants Ik2/2-1 and Ik2/2-2, Humboldt University Grant 98-649, Hübner Stiftung, Sonnenfeld-Stiftung, and National Institutes of Health Grants AG11355, DA05072, and HD37100.

1. Hauser, W. A. (1994) *Epilepsia* **35,** Suppl. 2, S1–S6.
2. Taylor, C. P. & Meldrum, B. S. (1995) *Trends Pharmacol. Sci.* **16,** 309–316.
3. Meldrum, B. S. (1996) *Epilepsia* **37,** Suppl. 6, S4–S11.
4. Brodie, M. J. & Dichter, M. A. (1996) *N. Engl. J. Med.* **334,** 168–175.
5. Gidal, B. E., Privitera, M. D., Sheth, R. D. & Gilman, J. T. (1999) *Ann. Pharmacother.* **33,** 1277–1286.
6. Speidel, B. D. & Meadow, S. R. (1972) *Lancet* **308,** 839–843.
7. Strickler, S. M., Dansky, L. V., Miller, M. A., Seni, M. H., Andermann, E. & Spielberg, S. P. (1985) *Lancet* **2,** 746–749.
8. Jones, K. L., Lacro, R. V., Johnson, K. A. & Adams, J. (1989) *N. Engl. J. Med.* **320,** 1661–1666.
9. Buehler, B. A., Delimont, D., Van Waes, M. & Finnel, R. H. (1990) *N. Engl. J. Med.* **322,** 1567–1572.
10. Holmes, L. B., Harvey, E. A., Coull, B. A., Huntington, K. B., Khoshbin, S., Hayes, A. M. & Ryan, L. M. (2001) *N. Engl. J. Med.* **344,** 1132–1138.
11. Zahn, C. A. (1998) *Epilepsia* **39,** Suppl. 8, S26–S31.
12. Farwell, J. R., Lee, Y. J., Hirtz, D. G., Sulzbacher, S. I., Ellenberg, J. H. & Nelson, K. B. (1990) *N. Engl. J. Med.* **322,** 364–369.
13. Reinisch, J. M., Sanders, S. A., Mortensen, E. L. & Rubin. D. B. (1995) *J. Am. Med. Assoc.* **274,** 1518–1525.
14. Sulzbacher, S., Farwell, J. R., Tenkin, N., Lu, A. S. & Hirtz, D. G. (1999) *Clin. Pediatr. (Philadelphia)* **38,** 387–394.
15. Thorp, J. A., O'Connor, M., Jones, A. M., Hoffman, E. L. & Belden, B. (1999) *Am. J. Perinatol.* **16,** 51–60.
16. Dessens, A. B., Cohen-Kettenis, P. T., Mellenbergh, G. J., Koppe, J. G., van De Poll, N. E. & Boer, K. (2000) *Acta Paediatr.* **89,** 533–541.
17. Ikonomidou, C., Bosch, F., Miksa, M., Vöckler, J., Bittigau, P., Dikranian, K., Tenkova, T., Turski, L. & Olney, J. W. (1999) *Science* **283,** 70–74.
18. Ikonomidou, C., Bittigau, P., Ishimaru, M. J., Wozniak, D. F., Koch, C., Genz, K., Price, M. T., Stefovska, V., Hörster, F., Tenkova, T., *et al.* (2000) *Science* **287,** 1056–1060.
19. DeOlmos, J. S. & Ingram, W. R. (1971) *Brain Res.* **33,** 523–529.
20. Gundersen, H. J. G., Bendtsen, T. F., Korbo, L. & West, M. J. (1988) *APMIS* **96,** 379–394.
21. Ishimaru, M. J., Ikonomidou, C., Tenkova, T. I., Der, T. C., Dikranian, K., Sesma, M. A. & Olney, J. W. (1999) *J. Comp. Neurol.* **408,** 461–476.
22. Ohmori, H., Ogura, H., Yasuda, M., Nakamura, S., Hatta, T., Kawano, K., Michikawa, T., Yamashita, K. & Mikoshiba, K. (1999) *J. Neurochem.* **72,** 1497–1506.
23. Huang, E. J. & Reichardt, L. (2001) *Annu. Rev. Neurosci.* **24,** 677–736.
24. Behl, C. & Manthey, D. (2000) *J. Neurocytol.* **29,** 351–359.
25. Hee Han, B. & Holtzman, D. M. (2000) *J. Neurosci.* **20,** 5775–5781.
26. Wlaz, P., Rolinski, Z., Kleinrok, Z. & Czuczwar, S. J. (1992) *J. Neural Transm. Gen. Sect.* **89,** 41–48.
27. Rataud, J., Debarnot, F., Mary, V., Pratt, J. & Stutzmann, J. M. (1994) *Neurosci. Lett.* **172,** 19–23.
28. Turski, W. A., Cavalheiro, E. A., Coimbra, C., da Penha Berzaghi, M., Ikonomidou-Turski, C. & Turski, L. (1987) *Brain Res.* **434,** 281–305.
29. Renfray, G., Schlinger, H., Jakubow, J. & Poling, A. (1989) *J. Pharmacol. Exp. Ther.* **248,** 967–973.
30. Walton, N. Y. & Treiman, D. M. (1989) *Epilepsy Res.* **4,** 216–221.
31. DeSarro, G., Di Paola, E. D., Aguglia, U. & De Sarro, A. (1996) *Pharmacol. Biochem. Behav.* **55,** 39–48.
32. Walker, M. C. (1998) *Curr. Opin. Neurol.* **11,** 149–154.
33. Kriel, R. L., Birnbaum, A. K. & Cloyd, J. C. (1999) in *Pediatric Neurology Principles and Practice*, eds. Swaiman, K. S. & Ashwal, S. (Mosby, St. Louis), pp. 692–718.
34. Walton, N. Y. & Treiman, D. M. (1992) *Epilepsy Res.* **12,** 199–205.
35. Dalby, N. O. & Nielsen, E. B. (1997) *Epilepsy Res.* **28,** 63–72.
36. Hengartner, M. O. (2000) *Nature* **407,** 770–776.
37. Venters, H. D., Dantzer, R. & Kelley, K. W. (2000) *Trends Neurosci.* **23,** 175–180.
38. Dobbing, J. & Sands, J. (1979) *Early Hum. Dev.* **3,** 79–83.
39. Trotter, A. & Pohlandt, F. (2000) *Ann. Med.* **32,** 608–614.